

Development of advanced cylinder liner conformation concepts of internal combustion engines with numerical simulation methods

Von der Fakultät für Maschinenbau
der Gottfried Wilhelm Leibniz Universität Hannover
zur Erlangung des akademischen Grades
Doktor-Ingenieur
Dr.-Ing.
genehmigte Dissertation

Von
M.Sc. Ahmad Alshwawra

2023

1. Referent: Prof. Dr. Friedrich Dinkelacker
 2. Referent: Prof. Dr. Gerhard Poll
 3. Referent: Prof. Dr. Ahmad Sakhrieh
- Tag der Promotion: 11.07.2023

Dedication

I dedicate this dissertation to my companions on this long journey:

my mother Majeda and my Father Dawood; their belief in me has kept my spirits and motivation high...

my soul mate Ayat; words cannot express my love and gratitude for having you in my life...

Dawood, Rasha, Zeinah, and Alharith; you are the ones who give meaning to my life...

Acknowledgments

I would like to express my sincere gratitude for Prof. Dr. Friedrich Dinkelacker. This endeavor would not have been possible without his guidance. I would like to thank him deeply for his support, directions and advices that helped me to develop personally and professionally. The thanks also goes to Prof. Dr. Gerhard Poll and Prof. Dr. Ahmad Sakhrieh who read, reviewed and refereed my work and to Prof. Dr. Jörg Wallaschek for chairing the Ph.D. committee.

Words cannot express my gratitude for my wife Ayat and my four children; Dawood, Rasha, Zeinah and Alharith. Those who endured the hardship of moving to a new country and a completely new life, so that I can complete my doctoral degree. I will be indebted to you for the rest of my life.

I would like to thank the funding agencies that facilitated the completion of my degree in Germany. First German Jordanian University (GJU) in Amman, who provided me with a research scholarship to do my Ph.D. in Leibniz University Hannover, the German Federal Ministry for Economic Affairs and Energy (BMWi), which funded my work through the cooperation project “Antriebsstrang 2025”, and last but not least, the equal opportunities office “Hochschulbüros für ChancenVielfalt” in Leibniz university Hannover who provided me with a partial fund through “Promotionsabschlussförderung” program.

I am also thankful to my colleagues here in ITV, especially Jan Wichmar, for giving me the required support whenever I asked. Many thanks for the tribological experimental group in ITV for sharing their experiences and doing the experiments required to validate my simulation. Thanks should also go to my colleagues in GJU, especially the president Prof. Al-Halhouli, who has been continuously backing me until the completion of this work.

Special big thanks for my friend Ahmad Almuhtady, who continuously motivated me to finish my PhD and for his help to improve the use of language in this thesis. I would like to extend my sincere thanks to my friend and office mate Lars Eichhorn for all the nice memories we shared together and for his help in the German part in this thesis.

I would be remiss in not mentioning my big family in Jordan and Palestine. My parents, grandmother, wife, children, sisters, Aunts, uncles, in laws, nephews, nieces and cousins: I am blessed by being part of this big lovely family.

Finally, I would also like to thank the bakery in Steintor that Lars used to buy my breakfast during my dissertation writing process, for their delicious food.

Abstract

Internal combustion engine (ICE) represents the main pillar of the powertrain in the majority of road, marine freight, and transportation worldwide. With the absence of a real alternative that can replace ICE over its full range of applications, enhancing the efficiency of ICE is of great interest to save energy and reduce greenhouse gas emissions. A great improvement potential is seen in the piston ring – cylinder liner (PRCL) coupling which is responsible to maintain the combustion pressure in the cylinder while preventing lubricant oil leak to it. Large frictional losses are associated with this sealing function. In order to improve the PRCL conformability with less friction, a rounder liner cross section is targeted in the hot operational state. The rounder the liner is, the better conformability exists. To achieve that, the engine must be started with a non-circular liner that deforms in a controlled manner under engine thermal and mechanical loads to form a circular liner bore during the fire operation. Further tribological improvement can be achieved by targeting a non-prismatic circular bore shape in the hot operational state. This cumulative thesis presents numerical investigations to this reverse engineering approach with the aim to reach a specific liner shape in the fire operation state from non-cylindrically produced liners in the cold state. It follows the relevant research hypothesis and provides quantitative analysis to show the advantages and limitations of such an approach. The presented numerical work is based on advanced simulation techniques established on the basis of finite element methods. Two physical models were considered; one for a series gasoline engine, and the second for a single cylinder diesel engine test rig. The models were validated using experimental data, then the local deformations of the liners were simulated. Harmonic analysis was used to investigate the orders of deformations and their trends over a set of operational points. Then different forms of non-circular liners were designed based on the reverse engineering concept. Geometrical performance indicators were developed and used in the comparative analysis. The results show a significant improvement in the geometrical performance when using non-circular liners. Special freeform liner can improve the bore roundness by 95% and the straightness by 75%. The concept of dominant deformation order can simplify the design significantly. For example, the elliptical conus liner is a good yet simpler alternative with 85% improvement in roundness and 65% in the straightness of the liner during fire operation. The freeform liner is susceptible to the engine load. However, some deformation orders are independent of operational points and can be considered in the liner design. The results presented here show a great potential of tribological improvement. A parallel experimental work shows a significant reduction of frictional losses by using one of the liners that was designed in this thesis.

Keywords: Cylinder liner; non-circular liner; freeform honed liner; elliptical liner; internal combustion engine; engine efficiency; piston ring – cylinder liner conformability.

Kurzfassung

Titel: Entwicklung innovativer Konzepte für Zylinderlaufbuchsen von Verbrennungsmotoren mit numerischen Simulationsmethoden

Ein erhebliches Potenzial zur Verbesserung von Verbrennungsmotoren liegt in der verbesserten Kopplung von Kolbenringen und Zylinder Laufbuchsen (Piston Ring Cylinder Coupling, PRCL). Um die Konformität von PRCL zu verbessern und die Reibung zu verringern, wird in einem gefeuerter Betrieb eine möglichst kreisförmige Querschnittsform der Laufbuchse angestrebt. Je weiter sich der Querschnitt der Laufbuchse eines Kreises annähert, desto besser ist die Konformität. Um dies zu erreichen, muss der Motor im kalten Zustand eine nicht-kreisförmige Laufbuchse haben, die sich unter thermischen und mechanischen Belastungen des gefeuerten Motors kontrolliert verformt und dann eine Laufbuchse mit ideal kreisförmigem Querschnitt bildet. Darüber hinaus können weitere tribologische Verbesserungen erzielt werden, indem im gefeuerten Betrieb eine nicht-prismatische, kreisförmige Laufbuchse angestrebt wird. Diese kumulative Arbeit präsentiert numerische Untersuchungen für diese Hypothese und liefert quantitative Analysen, um die Vor- und Nachteile mit nicht-kreisförmigen Laufbuchsen aufzuzeigen. Darüber hinaus werden Richtlinien für das Design nicht-kreisförmiger Freiformlaufbuchsen dargelegt.

Die Simulationsmodelle dieser Arbeit basieren auf der Finite-Elemente-Methode. Zwei physikalische Modelle wurden betrachtet: Eines für einen Serien-Gasmotor und ein zweites für einen Einzylinder-Forschungsmotor. Die Modelle wurden anhand experimenteller Daten validiert, woraufhin die lokalen Verformungen der Laufbuchsen simuliert wurden. Unter Anwendung der harmonische Analyse wurden die Deformationsordnungen für definierte Betriebspunkte untersucht. Darauf aufbauend wurden verschiedene Formen von nicht-kreisförmigen Laufbuchsen basierend auf dem Konzept des Reverse Engineering ausgelegt. Geometrische Indikatoren wurden definiert und in vergleichenden Analysen verwendet. Die Ergebnisse zeigen eine signifikante Verbesserung des geometrie-bedingten Verhaltens bei Verwendung von nicht-kreisförmigen Laufbuchsen. Eine speziell entwickelte Freiformlaufbuchse kann die Rundheit der Bohrung um 95 % und die Geradheit um 75 % verbessern. Das Konzept der führenden Deformationsordnungen ermöglicht eine signifikante Vereinfachung des Designs. Als Beispiel hierfür ist eine elliptische Konuslaufbuchse eine gute, jedoch einfachere Alternative, die eine Verbesserung der Rundheit um 85 % und der Geradheit der Laufbuchse um 65 % während des Betriebs aufweist. Die Freiformlaufbuchse ist empfindlich bezüglich der Motorenlast. Da bestimmte Deformationsordnungen jedoch unabhängig vom Betriebspunkt sind, können diese bei der Laufbuchsegestaltung besonders berücksichtigt werden. Die hier präsentierten Ergebnisse zeigen ein großes Potenzial zur tribologischen Verbesserung. Parallel stattfindende experimentelle Arbeiten zeigen eine signifikante Reduzierung der Reibungsverluste durch die Verwendung einer in dieser Arbeit entwickelten Laufbuchsen.

Schlagworte: Zylinderlaufbuchse; freiformgehonte Laufbuchse; elliptische Laufbuchse; Verbrennungsmotor; Motorwirkungsgrad; Konformität von Kolbenring und Zylinderlaufbuchse.

Table of contents

| | |
|---|-------------|
| Dedication..... | i |
| Acknowledgment..... | ii |
| Abstract..... | iii |
| Kurzfassung | iv |
| Table of contents | v |
| Nomenclature and Abbreviations | vii |
| List of Figures..... | viii |
| List of Tables..... | viii |
| Introduction | 1 |
| Shall we break the ICE?..... | 1 |
| Cylinder liner..... | 2 |
| State of the art..... | 4 |
| Contribution of the work | 8 |
| Theoretical background..... | 11 |
| Structural Thermal coupled field analysis..... | 14 |
| Summary and Interaction of Publications..... | 16 |
| List of Publications | 16 |
| Authors Contributions..... | 17 |
| Paper I | 18 |
| Paper II | 22 |
| Paper III | 25 |
| Paper IV..... | 27 |
| Paper V..... | 32 |
| Paper VI..... | 34 |
| Conclusion and recommendation | 39 |
| References | 43 |
| Appendix I: Paper I | |
| Appendix II: Paper II | |
| Appendix III: Paper III | |
| Appendix IV: Paper IV | |

Appendix V: Paper V

List of Publications

Supervised Thesis

Resume

Nomenclature and Abbreviations

| | |
|--------------------|--|
| FEM | Finite element method |
| FMEP | friction mean effective pressure |
| GHG | Greenhouse gas |
| ICE | Internal combustion engine |
| ITV | institute of technical combustion |
| PRCL | Piston ring – cylinder liner |
| A_p | Pressure area |
| A_s | Stress area |
| C_v | Specific heat at constant volume |
| h | Oil film thickness |
| K | Thermal conductivity matrix |
| l_l | Length of the liner |
| P_c | Cylinder pressure |
| Q | Energy density |
| r_l | Inner radius of the liner |
| T | Operating temperature |
| T_0 | Absolute reference temperature |
| T_{ref} | Strain free temperature |
| t | physical time |
| t_l | thickness of liner wall |
| U | Piston speed |
| α | Thermal expansion coefficient , and the, and the |
| β | thermoelastic coefficient |
| δ_i | Local deformation in i direction |
| ε_{el} | Elastic mechanical strain |
| ε_{th} | Thermal strain |
| σ | Normal stress |
| σ_h | Hoop stress |
| σ_L | Longitudinal stress |
| ρ | Density |

List of Figures

| | | |
|-------------|---|----|
| Figure 1.1 | Schematic for piston ring – cylinder liner coupling | 3 |
| Figure 1.2 | Hoop and longitudinal stresses | 12 |
| Figure 1.3 | Orders of cylinder liner deformation | 13 |
| Figure 2.1 | Physical and mathematical models for gasoline engine | 18 |
| Figure 2.2 | Summary of paper I main results | 19 |
| Figure 2.3 | Geometrical performance indicators | 21 |
| Figure 2.4 | Summary of paper II main results | 22 |
| Figure 2.5 | Summary of main results of paper III | 24 |
| Figure 2.6 | Freeform liner solution to enhance the geometrical performance of the liner | 26 |
| Figure 2.7 | Summary of paper IV main results | 28 |
| Figure 2.8 | Proposed freeform liner design to enhance the geometrical and tribological performances of cylinder liner | 29 |
| Figure 2.9 | proposed temperature control systems for cylinder liner | 31 |
| Figure 2.10 | Main parameters of physical and computational models for a single cylinder floating liner diesel engine | 33 |
| Figure 2.11 | Simulated deformation results for floating liner | 34 |
| Figure 2.12 | The proposed floating liner designs | 35 |

List of Tables

| | | |
|-----------|--|----|
| Table 2.1 | List of publications included in the cumulative thesis | 14 |
| Table 3.1 | Summary of results for testing the research hypotheses | 37 |

Chapter 1: Introduction

1.1 Shall we break the ICE?

In the current world of speed, the fast, powerful and efficient transportation sector represents one of the main pillars of societies' development and prosperity. Internal combustion engine (ICE) is dominating the transportation and freight sectors worldwide [1,2]. However, in the ongoing heated debate about the de-carbonization of the transportation sector, the internal combustion engine is always in the dock. The electrification is presented as a competitive alternative, backed by a broad team of scientist, politicians, and decision makers [3,4]. The standing argument for this team is to protect the environment and reduce global warming. However, they turned a blind eye to the fact that electricity is not a carbon free sector and will not be in the foreseen future [5]. Furthermore, they always avoid the discussion about more than 1.4 billion ICE vehicles operating on roads nowadays; what will be the size of the waste that environment has to deal with in case of retiring all the ICE cars.

Admitting the importance of the environment protection shall not lead to discarding one of the most established engineering technologies. Rather it should encourage the de-carbonization of the technology itself and enhancing its efficiency [6]. This rational conclusion is adopted in Germany that successfully convinced the EU to exempt e-fuels from 2035 ban on sales of ICE cars last March. Reducing the energy losses in ICE will improve the fuel efficiency and maximize the benefits of conversion to sustainable fuels such as synthetic fuels [7]. Additionally, some segments in the transportation sectors including submarines, heavy duty machineries, and long distance freight vehicles, will continue to use the large ICEs with high energy density fuels such as diesel [8]. Furthermore, stationary ICEs are ubiquitous for the power generation and industrial sectors. This magnifies the significance of enhancing the ICE's efficiency as it saves energy and reduces greenhouse gas (GHG) emissions.

Frictional losses within the piston assembly accounts for roughly half of the total mechanical energy losses in the internal combustion engine [9]. This represents approximately 4% - 7.5% of the total fuel energy in passenger cars [10]. The conformability between piston rings and cylinder liner affects the performance of ICE significantly as it is directly related to the consumption of fuel and lubricant oil. Up to 2.8% of the fuels consumption in diesel engines corresponds to the oil control ring alone [11]. This indicates that reducing the frictional losses in piston ring – cylinder liner (PRCL) coupling will have a considerable fuel saving, and consequently a potential operational cost cut as well as GHG reduction [12]. This conformability is altered due to the liner

deformation in the hot operational state [13]. The failure of the piston ring to conform to the deformed cylinder liner bore decreases engine efficiency and increases emissions due to the leak of lubricant oil into the combustion chamber and the loss of combustion pressure. Therefore, further tightness is required for the piston rings to maintain the needed sealing functionality. Unfortunately, this additional tightness increases the frictional losses and therefore decreases the engine efficiency and increases the emissions as more fuel energy is consumed [12,14]. Enhancing the geometry of the cylinder liner in the hot operational state represents a good solution for this dilemma [14–16].

1.2 Cylinder Liner

The cylinder liner or sleeve is a hollow cylindrical shell fitted in the engine block in which the combustion process takes place [17,18]. Since it encloses the combustion, the design of the cylinder liner is a crucial factor in the engine design as it is subjected to high stresses and works in a tough environment. The thickness of the cylinder liner should be adequate to handle the hoop stresses resulted from the direct exposure to the cylinder pressure [19]. Furthermore, the liner shall be designed to withstand thermal stresses, which are introduced by the significant temperature gradient between its inner and outer walls [20,21]. Additionally, the liner is subjected to slap force resulting from the piston's secondary movement [22].

One of the main functions for the cylinder liner is to provide a sliding surface for the piston rings while maintaining the best possible PRCL conformability; See figure 1.1. The efficiency of this interface relates directly to the engine efficiency and fuel consumption as mentioned in the previous section. Piston rings should glide on without oil leakage into the combustion chamber while supplying the lubricant in the clearances. At the same time, no gases shall leak from the combustion chamber into the crankcase [18]. A distortion of the cylinder liner disturbs the PRCL coupling and reduces these sealing properties. This reduces the overall engine efficiencies due to higher lubricant oil consumption, higher blow-by, and higher friction [23].

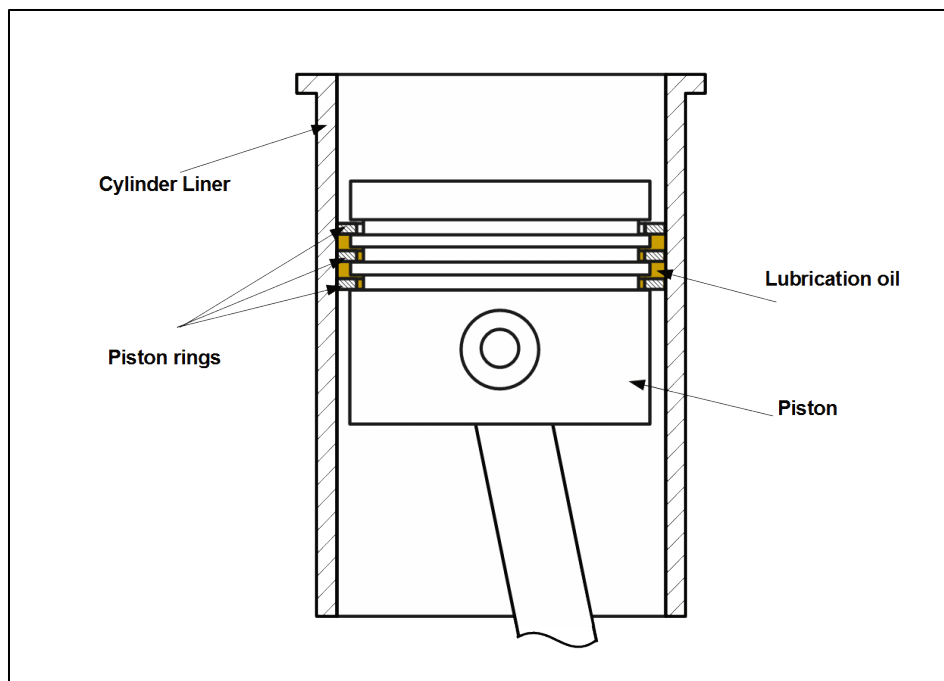


Figure 1.1: Schematic for the piston ring – cylinder liner coupling. [24]

The conformability of piston ring to cylinder liner is the ability of the piston ring to elastically deform in order to accommodate the variation in radius of the cylinder liner when the liner bore distorts [25,26]. The more bore distortion exists, the harder it is for the piston ring to conform. This means that the cylinder liner shall provide a good cylindricity for the piston ring in order to enhance the PRCL conformability. However, the liner bore distorts from its ideal circular cross section shape due to several reasons; including but not limited to; tolerances during the manufacturing processes, load which resulted from the assembly processes of the cylinder head and cylinder head gasket, variations in thermal expansion between different engine elements, combustion pressure, temperature gradients in the hot operation state, and mechanical load during fire operations [27–30]. More than 85 percent of the total liner bore distortion can be related to the operational thermal loads [14]. Analyzing the distortion trends can be significant for any design improvement that targets a better engine performance [31].

A cylinder liner should offer a good wear surface for piston and piston rings. Cast iron is widely used for liners due to its wear and anti-corrosion properties [32]. Furthermore, cast iron is considered as a self-lubricating material under sliding conditions; which is the case in the PRCL system. This could be attributed to the presence of graphite particles with layered crystal structure that acts as a solid-phase lubricating agent. Whenever a sliding shear force exists, the graphite particles come out from their pockets to form a tribofilm on the area of contact [33]. This improves the tribological characteristics

between the mating surfaces. Adding to that, cast iron has an excellent thermal conductivity that helps to transmit the combustion heat received through piston and piston rings to the coolant, which is another important function for the cylinder liner. However, cast iron, in its basic form, is not one of the strongest materials, therefore it is alloyed with other elements such like chromium, copper, and nickel with a concentration less than 5% [18].

Cylinder liners can be categorized into two types; wet liners and dry liners. The liner is considered as a wet liner if the coolant is in direct contact with the liner outer surface. This reduces the liner metal temperature and consequently, reduces the bore deformation as the thermal stresses are smaller compared to the dry liner concept. Wet liner configuration is usually preferred in heavy duty diesel engines [18,34,35]. In the dry cylinder liner configuration, there is no direct contact between the coolant and the liner outer wall. The temperature here is higher and the bore distortion is more significant. The Dry liner has a barrel shape with a flange at the top to fix it in the block. It could be of press-fitted or inserted type. For the press-fitted type, further attention should be given to make sure that the selected interference matches the operational temperature to prevent any loosening or additional stresses [18,36,37].

1.3 State of the Art

Due to their great influences on the engine performance, cylinder liner deformation as well as piston ring – cylinder liner conformability were investigated by many researchers. The works of Gintsburg represent one of the earliest analysis for the conformability of piston rings to a deformed cylinder liner [38,39]. The fundamentals of these early studies were later generally accepted in German technical literature and became known in engineering circles mostly through the piston ring manual of Goetze [40]. The works of Dunaevsky contributed greatly to the development of an analytical framework for the conformability problem. He developed the criterion of piston ring conformability that is based on the consideration that a full PRCL conformability can be achieved when the radii of the curvature of the piston ring and cylinder liner are the same at all points of contact [30,41–43].

The analytical studies for liner deformation are mainly based on a Fourier decomposition. In this approach the distorted liner bore is analyzed as a sequence of harmonic shapes up to n^{th} rank. Lu et al. used this method to analyze the tribological performance of PRCL coupling considering the liner bore distortion and the change in oil supply [27]. They focused in their model on the 4th order liner deformation as it is the most related to the lubricant oil consumption [27,36]. They concluded that liner bore distortion has a great

effect on the hydrodynamic friction force between the piston ring and cylinder liner, and consequently has impact on the power loss and overall engine performance. Similar results were reported by Selmani et al. [15] who analyzed the impact of different bore distortion orders on PRCL performance using the RINGPACK solver. They found that even third and fourth order contribution to the total liner distortion is smaller compared to 2nd order, as they generate higher blow-by value [15]. Some other examples about this approach can be found in [44–47] .

Experimental approaches were also used to investigate the liner deformation. Koch et al. studied the deformation of cylinder liner experimentally [14]. They went through different engine assemble and operation stages to measure liner deformation resulting from each stage. Specifically, they measured the liner distortion resulting from manufacturing tolerances. Then, they also measured the liner distortion resulting from assembling the cylinder head, and the ones which resulted from different thermal expansion coefficients between engine block, liner, and head. Finally, they measured the deformation resulting from thermal load in the hot operational state. According to their results, the majority of the liner deformation is caused by thermal load [14]. Other examples for such experimental approach can be found in [48–50].

Musashi Institute of technology in cooperation with Nissan Motor Co. developed a novel turning piston method to measure the deformation of the bore experimentally. Their test rig was based on a modified NISSAN engine with a dry liner configuration. In their test rig, they can measure the liner deformation as well as the cylinder wall temperature during the hot operational state. The liner can expand outward or inward depending on the clearance constraints. The maximum measured radial deformation at 4000 rpm was 32 μ m. They supported their experimental work with a finite element method (FEM) analysis. The measured block and cylinder temperatures were used as the boundary condition for the FEM model. The maximum simulated radial deformation was about 28 μ m [36,51–53]. Their experimental results were used to validate a part of the numerical analysis in this thesis.

With the great advances in the computational power, the numerical approach is heavily used by engine's developers and manufacturers to meet the challenges of efficiency improvement and emission reduction [1,54,55]. It is also used in liner deformation investigations in order to enhance the overall engine efficiency [13,27,56]. Such approaches are usually based on a three-dimensional representation of the engine and the liner using Finite Element Methods, where the local thermal and mechanical stresses can be simulated, and the resulting geometrical deformation can be obtained [14,29,44]. Using the Finite Element Method, developers can effectively analyze a large number of

technical design iterations within a relatively short period of time and lower cost [28,44,57,58]. FEM analysis is typically supported by a validation process, including in most of the cases detailed experimental work [1,59,60]. For example, Koch et al. used their experimental work results to build and validate a FEM simulation model that can deeply analyze more design parameters. Their engine model simulates the variation in the liner bore distortion with different bolt lengths, gasket materials, block materials, and during cold start [14].

ANSYS mechanical is a well-known numerical FEM software that has been used in this study. The robust algorithms of this software are capable of handling many non-linearities in FE model such as contact, dynamic, thermal, material and geometric non-linearities. ANSYS mechanical is used intensively in literature for analyzing the liner bore distortion [19,61–63]. Liang et al. used ANSYS to investigate the effect of static loads on liner bore distortion. Their model was based on a V6 diesel engine and the independent variables were the bolt preload, number of bolts, length of bolts and the distribution of bolts. It was found that the distortion in the upper half of the liner due to static load is higher than for the lower half, while the eccentricity was higher in the lower half [44]. Another example is Yang et al., who built a FE model based on a 4-cylinder gasoline engine, and then used ANSYS mechanical to solve the governing thermal and mechanical equations. They used their model to determine the dominant deformation order for different types of static and dynamic loads, and to optimize the best parameters in order to reduce the liner bore distortion. Their optimized model showed bore distortion for the cylinder liner compared with literature [29].

The high computational requirements and capacity represents the main challenges for FE simulation models. Solving FEM model requires long computing time and large computing powers. Here especially large memory capacity is needed to accommodate the excessive amount of generated data in each calculation step. Therefore, it is necessary to find sufficiently simple but yet accurate models to work with [29,64]. Barbieri et al. proposed a numerical methodology that aims to simplify the FE analysis for the cylinder liner deformation in an 8-cylinder V-type engine. A simplified geometry for the cylinder head was used, also some of the engine geometries were replaced by equivalent forces in order to reduce the solving time. Their simulated deformation had a good agreement with the experimental results [65].

A floating liner test rig is one of the most common techniques to measure the piston group friction during fired operation conditions. Its concept is based on decoupling the cylinder liner from the crankcase and constraining its radial movement, while allowing it to make free and infinitesimally small displacement in the axial direction. This axial

movement is caused mainly by the frictional forces in the piston/liner system and can be detected by force transducers located under the floating liner [66–70]. In a cooperation between the Institute of Technical Combustion (ITV) and Rolls-Royce Power Systems, the floating liner technique was used to measure the friction in the piston ring – cylinder liner coupling in order to validate and support a dynamic simulation of the coupling [59,60]. The friction measurements were done under fired and motored engine condition in order to derive the contribution of each ring in the total frictional loss. The temperature distributions of the piston and the liner were measured in order to calibrate the thermal deformations of the piston group in the simulation model. This led to a development of a novel automatic optimization simulation strategy that considered the cycle to cycle variation of the inter ring pressure [59,60].

Honing is a precise surface finishing using a grinding tool along a specific path. It is applied to the inner liner wall to provide a microstructure that stores lubricant oil and decreases the contact area on PRCL interface [71]. The vast majority of the published literature related to liner honing focuses on enhancing the tribological performance of the PRCL system through honing texture, roughness, and orientation [72–75]. Only one published work has discussed using the honing techniques to enhance the PRCL performance through the improvement of the liner geometry in the hot operation state [76].

In this regard, the German honing company Gehring developed an advance machining technique to apply freeform honing profile to the liner bore in order to achieve better cylindrical shape in the hot operational state [16]. This technique was mainly applied to get a bottle shape liner bore where the top half is kept small while the diameter of the bottom half is gradually increased. The reason behind that is the uneven supply of the combustion heat to the cylinder along the axial direction; the top of the liner is hotter than the bottom. This form was intended to lead to a better cylindrical shape of the liner in the hot operation state, where there is no secondary movement of the piston in the top of the liner and less friction in the bottom of the liner [18]. This bottle shape is applied to some BMW series engines [77]. However, there is no published record about the use of a completely freeform honed liner in an internal combustion engine.

So far, the bore distortion of circular cylinder liners has been studied intensively in literature. Only rarely, non-circular bore liners are investigated [25]. Furthermore, the literature mostly discussed the performance of the liners with a conventional cylindrical shape. Only a few recent publications investigated starting the engine with non-cylindrical liners; namely, bottle shape liner. Edtmayer et al., used floating liner technique and advance simulation model to study the effect of material thermomechanical properties, liner surface finish and bore shape on engine friction experimentally and numerically. In

their work, they compared the tribological performance of a conventional cylindrical liner with a bottle shape liner. They found that increasing the liner diameter at the bottom decreases the friction significantly [22].

Halbhuber and Wachtmeister used a floating liner test rig to evaluate the potential for friction saving that can be achieved by a conus honed liner. They also studied the change in this potential with different engine materials and different cooling scenarios. It was found that for an aluminum engine block, the effect of the conus shaped liner is low if sufficient cooling is provided. For a grey cast iron engine block, the friction mean effective pressure (FMEP) is reduced by 6% with conus liner if sufficient cooling is provided, and up to 12% in the absence of piston cooling. They concluded that the use of a honed liner should be connected to several design parameters and operation strategies, otherwise the maximum benefit of using honed liner will not be achieved [78].

1.4 Contribution of this work

This work contributes to the existing piston group literature in several ways. Firstly, the vast majority of the published literature discussed fully cylindrical liner with strictly circular cross section. This kind of conventional liner has been studied thoroughly with deep details in the last decades. The topic of the non-prismatic liner is the state of the art, but the subject of its combination with a non-circular cross section is only superficially addressed in the literature.

Many studies have discussed the improvement of the tribological performance of PRCL coupling [48–50]. However, their focus was mainly on the honing texture, orientation and roughness [72–75]. Enhancing PRCL conformation by improving the geometrical performance of the cylinder liner has not been investigated thoroughly before. Moreover, a detailed work on the quantification of the geometrical performance of the cylinder liner through specific quantified indicators was not existing in published literature before.

As mentioned before, the German honing company Gehring raised the topic of freeform honing in 2015 [16]. Since then, there has been no published investigation about the topic. The essential new contribution of this work is, to relate the freeform honing technique to the operational points and to investigate its behavior if the engine load changes with theoretical analysis and numerical simulation. The harmonic analysis provided in this work aims at presenting a road map for selecting the deformation orders of the freeform honing with relation to the engine operation cycles. Additionally, the experimental validation, being done by the experimental tribology group within ITV, gives a solid evidence for the tribological improvement achieved by this freeform honing techniques [79]. Finally, an essential outcome of this work is that the combination of a

slightly elliptical shaped cross section in combination with a conus liner might be an effective compromise between the challenges of fully freeform honing and sufficient improved liner form.

An additional possibility of advanced numerical simulation of the thermal and mechanical stresses of the piston and liner system is that it could be combined with the new methods of additive manufacturing. The additive manufacturing techniques are the techniques for the future. So far, many studies have been conducted on the performance of additively manufactured engine components, especially, the piston. However, using these advanced techniques for liner manufacturing has not been addressed in the literature. One first study in this direction is part of this thesis. It shows the potential to improve the liner design significantly due to the new design possibilities of additive manufacturing.

The thesis is written as a cumulative thesis, where different topics are included in five published and one planned publication. Through the published papers, this cumulative thesis addresses the following research questions (R) and subsequent hypotheses (H):

R1: How can the use of a non-circular liner improve the PRCL conformation in hot operational states?

H1.1: Non-circular liner in its cold state deforms due to thermal and mechanical engine operation loads in a controlled manner such that a rounder shape is reached in the hot operational state. Consequently, this will improve the PRCL conformation and reduce friction losses.

R2: What is the improvement in the cylinder liner's geometrical performance that can be achieved by starting the engine with a non-prismatic liner profile?

H2.1: A suitably formed conical liner can be deformed into a better cylindrical shape in the hot operational state.

H2.2: Cylindrical bore shape in the hot operational state is not the optimal bore shape for a cylinder liner from a tribological point of view.

H2.3: There are some deformation orders that vary along a liner's depth, hence a suitable non-prismatic bore shape improves the geometrical performance of the liner.

R3: How do the engine operational points influence the freeform honed liner performance?

H3.1: There are some deformation orders that vary with engine load, therefore changing operational point alters the deformation pattern of the freeform honed liner and consequently increases or decreases its performance.

H3.2: Operating a freeform honed liner at an operational point other than the reference one where the liner bore is reversed based on it, reduces the expected benefit of utilizing the totally reversed honed liner.

H3.3: There are some deformation orders that are independent of the operational load and therefore shall be considered to be most relevant for a freeform honed liner design regardless of the load.

R4: Gehring formulated in [16] the vision of the totally reversed freeform honed liner concept. Are there possibilities to get simplified reversed geometries which are easier to produce?

H4.1: There is a dominant deformation order in the total order deformation. Reversing only this dominant order simplifies the honed shape significantly while considerably improving the PRCL performance. For example, considering an elliptical liner in the case of second order domination.

H4.2: Cylinder liner is deformed in a controlled manner and therefore a better shape other than a cylindrical liner can be achieved in the hot operational state. This shape improves PRCL conformation and improves its tribological performance.

R5: What improvement to the tribological performance of an engine can be achieved by enhancing the PRCL conformation?

H5.1: Improving PRCL conformation can simultaneously reduce several tribological issues, such as engine friction, blow-by and lubricant oil consumption.

R6: What is the relationship between the liners' material and its geometrical performance?

H6.1: Young modulus, Poisson's ratio, thermal conductivity and thermal expansion coefficient influence the geometrical performance of a cylinder liner.

H6.2: The deformation orders' variation trends with operational points and over liner depth are independent of liner material.

R7: What are the potential impacts of utilizing additive manufacturing materials as cylinder liner material on its geometrical performance?

H7.1: The use of common AM metallic materials will not cause a failure due to excess structural deformation in the cylinder liner during engine operation.

H7.2: The common AM metallic materials can improve or worsen the geometrical performance of the liner depending on its properties.

To answer those research questions and test the above mentioned research hypotheses, advanced finite element simulation techniques are implemented using validated mathematical models. Based on the results of these simulations, three designs for a freeform honed liner are suggested, considering improving both PRCL conformation and its tribological performance. Within the joint research project "Antriebsstrang 2025" [80], one of these designs was manufactured using advanced manufacturing techniques by research partners, and then it was tested by the experimental tribological group at ITV [79].

1.5 Theoretical background

A cylinder liner is subjected to different types of loads that generate different stresses. Mechanical loads resulting from combustion pressure generate hoop and longitudinal stresses. Furthermore, the temperature gradient between the inner and outer walls of the liner causes thermal stress. The stress caused by combustion pressure can be found by:

$$\sigma = \frac{P_c A_p}{A_s} \quad (1.1)$$

Where; σ is the stress, P_c is the cylinder pressure, A_p is the pressure area, and A_s is the stress area.

Hoop stress (σ_h) is the stress resulting from combustion pressure and acts in the circumferential direction. For the hoop stress, A_p and A_s can be found from the following equations as indicated in Figure 1.2 (a),

$$A_p = 2r_l l_l \quad (1.2)$$

$$A_s = 2l_l t_l \quad (1.3)$$

Where; r_l is the inner radius of the liner, t_l is the thickness of liner wall, and l_l is the length of the liner.

Substitution of equations 1.2 and 1.3 in equation 1.1 leads to:

$$\sigma_h = \frac{P_c r_l}{t_l} \quad (1.4)$$

Longitudinal stress (σ_L) is the stress resulting from the combustion pressure and acts in the axial direction. For longitudinal stress, A_p and A_s can be found from the following equations as indicated in Figure 1.2 (b),

$$A_p = \pi r_l^2 \quad (1.5)$$

$$A_s = 2\pi r_l t_l \quad (1.6)$$

Substitution of equations 1.5 and 1.6 in equation 1.1 gives:

$$\sigma_L = \frac{P_c r_l}{2t_l} \quad (1.7)$$

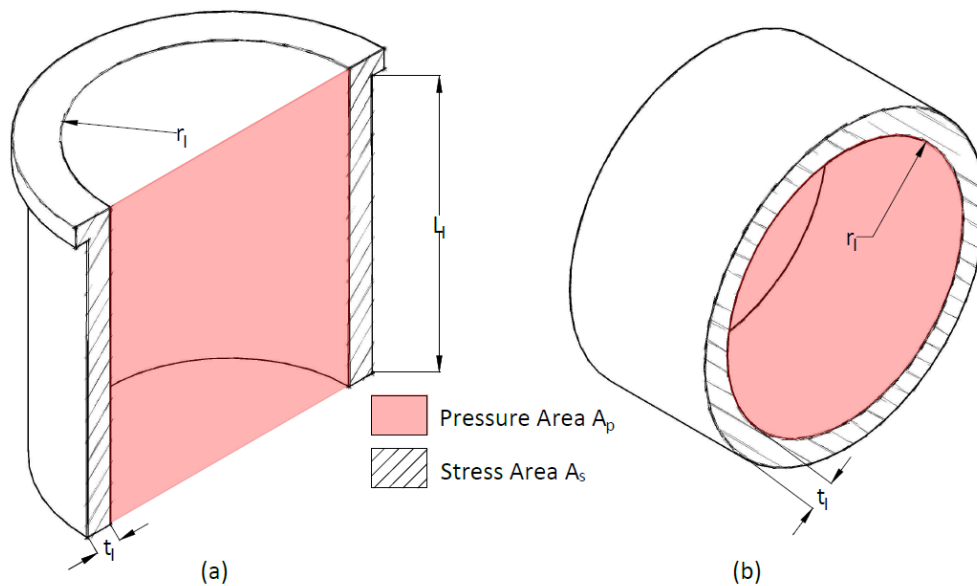


Figure 1.2 Hoop and longitudinal stresses

As could be seen from the previous set of equations, the value of hoop stress is higher than the one of longitudinal stress (since $t_l \ll 1m$) and therefore, it is the most critical one in determining the liner wall thickness. These equations assume that the material properties of the liner are isotropic, homogeneous, and within the elastic range. Further, the diameter to wall thickness ration must be greater than 10.

The local elastic mechanical strain vector $\{\varepsilon_{el}\}$ can then be calculated using Hook's law:

$$\{\varepsilon_{el}\} = [D]^{-1}\{\sigma\} \quad (1.8)$$

Here $\{\sigma\}$ represents the stress vector and $[D]$ represents a matrix related to the material's mechanical properties. Thermal strain $\{\varepsilon_{th}\}$ can be calculated

$$\{\varepsilon_{th}\} = (T - T_{ref})\{\alpha_x \ \alpha_x \ \alpha_x \ 0 \ 0 \ 0\}^t \quad (1.9)$$

with the thermal expansion coefficient α , the strain free temperature T_{ref} , and the operating temperature T . The total strain ε equals the summation of thermal strain and elastic mechanical strain, or in other words:

$$\{\varepsilon\} = \{\varepsilon_{el}\} + \{\varepsilon_{th}\} \quad (1.10)$$

Then the local deformation in i direction (δ_i) equals to:

$$d\delta_i = \varepsilon(i)di \quad (1.11)$$

Cylinder liner deformation can be represented approximately using a Fourier decomposition. The variation of the cylinder liner radius from the ideal circular shape ΔR can be represented as:

$$\Delta R = A_0 + A_1 \cos \theta + B_1 \sin \theta + A_2 \cos 2\theta + B_2 \sin 2\theta + \dots + A_n \cos n\theta + B_n \sin n\theta \quad (1.12)$$

where A_n, B_n are the Fourier's coefficients, θ is the angular position, and n is the deformation order. For each n^{th} order, the maximum bore deformation $U_{max,n}$ and the phase angle ϕ_n can be calculated by

$$U_{max,n} = \sqrt{A_n^2 + B_n^2} \quad (1.13)$$

$$\phi_n = \frac{1}{n} \tan^{-1} \frac{B_n}{A_n} \quad (1.14)$$

Using the harmonic series, the variation of the radius ΔR can be rewritten as:

$$\Delta R = A_0 + \sum_{n=1}^i [U_{max,n} \cos\{n(\theta - \phi_n)\}] \quad (1.15)$$

Different deformation orders describe different distortion patterns, see Figure 1.3. Generally, higher deformation orders ($n \geq 5$) contribution to the total liner deformation is negligible [15,27,57].

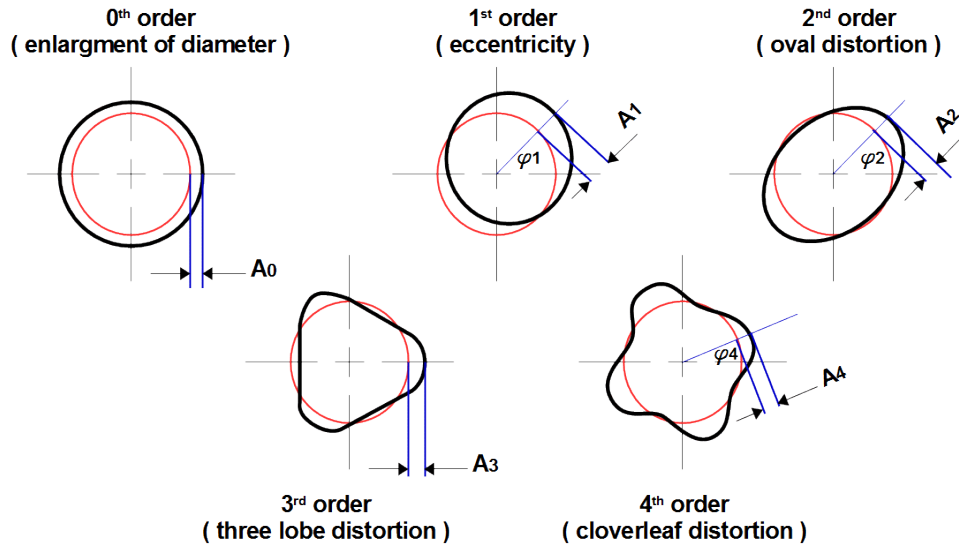


Figure 1.3 Orders of cylinder liner deformation. [24]

1.6 Structural thermal coupled field analysis

A direct structural – thermal coupled field approach was used in this work to model the cylinder liner deformation. In this approach, the equation of motion in terms of stress and the conservation equation of heat flow are strongly coupled by thermoelastic constitutive equations. Here the simplified thermoelastic constitutive equations for isotropic conductor suggested by Nye was used [81]. The equation was derived based on the balance of entropy and conservation laws of energy and momentum. Its final form is presented as follows:

$$\frac{\partial Q}{\partial t} = T_0 \{\beta\}^T \frac{\partial \{\varepsilon\}}{\partial t} + \rho C_v \frac{\partial (\Delta T)}{\partial t} - \nabla \cdot ([K] \nabla T) \quad (1.16)$$

here, Q is the generated heat per unit volume, t is the physical time, T_0 is the absolute reference temperature, $\{\beta\}$ is a vector of thermoelastic coefficients, ρ is the density, C_v is specific heat at constant volume, $[K]$ is the thermal conductivity matrix, T is the local operation temperature, and ΔT is the temperature difference which equals to:

$$\Delta T = T - T_{ref} \quad (1.17)$$

In equation 1.16 above, the left hand side represents the energy received by the combustion process. It is represented in the model by a heat source that keeps the temperature distribution on the inner surface of the cylinder bore constant. The first term on the right hand side is related to the work done by the system in the form of structural deformation. The second term is related to the heat used to increase the material

temperature at constant strain, while the last term is related to the heat flux. Further details about the strongly coupled finite element matrix can be found in [82].

Chapter 2: Summary and Interaction of Publications

2.1 List of Publications

This cumulative thesis contains five published papers in addition to one manuscript currently under preparation. Table 2.1 summarizes the papers included in this cumulative thesis. In the five already published papers, the candidate was the first author.

Table 2.1: List of publications included in the cumulative thesis

| No. | Title | Authors | Journal | Year |
|-----------|--|---|--|------|
| Paper I | Increasing the roundness of deformed cylinder liner in internal combustion engines by using a non-circular liner profile | A. Alshwawra H. Pasligh H. Hansen F. Dinkelacker | International Journal of Engine research | 2021 |
| Paper II | Enhancing the Geometrical Performance Using Initially Conical Cylinder Liner in Internal Combustion Engines— A Numerical Study | A. Alshwawra F. Pohlmann-Tasche F. Stelljes F. Dinkelacker | Applied Sciences | 2020 |
| Paper III | Cylinder Liner Deformation - An Investigation of its Decomposition Orders under Varied Operational Load | A. Alshwawra F. Pohlmann-Tasche F. Stelljes F. Dinkelacker | SAE Technical Paper | 2022 |
| Paper IV | Effect of Freeform Honing on the Geometrical Performance of the Cylinder Liner— Numerical Study | A. Alshwawra F. Pohlmann-Tasche F. Stelljes F. Dinkelacker | SAE International Journal of Engines | 2023 |
| Paper V | Structural Performance of Additively Manufactured Cylinder Liner—A Numerical Study | A. Alshwawra A. Abo Swerih A. Sakhrieh F. Dinkelacker | Energies | 2022 |
| Paper VI | Improving engine tribological performance through enhancing cylinder liner geometry | F. Stelljes A. Alshwawra F. Pohlmann-Tasche F. Dinkelacker | Under preparation | |

The research work of this cumulative thesis deals with the mathematical modeling and numerical simulation of the shaping of the cylinder liner under thermal and mechanical

stresses, which leads to deformations. This research work is part of a frame of investigations of the reduced friction in cylinder liners where experimental work was also done. While the coworkers did the experimental work, all the numerical simulation work was done by the candidate. The experimental research work and some parts of the numerical one were part of a joint research project "Antriebsstrang 2025" together with two other institutes and industrial partners [80]. The numerical work, however, was significantly extended beyond this research project, as is described within this thesis. The main idea in all this work is that if the appearing deformations of the cylinder liner under thermal and mechanical stresses can be predicted numerically, then using an inverse engineering approach, the shape of the cylinder liner could probably be produced in non-cylindrical form in such a way that, during the hot engine operation conditions a better liner bore form can be reached which would minimize the piston-liner friction.

In paper V, a newly developed idea is contained, to add more functionality to the enhanced cylinder liner of the future by also allowing additive manufacturing methods. With that also, for instance, the cooling channel structure within the engine bed around the cylinder liner can be regarded. This paper describes the first numerical study to evaluate the potential of this method. This was done mostly by the candidate and a master student (Abo Swerih) being supervised by the candidate. During the discussion of these ideas, essential ideas also came from the candidate's earlier academic advisor (Prof. Sakhrieh) and from the current advisor (Prof. Dinkelacker), so that they are co-authors of this paper.

2.2 Authors Contributions

The candidate developed the mathematical model and performed the simulations. He validated the computational model and performed the grid independence test. The different non-conventional shapes of the liner were developed by the candidate who numerically calculated their deformations based on the validated model. A comparative technique was suggested and implemented by the candidate who developed the required codes for the comparative analysis. The candidate also performed the post processing of the simulated data and the harmonic analysis of the liner deformation. The candidate wrote and revised the papers, including most of the literature review and made all the figures. The coauthors shared their experiences in engine tribology and contributed with their experience from the experimental work on tribological engine test rigs. The experimental work in paper VI was done by Pohlmann-Tasche and Stelljes. Stelljes wrote the experimental part in the paper and prepared the required figures for it. In particular, the work in paper VI is related to the joint research project "Antriebsstrang 2025", while the papers I to IV are partly related to that project, as here the preparation and

development of the simulation methods are described, being then applied to the project work, as figured out in paper VI.

Paper V is based on the candidate's work on numerical simulation of the impact of possibilities of additive manufacturing on tribological behavior. Part of the work was done together with his master student, Abo Swerih. Essential ideas were also given in scientific discussions by Prof. Sakhrieh and Prof. Dinkelacker, and they contributed to the final version of the manuscript.

2.3. Paper I

Paper I is entitled *“Increasing the roundness of deformed cylinder liner in internal combustion engines by using a non-circular liner profile”*. Its main hypothesis is that starting the engine with a non-circular liner cross section in the cold operational state will lead to a rounder liner cross section in the hot operational state. The rounder the cylinder liner is, the better conformation between piston ring and cylinder liner is reached. This eventually allows an increase in the efficiency of the engine. To test that hypothesis, a computational model for a gasoline engine was built and validated, where experimental data of the deformation during the operation have been described by Hitosugi et al. in [36]. This experimental test case allowed to develop and validate the numerical approach which is the basis of this thesis. It also allowed to simulate the deformation of different liner cross sectional shapes under typical engine operation conditions. Finally, the roundness errors of a non-circular liner were compared with the ones of conventional circular liner.

The development of the simulation model is based on experimental data from an engine test bench designed by Hitosugi et al. [36]. It is a modified NISSAN CA18 four-stroke gasoline engine. It has four cylinders arranged in a row with a cylinder bore of 83 mm and a piston stroke of 83.6 mm. Cast iron is used as a block material while aluminum alloy is used for the cylinder head. The engine was modified so that a dry liner configuration could be used. The liner is made of cast iron with a thickness of 1.6 mm. The numerical study was done on the terminal cylinder as the deformation values were available experimentally at 4000 rpm / full load. For that, one and half cylinder were simulated to capture the thermal loads from adjacent cylinder. The temperature of the cylinder inner walls was set to 130 °C and the temperature of the block outer wall was set equal to the coolant temperature (80 °C). These boundary conditions were set based on Hitosugi et al. experimental and simulation work [36]. The bolt pretension is 80 kN.

A grid independence test was performed and the results showed that there is a less than 2 μm average difference in the calculated deformation with a mesh of 100,000 nodes compared with a mesh of 1 million nodes. The circumferential position dependent

deformation for two mesh sizes of 200,000 nodes and 325,000 nodes shows almost identical deformations at different levels. Based on that, a mesh consisting of about 200,000 nodes (exactly: 197,666 nodes and 112,944 elements) was selected. A Direct coupled approach was used to solve the model. In this approach, the mechanical and thermal matrices are solved simultaneously. The simulation results show that the liner deformation values are in the range of 30 μm . The simulated trends and values of liner deformation were compared with the experimental results at two different levels. A good agreement was found and therefore the model was considered valid. Figure 2.1 summarizes the details of the physical and mathematical model.

Three different non-circular cross sections were selected for the prismatic liner in the cold state; Elliptical form (EL), half circle-half ellipse form (HCE), and non-symmetrical ellipse form (NSE). These designs were based on reversing the direction of the maximum deformation and pre-applying it to the liner in the cold state. The deformations of these non-circular liners were simulated under the same operational conditions. It is expected to have better liner roundness in the hot state as those pre-applied deformations were compensated for during engine operation.

Codes were developed to calculate the roundness error in different liner's cross sections using the least squares circle method. The least squares circle is a unique circle fitted within the cross sectional profile such that the sum of the squares of the radial ordinates between the circle and the profile is as minimal as possible. Then two concentric circles with the least squares circle are drawn. One is the maximum inscribed circle that is contained by all the points in the cross sectional profile and the other is the minimum circumscribed circle that contains all the points in that profile. The radial distance between those two circles represents the roundness error, see Figure 2.2.

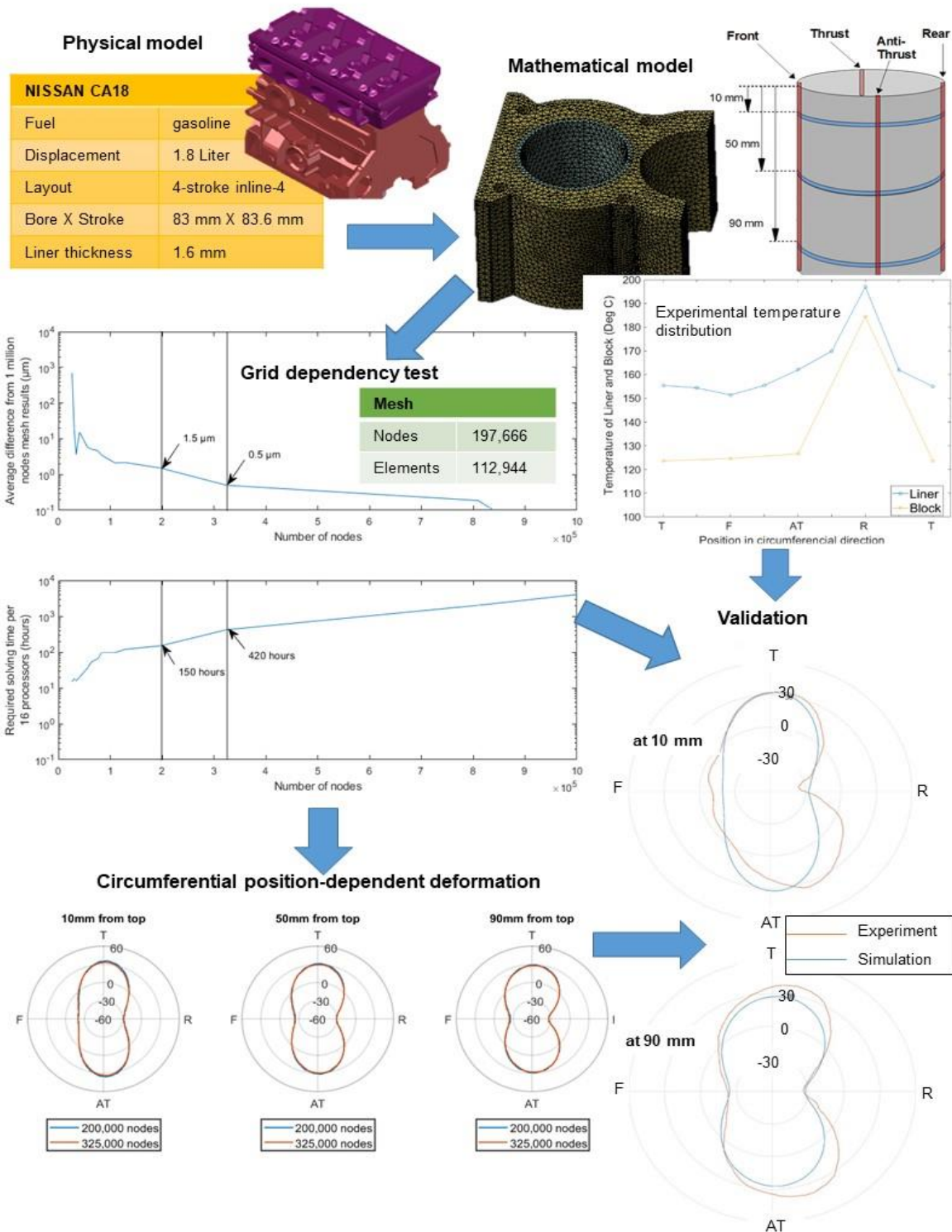


Figure 2.1: Physical and mathematical models for gasoline engine

The results show that non-circular liners have a lower roundness error than conventional circular liner under typical operational conditions. The elliptical (EL) liner reduced the roundness error by 75% and 85% at the top and bottom of the liner, respectively. This reduction indicates a significant improvement in the PRCL conformation and therefore, better engine performance. The non-symmetrical ellipse (NSE) and half circle-half ellipse (HCE) reduce the roundness error between 25% - 30%. Figure 2.2 presents the main findings of the paper.

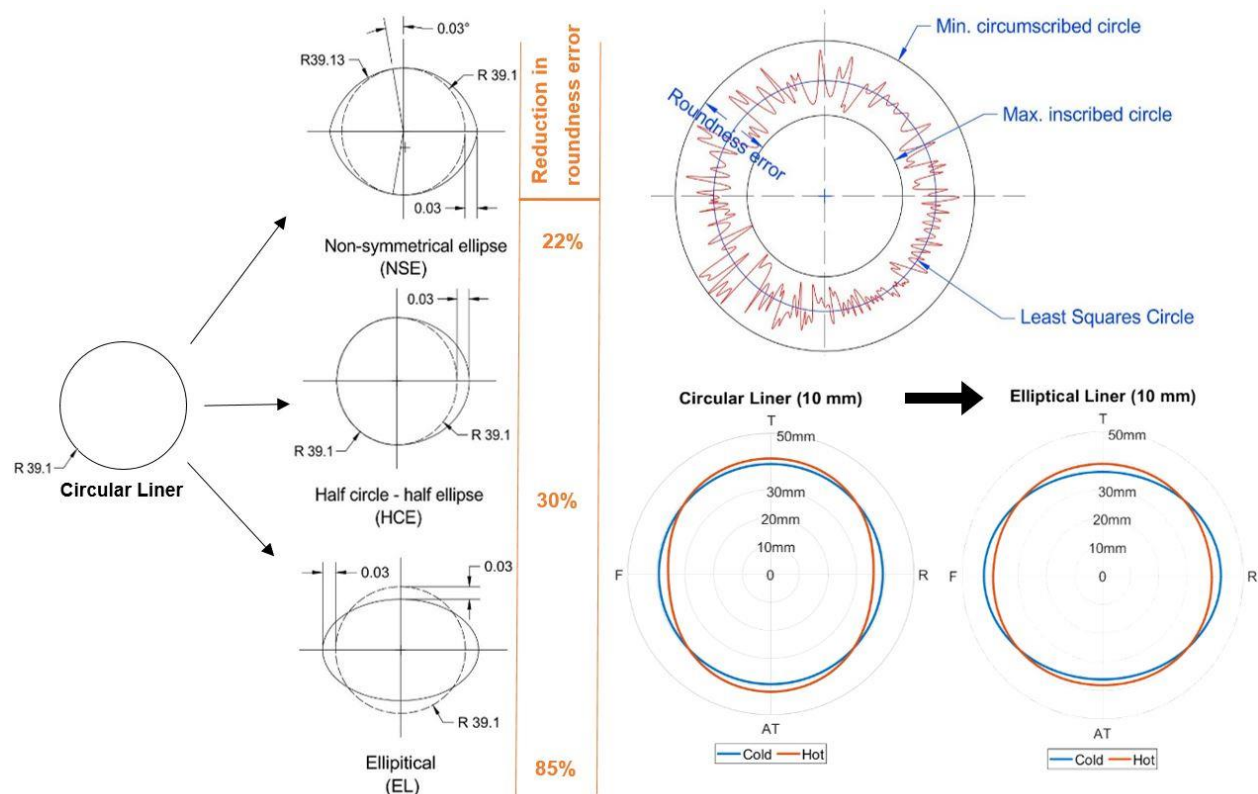


Figure 2.2: Summary of paper I main results

The reduction in the roundness error for the EL case is much greater than for the other two cases; HCE and NSE. For this reason, the last two have not been analyzed further. The focus on the elliptical cross section can be justified not only by the significant reduction in the roundness error achieved but also by its simplicity, which will require a less complicated honing technique compared with the other freeform honed liners.

The analysis in this paper focused on the radial deformation in the circumferential direction at three specific levels; 10 mm, 50 mm, and 90 mm. These three levels were selected to indicate the top, middle and bottom of the liner respectively. However, the values of the roundness error in the hot state vary at those levels even when the engine was started with a prismatic liner in the cold state. This variation between the top and

the bottom reaches more than 40% in the elliptical (EL) liner. This indicates the radial deformation in the longitudinal direction should be analyzed too. This will be the scope of paper II.

2.4. Paper II

Paper II is entitled “*Enhancing the Geometrical Performance Using Initially Conical Cylinder Liner in Internal Combustion Engines—A Numerical Study*”. The main hypothesis in this paper is that starting the engine with a suitably formed conical liner in the cold operational state can lead to a liner with a nearly cylindrical profile in the hot operational state. The cylindrical profile includes straighter and more parallel walls. This will enhance the piston ring – cylinder liner conformation and lead to a more efficient engine. To test that hypothesis, the deformations of various straight and conical liners were determined numerically using the validated gasoline engine model under typical engine operation conditions. Geometrical performance indicators were developed to quantify the cylinderness parameters of different liners. Finally, a comparative analysis was performed.

Firstly, the validated simulation model presented in “paper I” was used to numerically calculate the deformation of the cylinder liner in the hot operational state. Then, the simulated local bore distortion was subtracted from the originally cylindrical liner shape in order to shape conus liners in the cold state with different cross sections. Liner deformations for these modified liners were simulated and compared with the conventional cylindrical liner.

Four liners were considered in this comparative analysis; the conventional circular liner, the prismatic elliptical liner, a conical shaped circular liner, and a liner with both a conical and elliptical shape in its cold state. The elliptical cross section was selected because of its potential to reduce the roundness error in the hot operation state as shown in “paper I”. The selection of taper angle for the conus liner was based on reversing the angle resulting from the deformation of an initially cylindrical liner. It was formed with a 5 μm increment of the lower liner bore radius compared with the upper bore radius. There is a general agreement between this design and the known shapes of non-prismatic liners used by some manufacturers.

The deformations of all liners were numerically simulated at one selected operation condition; 4000 rpm/ full load, at the main sides of the liner; the thrust, anti-thrust, front, and rear sides. The results show that the conus liners with the right initial increment deform to a better parallel and straight shape in the hot operation state. For all liners, the section in thrust – anti-thrust orientation was straighter and more parallel than the section in front – rear orientation. This is mainly due to symmetrical cooling boundary

conditions in the thrust – anti-thrust orientation, while in the front – rear orientation, the adjacent cylinder supplies additional heat to the rear side.

Three geometrical indicators were defined to compare the geometrical performance of the four liners. The first is the roundness error that is based on the least squares circle method as defined in “Paper I” above. It represents the change in bore radius in circumferential direction and was calculated at the top, middle, and bottom of each liner. The second is the straightness error, which represents the change of the bore radius in the axial direction. It equals the minimum distance between two straight lines that contain all the deformed points of a specific side of the liner bore. It was measured at thrust, anti-thrust, front, and rear sides of each liner.

The last indicator is the parallelism error, which is calculated as the difference between maximum and minimum distances between points at identical elevation on two lines facing each other, see Figure 2.3. The parallelism error represents the change of diameter over length, and thus shows the change in the bore tightness in a certain orientation. The maximum value of the parallelism error between two lines should not exceed the summation of the straightness error of those two lines. The reason for using both straightness and parallelism errors in this work is to predict the closeness of the liner’s wall to the required straight parallel shape, as the parallelism error alone cannot predict the existence of parallel curved walls.

The results show that conus liners have better straightness and parallelism. Conus liners reduced the parallelism error by more than 60% in thrust – anti-thrust direction and up to 70% in front – rear direction compared to the prismatic cylindrical liner. In terms of straightness error, the conus liner reduced it by up to 65% on thrust and anti-thrust sides, and up to 50% on the front and rear sides. Furthermore, combining the conus liner concept with an elliptical liner cross section shows performance improvement in roundness, straightness, and parallelism of the liner bore. This makes the conus elliptical bore shape a promising competitor and will be considered in further analysis. Figure 2.4 presents the main findings of the paper.

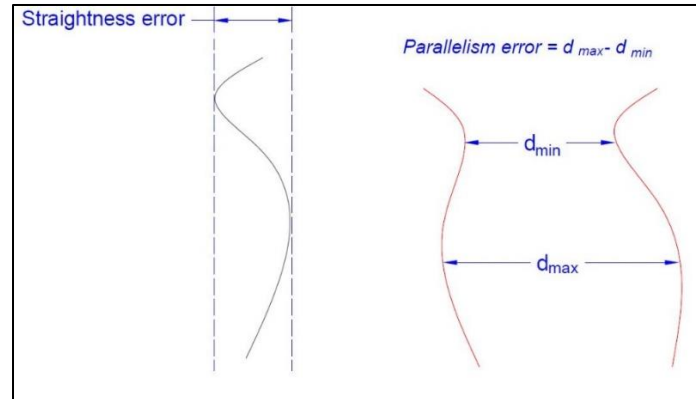


Figure 2.3 Geometrical performance indicators

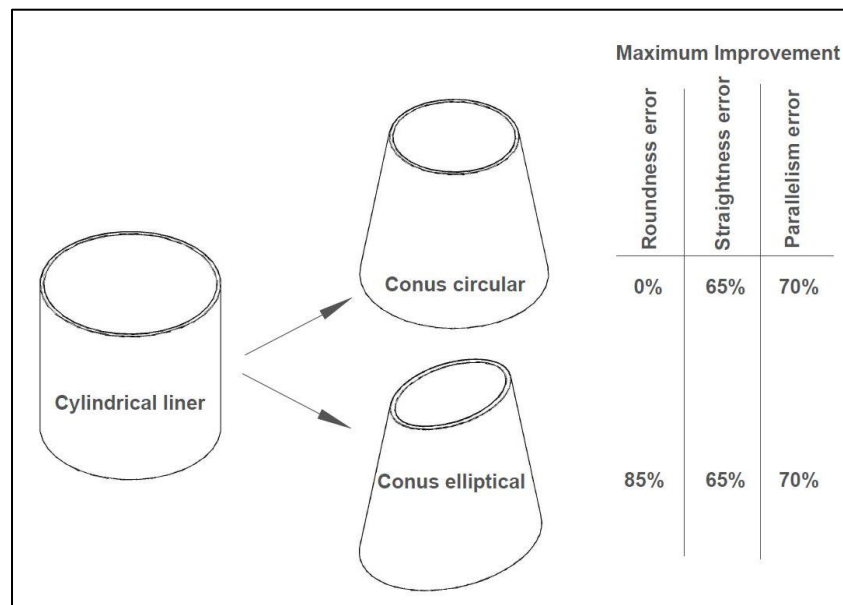


Figure 2.4: Summary of paper II main results

It is expected that the deformation at the top of the liner is higher than the lower part as the heat supply from the combustion gases to the upper part of the liner is higher. Therefore, increasing the liner diameter in the bottom half would lead to a straighter liner wall in the hot operation state. However, the straightness of the wall is not the only reason that led some of the engine manufacturers to increase the liner diameter in the bottom half compared with the top. Increasing the liner diameter in the lower part will lead to less contact between the liner walls and the piston skirts. This means less friction and less mechanical energy loss and therefore better engine efficiency. Furthermore, it increases the lubricant oil thickness for the upper two piston rings as it allows more oil feeding for them. At the same time, keeping a tight liner diameter in the top part is

necessary, to reduce the piston slap force due to its secondary motion. Moreover, a good compression ring sealing will be essential to avoid the blow by and the loss of combustion pressure.

However, an excess increase in the liner diameter in the bottom part or tightness of the upper part can have a catastrophic impact on the engine performance. Therefore, it is important to select a suitable taper angle that is safe for the whole engine's operation points. So the analysis was done for multiple operational points in the further works (paper III and paper IV). Another interesting question is whether the straight wall liner in the hot operation state is the optimal or if there is a better shape. This question will be considered in the experimental work section at the end of this chapter.

2.5. Paper III

Reaching the required round liner bore cross section in the hot operation state starting from a non-circular liner in the cold state requires a deep understanding of the liner bore deformation and deformation trends. That was the reason behind paper III, which is entitled "*Cylinder Liner Deformation – An Investigation of its Decomposition Orders under Varied Operational Load*". The paper discusses the variations trends of each deformation order over liner's depth and engine operational points. This knowledge is essential to understand the PRCL coupling behavior in the hot operational state, in order to enhance its geometrical performance. To answer this research question, first, deformations of a circular liner were numerically simulated at three operational points, namely; 3000 rpm, 4000 rpm, and 5000 rpm at full load. The validated simulation model for the NISSAN engine was used for this purpose. Then the simulated deformations were analyzed analytically using Fourier decomposition to determine the variation trends as explained in section 1.5.

The results show that the second order deformation is dominating the liner deformation, regardless of the operation point. This order of deformation is a function of the operational point; i.e. increasing the load increases the second order deformation. This is expected as this order of deformation is directly related to the thermal and mechanical operational load. Furthermore, this order of deformation slightly decreases with elevation increase as the thermal load decreases in this direction. Note that elevation (or depth) increases in the direction toward the bottom of the liner as shown in Figure 2.1 above.

The fourth order is the second largest contributor in the total liner deformation. This order of deformation is less sensitive to the operational point. However, its value decreases significantly with elevation increase. This order of deformation is mainly related to the bolt pre-tightening and the constraining conditions of the cylinder liner.

The first order deformation is the least contributor to the total liner deformation. It represents the eccentricity of the liner bore. It increases with the increase of operational load and elevation.

Third order deformation is related to unsymmetrical thermal load. It increases as this asymmetry increases. Therefore, it is clearer in the terminal cylinder compared to intermediate cylinders. Also, it reaches its minimum value in the middle of the cylinder liner as the unsymmetrical temperature gradient is the lowest here. The slope of the third order deformation in the upper half of the liner is sharper than in the lower half. This indicates larger temperature gradients in the upper half. The third order deformation has an indirect relation with the operational load; when the load increases, the asymmetry increases. Figure 2.5 presents the main findings of the paper.

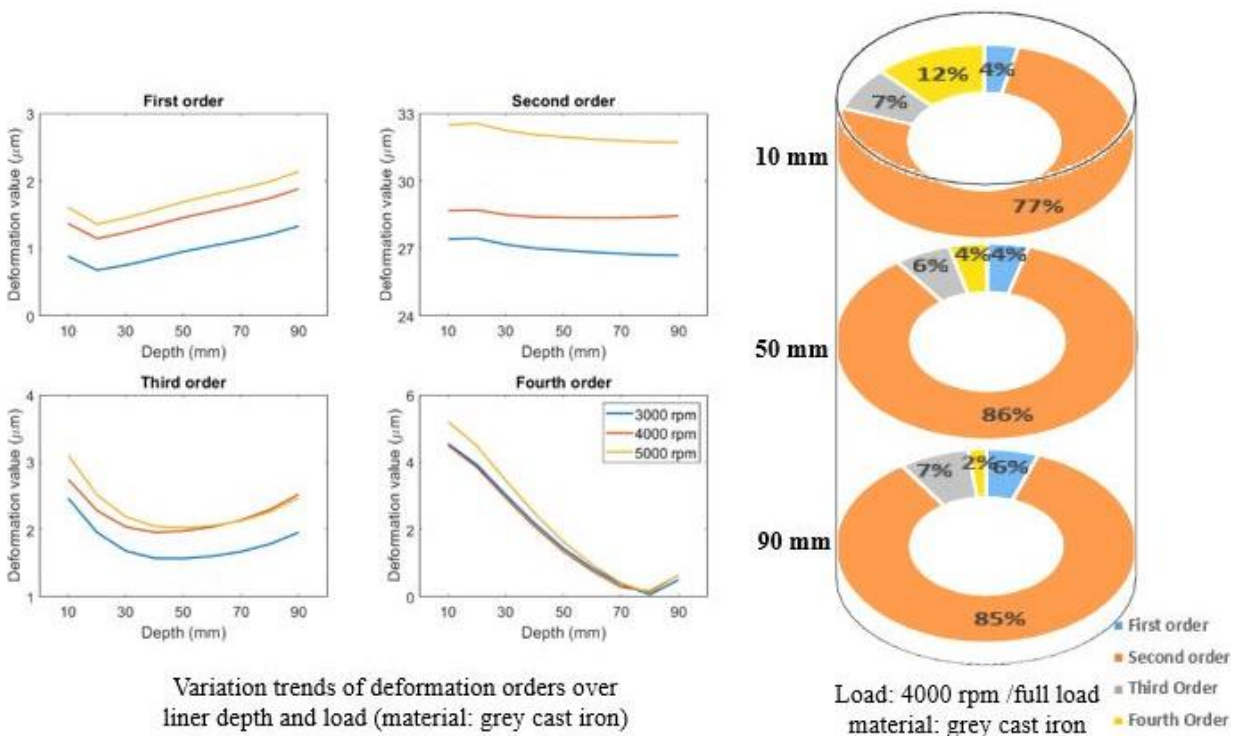


Figure 2.5: Summary of main results of paper III

To make sure that this deformation pattern is independent of the liner material, the grey cast iron liner used in the upper analysis was replaced by an aluminum liner. The same methodology was implemented for the new aluminum liner. It was found that although the deformation values differ, the pattern and trends of the deformation order is almost the same as for the grey cast iron liner.

The above analysis and findings can significantly help in improving the cylinder liner bore design by utilizing a freeform liner bore shape that deforms into a circular bore during

engine operation. This freeform shape can be seen as a sequence of harmonic shapes that can be applied to the liner through recently advanced honing techniques. As some of the liner deformation orders depend on the operational load, this methodology can be seen to be especially effective for engines that work for a long time at a single operational point, like generators and ship engines, and eventually for some transportation vehicles engines.

The findings of this paper agree with existing cylinder liner literature. The domination of the second order deformation and the significance of the fourth order in total liner deformation is shared by other researchers who also recognize the insignificance of the higher deformation orders [29,44]. Furthermore, some of their results show that the third order deformation is clearer in the terminal cylinders compared with intermediate cylinders [29]. Additionally, in "Paper I" it was shown that starting the engine with an elliptical liner bore can reduce the roundness error up to 85%. This can be explained by the results of this paper that found the second order deformation is dominating the liner deformation. The second order deformation represents the elliptical shape as shown in Figure 1.3.

The difference in the deformation value between the grey cast iron liner and the aluminum liner is also worth investigating. It is definitely related to the different material properties, and mainly to the thermal properties. However, detailed analysis will be implemented to check the impact of thermal and mechanical material properties on the geometrical performance of the liner. This is included in the scope of Paper V.

Another important question coming from this analysis is, how to select the operational point for the freeform honed liner design and what will be the impact on the liner performance if a liner operates at load other than the one that's liner bore was reversed according to it? For example, if the deformation of 4000 rpm / full load was selected to design the honed freeform shape of the liner for a specific engine, how will the engine perform when it operates at 3000 rpm / full load or 5000 rpm / full load. This research question will be investigated in paper IV.

Another useful finding in this paper is that the fourth order deformation is a static load, which means that it is independent of the operational load. This indicates that it could be considered in any freeform honed liner regardless of the design operational point. This fourth order deformation was recognized in the literature with its large effect on lubricant oil consumption [36]. This means that eliminating this order of deformation is expected to decrease the lubricant oil consumption.

2.6. Paper IV

Paper IV is entitled "*Effect of Freeform Honing on the Geometrical Performance of the Cylinder Liner – Numerical Study*". The main objective of this paper is to show the

geometrical improvement achieved by using a freeform honed (TR) liner compared with other investigated shapes of the liner bore. The freeform honed liner concept is based on the approach of reversing the local deformation of a conventional circular liner. The main hypothesis here is that this type of honed liner bore will significantly improve the geometrical performance of the cylinder liner in the hot operational state. This will be followed by a significant improvement in PRCL conformation and the whole engine efficiency. The methodology followed in this paper is quite similar to the previous papers. However, the scope of investigation is broader.

The validated gasoline simulation model is used to numerically calculate the local bore deformations of a conventional circular-cylindrical liner at three operational points; 3000 rpm/full load, 4000 rpm/full load and 5000 rpm/full load. The TR liner bore shape is designed based on reversing the local deformations of the cross section at the reference load. Then the designed liner is simulated using the operational load, see Figure 2.6. The reference load can be similar to the reference load or both loads can be mixed. Additionally, three non-prismatic optimized (Opt) liner bore shapes are designed based on reversing the average liner local bore deformations of all considered operational points. Moreover, the predefined elliptical (EL) liner from paper I and the conus elliptical liner from paper II were considered here too.

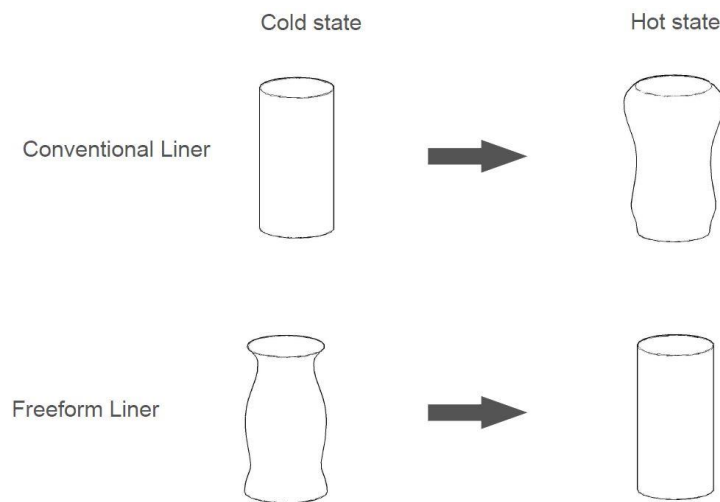


Figure 2.6: Freeform liner solution to enhance the geometrical performance of the liner

These non-circular liners are then simulated and their deformation in the hot operational state is numerically calculated. It was found that the TR cases give almost a circular cross section in the hot operational state when the operational load is similar to the reference load. They reduce the average roundness error by up to 95% compared to the circular liner. Furthermore, in these cases, the liners have straighter walls in the hot operational

state with the straightness error reduced up to 75% compared with the circular liner. This indicates a significant improvement in PRCL conformation and therefore improves the overall engine performance.

EL and NEL deform to a rounder cross-section compared to the circular liner. They reduced the average roundness error by up to 87%, which makes them a competitive alternative to the TR liner as they have a less complicated shape. In terms of straightness error, the EL liner does not provide much improvement, while the NEL liner improves the straightness error by up to 64%. However, the NEL liner shows a wider diameter in the hot operational state compared with TR liners.

When a TR liner is used for an operational load less than its reference load, it leads to a reduction in the diameter in thrust – anti-thrust direction and increase in the diameter in front-rear direction. This can be justified as the mechanical and thermal loads at a lower operational point are not able to cause enough deformation to compensate for the pre-deformed liner that was designed based on a higher operational point. Even the reduction in the diameter in these cases is less than the reduction in the diameter in the case of the circular liner, one can conclude that operating a TR liner at an operational load less than its reference load decreased the potential enhancement that can be achieved by using a TR liner.

On the other hand, when a TR liner is used with an operational load higher than its reference load, a good tribological performance is expected as there is no noticed reduction in the liner diameter. Nonetheless, in both cases, i.e. a TR liner operates at a higher or lower than its reference load, a significant reduction in the roundness and straightness error achieved. The average roundness error is reduced by 75% when a liner designed at a reference load of 5000 rpm/full load is operated at 3000 rpm/full load. In the opposite case, i.e. a TR liner designed at a reference load of 3000 rpm/full load operates at 5000 rpm/full load, the average roundness error decreased by 90%. The straightness error varies in the range of 5% when the reference load is not similar to the operational load.

The Opt liner shows the same pattern as the TR liners with mixed load. It also reduces the roundness error by 82%, 91%, and 94% when it operates at 3000 rpm/full load, 4000 rpm/full load and 5000 rpm/full load respectively. Furthermore, it reduces the straightness error by 61%, 64%, and 69% for the same operational point respectively.

The figures also show that the remaining deformation orders when using TR liners at operational load other than its reference load is a pure second order deformation. The fourth order deformation is eliminated completely, which implies a better sealing

capability for the piston ring. Third and first orders of deformation are also compensated as the differences in their values are less than $1\mu\text{m}$ between the maximum and minimum operational points. Being a pure second order deformation with a smaller value compared to the circular liner indicates that the piston ring elasticity can absorb it with ease as indicated in literature. Figure 2.7 summarizes the main findings of the paper.

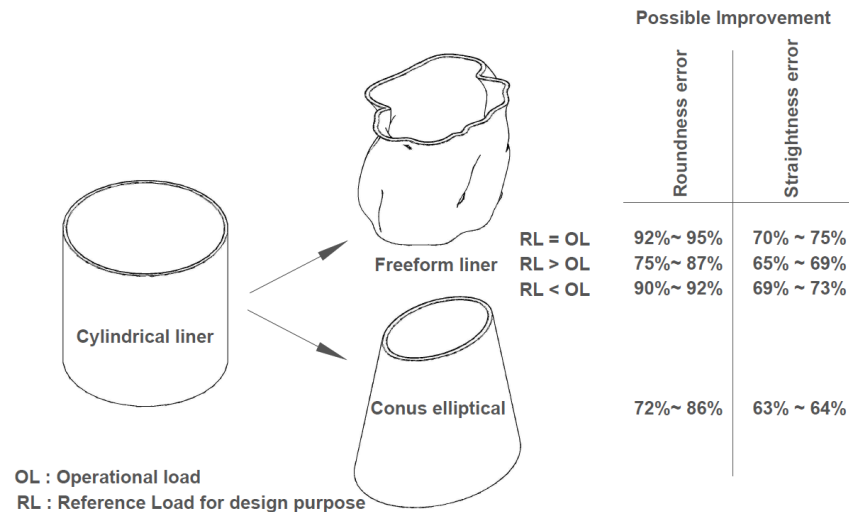


Figure 2.7: Summary of paper IV main results

The results of this paper raise two important questions. First, it was mentioned that the performance enhancement achieved by the TR liner may be lowered if it is used for operational points less than its reference load. The cold start represents the extreme case for operating the liner at a lower operational point. Based on that, one can ask if it is possible that the freeform honed liner gives negative results in the cold state, and consequently, during the startup procedure of the engine, especially for the cold start?

The total friction reduction that could be potentially achieved by using TR liners must be found based on detailed calculations that take into consideration the total engine running cycle, the frequency and the duration of each operational point, frequency and duration of different engine operational conditions, etc. This means that friction increasing during the startup stage might be compensated by a major friction reduction in the other engine running stages. Furthermore, fourth order deformation exists in the cold state. Eliminating this may reduce the negative effect of using a TR liner in the cold state. Additionally, the tolerance between the piston and the liner in the cold state will also contribute to the cold start problem reduction.

The second question is: does the freeform honed liner interfere with the piston expansion during the hot operation state? It seems to be a reasonable assumption that the piston keeps its circular shape in the fired state [19]. Increasing the roundness of the cylinder

liner in the hot state makes it more compatible with the piston's circular shape. Therefore, if the piston clearance is maintained in the hot state, better liner roundness will lead to better PRCL coupling.

Finally, one important aspect shall be discussed based on the presented results. The suggested methodology shows that it is possible to reach the cylindrical liner bore shape in the hot operational state by applying a specific freeform honing in the cold state. This implies that it is possible to achieve any other desired liner bore shape in the hot operational state by applying a suitable freeform honing. Figure 2.8 presents an example of a proposed liner design. The target hot state shape in this example has a tight diameter in the upper part of the liner to prevent the piston slap, a large diameter middle part of the liner to enhance the lubricant oil feeding and an intermediate diameter at the bottom of the liner to decrease the friction while preventing any secondary movement of the piston. However, in all parts of the liner, the round cross section should be maintained in the hot state.

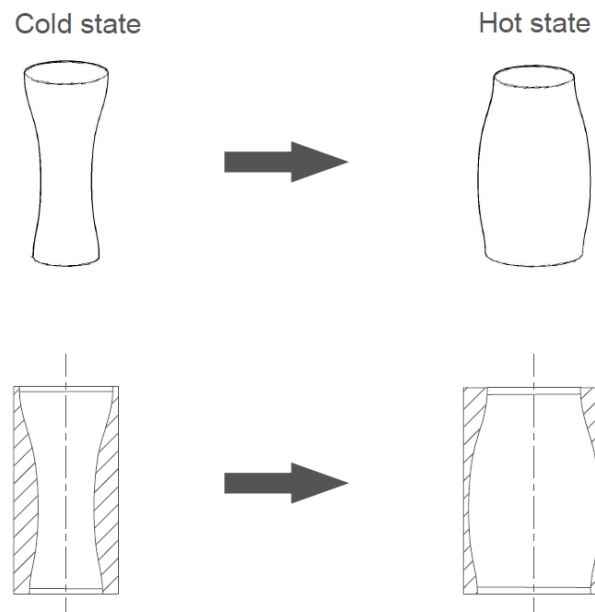


Figure 2.8: Proposed freeform liner design to enhance the geometrical and tribological performances of cylinder liner

Knowing that any liner bore shape can be targeted in the hot operational state, the applied freeform honing can be adjusted to compensate for many other variables such as cold start, manufacturing limitations and piston expansion. As a starting point for experimental work, the hot state radius of any initially non-circular liner should not be smaller than the one for the initially circular liner. Moreover, it is possible to target different hot state radii at different elevations for a better tribological performance [31]. This point will be further discussed in the experimental work section.

2.7. Paper V

Additive manufacturing technology has gained more attention in the engine manufacturing industry. AM technology's ability to freely shape complex parts is one of its main advantages. By using AM techniques, non-traditional liner cross section can be achieved to improve the geometrical and tribological performance of the liner and therefore, enhancing the engine efficiency. Paper V, "Structural performance of additively manufactured Cylinder Liner – A numerical Study", aims to investigate the compatibility of additively manufactured materials for the fabrication of cylinder liner from a structural and geometrical perspective. This is important in order to be able to use the additive manufacturing (AM) technologies in engine development in order to improve its design and performance.

The validated computational FEM model of the gasoline engine was used to numerically simulate the deformation of liners made of five different AM materials. If the deformations of these liners are comparable to the grey cast iron, this gives an indication that possibly no failure due to structural thermal deformation has to be expected. In this case, the thermal stresses will not cause an excess deformation that leads to excessive friction, blow-by or lubricant oil leakage. Further, geometrical performance can be measured using the geometrical indicators to check the potential improvement.

The five AM materials that have been considered in this paper are Inconel 625, Inconel 718, 17-4PH stainless steel, AlSi10Mg, and Ti6Al4V. Their mechanical properties are presented in the paper. It is worth to mention that the thermal expansion coefficient for those materials is in the range of 10 – 13 $\mu\text{m}/\text{m}^\circ\text{C}$ except for AlSi10Mg where the thermal expansion coefficient is almost the double; 23.6 $\mu\text{m}/\text{m}^\circ\text{C}$. This means that it is expected to have almost a double value of the deformation for this material compared to the others. The simulation results show that there was no structure failure due to the thermal and mechanical stresses in the liner. Additionally, the maximum deformation of all liners is within the ranges known in the field. Some of the materials like Ti6Al4V decreased the maximum deformation more than 30%, which indicates its competitiveness as cylinder liner material if the cost issue would be solved.

To investigate the geometrical performance of the AM liners, roundness error and straightness error were used. The results show that Ti6Al4V and 17-4PH have a significant improvement in roundness compared to grey cast iron. The use of Ti6Al4V reduces the average roundness error by about 30% compared to grey cast iron. However, the lower side of the liner in the case of Ti6Al4V has a higher roundness error compared to the top of the liner. AlSi10Mg increases the roundness error significantly as it deforms more than the others. In terms of straightness error, Ti6Al4V reduces the straightness error to half except on the rear side where the straightness error increases even more than for the

grey cast iron. These results show that AM materials can be used as an alternative to conventional grey cast iron material in liner manufacturing from the structural point of view, and therefore the AM technology might be utilized to manufacture the cylinder liner. However, other aspects must be investigated, such as residual stresses, structural local inhomogeneities, the manufacturing process of the liner, etc.

Additive manufacturing technology can help in developing the liner design. One potential improvement can be achieved by applying a cooling system inside the liner walls that takes the heat from the high temperature points in the liner (like the top of the liner) and dissipates it into the points with low temperature (like the bottom of the liner), see Figure 2.9. By that, the liner deformation can be controlled in order to get a rounder liner shape in the hot operational state or to reach a certain liner bore shape in order to enhance the tribological performance of the PRCL coupling. This can be an outlook for future development and research.

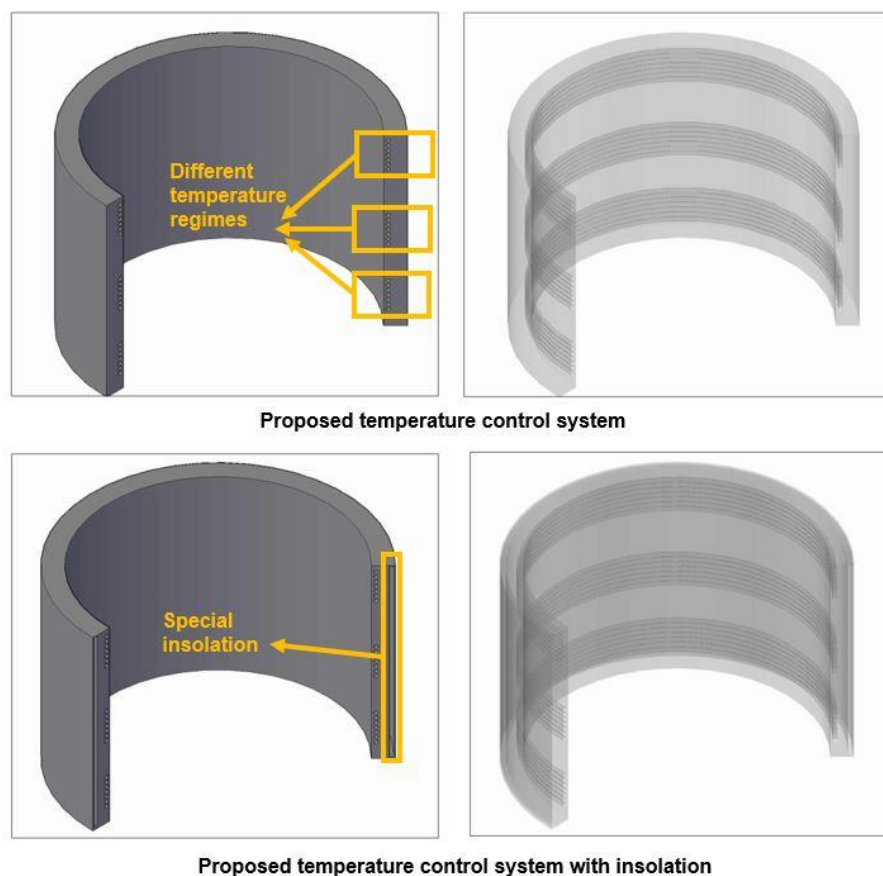


Figure 2.9: proposed temperature control systems for cylinder liner

The previous results show that there is a strong relationship between the cylinder liner's material and its deformation values and patterns. Koch et al. indicates that fourth order

deformation increases in weaker materials due to lower Young's modulus and higher thermal expansion coefficient [14]. This would be the case for AlSi10Mg. On the other hand, it seems that Ti6Al4V, which is considered as a strong material with low thermal expansion coefficient, has a higher first and third order deformation. This could be the reason for increasing the roundness error on the bottom of the liner (high eccentricity), and increasing the straightness error on the rear side (unsymmetrical heat supply). This could be an outlook for future investigations.

To investigate the material properties impact on the liner deformation and its geometrical performance, a study was implemented by a master student under the supervision of the candidate [82]. The detailed results that were published in the master thesis are not included in this cumulative thesis. However, summarizing some of the main findings will help to understand the results of paper V.

The study analyzed numerically the impact of the thermal expansion coefficient, young's modulus, Poisson's ratio, and thermal conductivity on the liner deformation and geometrical performance. It used the FEM simulation model for the gasoline engine. The effect of each material property is analyzed by changing it gradually while fixing all other properties and boundary conditions. The results show that the thermal expansion coefficient has the largest effect on the liner deformation and its geometrical performance. Increasing Young's modulus and thermal conductivity will slightly increase the liner deformation and the roundness error. The relation between Young's modulus and the deformation is linear, which is also in accordance with Hook's law. The change in Poisson's ratio shows no effect on the liner deformation.

2.8 Paper VI: Experimental validation

In order to test the approach suggested in this work, an experiment was planned using the single cylinder floating liner test rig in ITV. To prepare that, a simulation model was built based on the physical model of the engine test rig. The local deformation was then numerically calculated using developed advanced FEM techniques. These deformations were used to design three freeform honed shapes for the liner. One of these shapes was manufactured and tested experimentally for the improvement in friction and blow-by. (Due to problems with the manufacturer and limited rest time within the project Antriebsstrang2025 the other two options could not be produced.)

The physical model is based on MTU-Series 2000 single cylinder diesel engine test rig with a bore of 130 mm and stroke of 150 mm. It was provided with special housing that contains the floating liner system [83,84]. Despite being a test rig, the cylinder liner is closed to the series one in terms of the coolant jacket design. The floating liner itself is a

wet liner with a wall thickness of 8.1 mm in the top and 9.6 mm in the middle with a total height of 240 mm. It is provided with a slot for the hydrostatic bearing at the top and a built-in flange at the bottom. The piston is equipped with two compression rings above on oil control ring [69,83].

The simulation model was carried out on a simplified geometry following the methodology suggested by [65], in which some of the engine elements were replaced by forces/constraints to simplify the model. The simulation is done for an operational point at 1300 rpm and a load of 15.5 bar mean effective pressure. The temperature distribution for this operation point was measured experimentally. The simulation is done at a crankshaft angle equal to zero, in which the piston is at the top dead center in the third stroke and the cylinder pressure has a value of 112 bar. The hydrostatic bearing applies a pressure of 37 bar in its four pockets. The temperature of the coolant in the jacket is maintained at 80 °C.

An adaptive meshing technique was adopted and the final optimum mesh has 501,056 elements and 321,618 elements. Grid independency tests were performed at different adaptive mesh sizes and the results show that the simulated deformations are independent of mesh size. That model was again solved using a direct coupled approach. In this approach, the mechanical and thermal matrices are solved simultaneously. To solve this model, 160 cores with a maximum of 1.5 GB of RAM/core were used. The solving time was more than 150 hours. Figure 2.10 summarizes the main aspects of the physical and computational model.

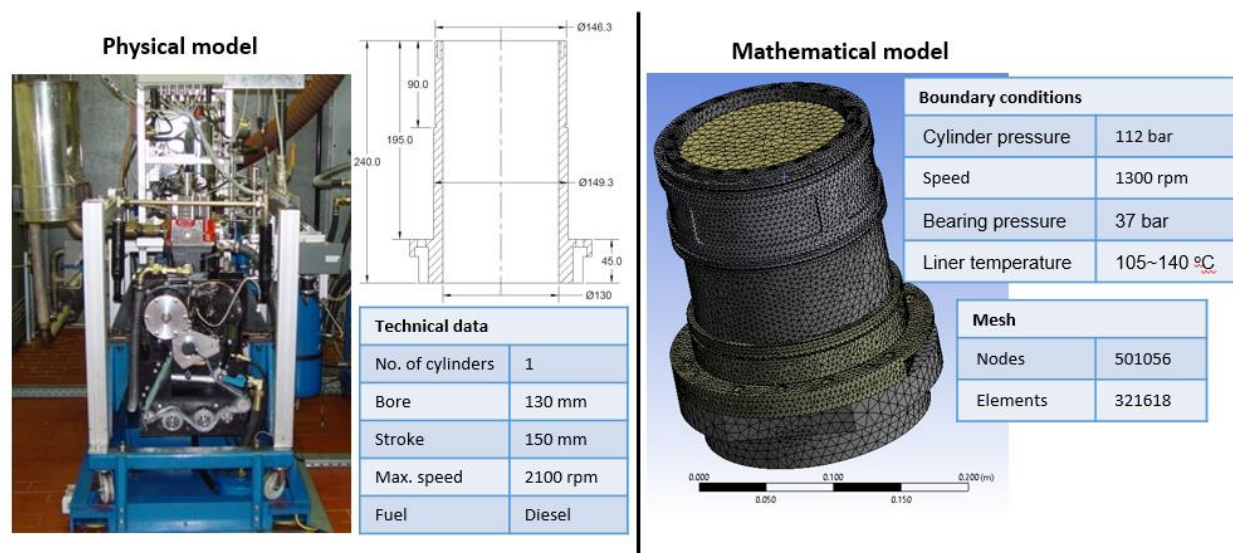


Figure 2.10: Main parameters of physical and computational models for a single cylinder floating liner diesel engine (left photo is taken from ITV website)).

To validate the model, an experiment work was implemented to measure the liner deformation using strain gauges in the hot operation state. The strain gauges were located at specific points at different levels and directions. The strain gauges were oriented such that they could measure the hoop strain. Using the hoop strain, the radial deformation can be calculated. The measured deformation at these points show a good agreement with the simulation results.

The maximum liner radial deformation was in the range of 100 μm at the top of the liner in the outward direction. The hydrostatic bearing pressure limits the radial expansion of the liner and reduces it to 40 μm at 50 mm elevation. The flanges constrain the outward expansion of the liner and cause a reduction in the radius in the range of 30 μm at 180 mm elevation. The Fourier analysis indicates a homogenous thermal distribution around the liner as the zeroth order is dominating the deformation. This indicates that the liner expands while keeping a considerable roundness. Another evidence of a homogeneous thermal distribution is the disappearance of the third order deformation over most of the liner length. The effect of the hydrostatic bearing is obviously in the upper part of the liner as the contribution of the fourth order deformation to the total liner deformation exceeds 15%.

In good agreement with the harmonic analysis, the roundness error values were relatively small compared to the value of the maximum deformation. The majority of the roundness error in the upper part of the liner are related to the fourth order deformation. On the other hand, the straightness error is large as the liner deforms upward at the top and inward at the flanges location. The values of the straightness error are comparable to each other on all four main sides of the liner. Figure 2.11 presents some of the main findings of the simulation.

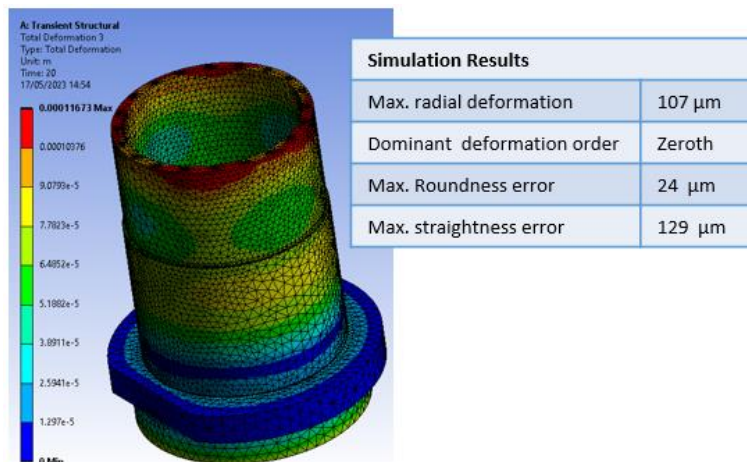


Figure 2.11: Simulated deformation results for floating liner

Based on the simulation results, a freeform liner shape was designed based on Gehrings totally reversing approach by subtracting the local liner deformations from the originally cylindrical liner in the hot operational state. This will be denoted as variant 1. However, this design approach suffers from some shortages. In this approach, the liner is pre-deformed in a cold state in order to reach a cylindrical liner with a radius of 65 mm in the hot state. This requires a reduction in the liner radius in the cold state by more than 100 μm at some points. This will exceed the piston-liner clearance (clearance = 65 μm in cold state). Further, the piston expands under the fire condition and the experimental measurements show a maximum increment of 60 μm in the piston radius during fire operation. In order to overcome those two shortages, the bore radius of the liner in the cold state was increased by 65 μm before applying the reversed pre-deformation freeform honing. Therefore, the liner will deform to a cylindrical bore in the hot state with a radius of 65.065 mm. This will be denoted as variant 2.

Another possible improvement to enhance the tribological performance of the liner is tightening the liner at the upper part. This will increase the sealing of the compression ring and keep the cylinder pressure inside, which enhances combustion efficiency. Further, it will reduce the piston secondary movement at the top dead center, which will reduce friction significantly. However, attention should be given to avoid negative piston clearance in both cold and hot state. For that, a bottle shape liner is targeted in the hot operation state with a radius of 65.055 mm at the top 20 mm and a prismatic radius of 65.065 from 60 mm and below. This will be denoted as variant 3.

A final possible improvement is to increase the oil film thickness (h) through increasing the lubricant oil flow through the oil control ring to the two upper rings. This will reduce the shear stress (τ) in the hydrodynamic lubrication regime. To achieve that, a further increase in the liner radius is targeted in the middle part of the liner; starting from 80 mm to 200 mm, the target liner radius is 65.1 mm. However, to reduce the possible piston secondary movement in the bottom dead center, a radius of 65.04 mm is targeted in the lower 20 mm of the liner. With the tight upper part of the liner discussed in variant 3, the final shape of this variant is a mix between a bottle and a barrel liner bore shape. Such a shape has never been proposed in literature before. This variant is denoted by variant 4. Figure 2.12 gives a visual representation of the four variants.

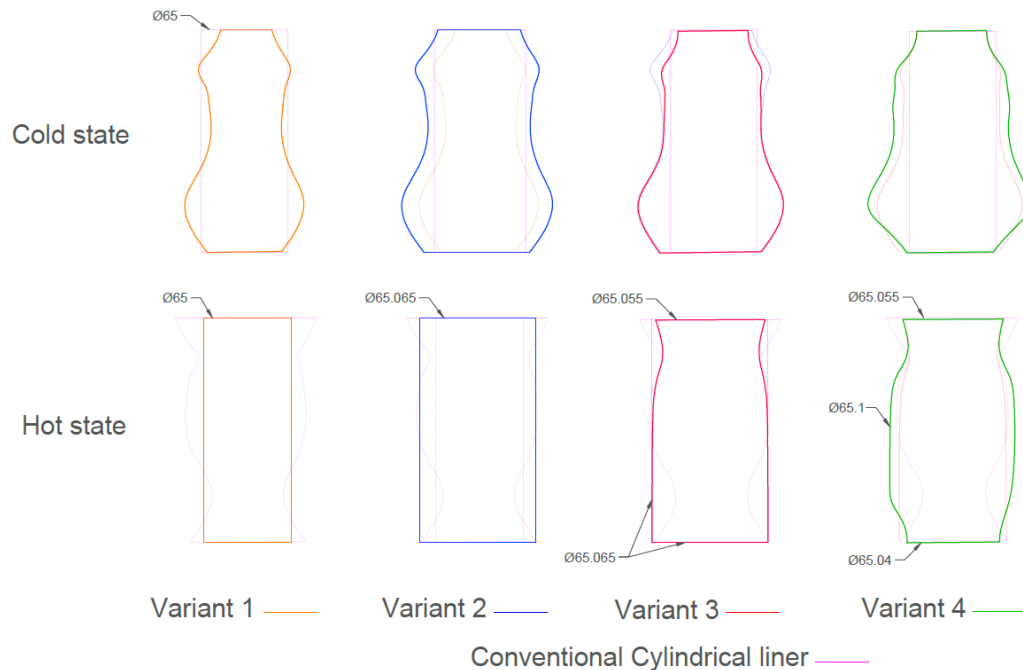


Figure 2.12: The proposed floating liner designs. Dimensions are in mm

Variant 3 was manufactured within the research project "Antriebsstrang 2025", using resource efficient process chain approach. The processing contains a piezoactuated hybrid tool for non-circular turning and micro-structuring. Further details about the liner manufacturing can be found in [85,86]. The freeform honed liner was tested using the single cylinder floating liner test rig. The results show that 17% of friction saving can be achieved compared to the conventional cylindrical liner [80]. The details of these experimental results will be prepared by the experimental group in ITV and included in the paper. Later, more details can be added here. The paper is planned to be submitted before the final printed version of this thesis.

Even without these details, this combined numerical and experimental work shows already clearly, that the aim of this thesis with this inverse engineering approach for the shaping of the cylinder liner has found already very impressive confirmation.

Chapter three: Conclusion and recommendation

Improving the efficiency of internal combustion engines is of great interest for sustainable development and greenhouse gas emission reduction. A great potential is seen in improving the piston ring – cylinder liner (PRCL) coupling. As the thermal load during the fired state of the engine causes the liner to deform, more tightness is required so far for the piston ring to conform to the cylinder liner in order to keep its sealing functionality to reduce blow by and lubricant oil consumption. This additional tightness increases the friction and therefore, reduces the engine efficiency and increases emissions. A good solution for this dilemma is to change the shape of the liner from the strictly cylindrical shape in the cold state, being common so far, to an advanced shaped liner.

This work addressed seven research questions and suggested fourteen hypotheses, to find answers to these questions. To test these hypotheses, two advanced FEM model were used; one for the terminal cylinder in a gasoline NISSAN CA18 engine, and the other is for the single cylinder floating liner diesel engine test rig, being experimentally investigated within the institute. Both models were validated using experimental data. The FEM models were used to simulate the local liner deformations. Based on that, harmonic analysis was performed to investigate these deformations. Following this analysis, different liner designs and shapes were suggested and implemented. The geometrical performance for these new liners were tested numerically using numerical modeling and developed geometrical performance indicators. One of the liners was manufactured and tested experimentally. A very impressive reduction of the liner friction of up to 17% confirms also from the practical side the success of the overall approach.

Table 3.1 summarizes in detail the results of testing the research hypotheses. Ten of the hypotheses were completely satisfied, two are partially satisfied, while a general conclusion was not possible for the remaining two. The main finding of this work is to show the potential improvement that can be achieved by using non-circular liner and the limitations for this improvement. The results show that a suitable formed non-circular liner deforms in a controlled way such that a circular liner bore in a hot state is possible. The rounder the liner is in the hot state, the better the engine efficiency is. Different variations of unconventional liners were considered; however, the conus elliptical liner has demonstrated great potential for friction reduction in four cylinder engines. Totally reversed freeform honed liners will be extremely efficient, specifically, if the engine will run for long time on one operational point, as in the case of ship engines and electricity generators.

To design an efficient freeform honed liner, harmonic analysis must be performed to determine the dominant order. Then the freeform shape is determined considering the

significance of the orders and the target liner bore shape in the hot operational state, such that better tribological performance is achieved. The analysis in this work shows that one of the limitations of using totally reversed freeform honed liner is the dependency of its performance on the operational point. The freeform honed liners perform better when they operate at a load higher than their reference load compared with other way around. However, the best performance is achieved when the liners operate at their reference load. Nonetheless, an improvement was seen in all cases considered in this study, compared with conventional liners.

The liner material has a significant effect on its geometrical performance. Mainly the thermal expansion coefficient of the material influences the deformation, as the major part of the liner deformation is due to thermal load. Additive manufacturing techniques can be used in liner manufacturing. It was shown that no structural failure is predicted due to thermal load when using AM materials, with regard to the overall material properties. These techniques can be used to improve the liner design. A potential improving example is given in this thesis, addressing an arteries like the cooling system inside the liner walls that takes the heat from the high temperature points in the liner and dissipate it into the points with low temperature. Such system might be able to control the deformation and enhance the tribological performance with less complicated honed liner shapes.

The results presented in this cumulative thesis show a great potential improvement. They present a solid ground to carry out further experimental investigations on the tribological performance of non-circular liners. One of the main challenges is the ability of current manufacturing techniques to provide an accurate honing profile. The technique used to manufacture the liner designed in this thesis was limited to a minimum surface machining depth of 40 μm . Thus the smaller details could not be included. Therefore, the concept of dominant deformation order shall be considered seriously to reduce the complexity of the freeform honed shape. Further investigation should be carried out on the piston ring design for non-circular liners. If a better PRCL conformation can be achieved with non-circular liners, then the piston rings can be redesigned to provide less tension, and therefore less frictional losses.

Table 3.1: Summary of results for testing the research hypotheses.

| Hypothesis | Supported | Paper | Comments |
|------------|---------------------------|------------|--|
| H1.1 | Supported | I, IV, VI | The deviation from perfect circle for the liner cross section decreases significantly when starting the engine with non-circular liner. Elliptical liner reduces the roundness error up to 85% while the freeform honed liner decreases the roundness error up to 95% compared with conventional circular liner. |
| H2.1 | Supported | II, IV | The use of conus liner reduces the straightness error by up to 65% compared with cylindrical liner. This mean the liner is closer to the cylindrical shape in the hot operation state. |
| H2.2 | No conclusion is possible | IV, VI | An improvement in tribological performance was noticed when targeting non – cylindrical liner in the hot operational state. However, manufacturing a freeform liner that deforms into a perfectly cylindrical shape was not possible due to limitations in the available manufacturing techniques. |
| H2.3 | Supported | III, IV | The harmonic analysis shows that second and fourth deformation order decrease towards the bottom of the liner, while the significance of the first order deformation increases in the same direction. |
| H3.1 | Supported | III, IV | The second and third deformation orders increase with the load increase. |
| H3.2 | Supported | IV | Operating the freeform honed liner at operational points other than its reference load decreases its geometrical performance. For example, a liner designed at reference load 4000 rpm / full load improves the roundness by 95%, when it operates at the same load. This value is reduced to 87% and 91% when operating the liner at 3000 rpm and 5000 rpm / full load; respectively. |
| H3.3 | Supported | III, IV | Harmonic analysis shows that fourth order deformation is independent of the operational point. |
| H4.1 | Supported | I, III, IV | Harmonic analysis for the gasoline engine shows that the second order deformation is dominant. The |

| | | | |
|------|---------------------------------------|--------|---|
| | | | roundness values show that an elliptical liner reduces the liner's roundness error in the hot operation state by up to 85%. |
| H4.2 | Supported | IV, VI | Starting the engine with a freeform honed liner that deforms into non-cylindrical shape reduces the friction by up to 17%, as has been shown experimentally for such a shape designed numerically. |
| H5.1 | Partially Supported | VI | Improving the PRCL conformation through the enhancement of the geometrical performance of the liner reduces the frictional losses in the engine. A slight increase in the blow-by values is witnessed experimentally so far. No accurate data about the lubricant oil consumption is available. |
| H6.1 | Partially Supported, partially denied | V | Thermal expansion coefficient has a large influence on the geometrical performance of the liner. Young's modulus influence is relatively low. While no influence was noticed for changing Poisson's ratio and thermal conductivity. |
| H6.2 | No conclusion is possible | III, V | A comparable variation trend for the deformation orders in different materials is witnessed. However, some anomalies were seen too. |
| H7.1 | Supported | V | The deformations of additively-manufactured liners are comparable to the ones of grey cast iron liner. Therefore, no structure failure is assumed. |
| H7.2 | Supported | V | Some additively-manufactured materials, like Ti6Al4V is predicted to improve the geometrical performance, while others like AlSi10Mg would require stronger deviations from the perfectly cylindrical shape in the cold state. |

References

1. Reitz, R.D., Ogawa, H., Payri, R., Fansler, T., Kokjohn, S., Moriyoshi, Y., Agarwal, A., Arcoumanis, D., Assanis, D., Bae, C., Boulouchos, K., Canakci, M., Curran, S., Denbratt, I., Gavaises, M., Guenther, M., Hasse, C., Huang, Z., Ishiyama, T., Johansson, B., Johnson, T., Kalghatgi, G., Koike, M., Kong, S., Leipertz, A., Miles, P., Novella, R., Onorati, A., Richter, M., et al., "IJER editorial: The future of the internal combustion engine," *Int. J. Engine Res.* 21(1):3–10, 2020, doi:10.1177/1468087419877990.
2. Dargay, J., Gately, D., and Sommer, M., "Vehicle ownership and income growth, worldwide: 1960-2030," *Energy J.* 28(4), 2007, doi:10.5547/ISSN0195-6574-EJ-Vol28-No4-7.
3. Pereirinha, P.G., González, M., Carrilero, I., Anseán, D., Alonso, J., and Viera, J.C., "Main Trends and Challenges in Road Transportation Electrification," *Transp. Res. Procedia* 33:235–242, 2018, doi:10.1016/j.trpro.2018.10.096.
4. Yuan, M., Thellufsen, J.Z., Lund, H., and Liang, Y., "The electrification of transportation in energy transition," *Energy* 236:121564, 2021, doi:10.1016/j.energy.2021.121564.
5. Gordic, D., Nikolic, J., Vukasinovic, V., Josijevic, M., and Aleksic, A.D., "Offsetting carbon emissions from household electricity consumption in Europe," *Renew. Sustain. Energy Rev.* 175:113154, 2023, doi:10.1016/j.rser.2023.113154.
6. Yu, X., LeBlanc, S., Sandhu, N., Wang, L., Wang, M., and Zheng, M., "Decarbonization potential of future sustainable propulsion—A review of road transportation," *Energy Sci. Eng.*, 2023, doi:10.1002/ese3.1434.
7. Alshwawra, A., Abo Swerih, A., Sakhrieh, A., and Dinkelacker, F., Structural Performance of Additively Manufactured Cylinder Liner—A Numerical Study, *Energies* 15(23), 2022, doi:10.3390/en15238926.
8. Herdzyk, J., "Decarbonization of Marine Fuels—The Future of Shipping," *Energies* 14(14):4311, 2021, doi:10.3390/en14144311.
9. Kurbet, S.N. and Malagi, R.R., "Review on Effects of Piston and Piston Ring Dynamics Emphasis with Oil Consumption and Frictional Losses in Internal Combustion Engines," *SAE Technical Papers*, 2007, doi:10.4271/2007-24-0059.
10. Anderberg, C., Dimkovski, Z., Rosén, B.G., and Thomas, T.R., "Low friction and emission cylinder liner surfaces and the influence of surface topography and scale," *Tribol. Int.* 133:224–229, 2019, doi:10.1016/j.triboint.2018.11.022.
11. Holmberg, K., Andersson, P., and Erdemir, A., "Global energy consumption due to friction in passenger cars," *Tribol. Int.* 47, 2012, doi:10.1016/j.triboint.2011.11.022.
12. Styles, G., Rahmani, R., Rahnejat, H., and Fitzsimons, B., "In-cycle and life-time friction transience in piston ring-liner conjunction under mixed regime of

- lubrication," *Int. J. Engine Res.* 15(7):862–876, 2014, doi:10.1177/1468087413519783.
13. Liu, N., Wang, C., Xia, Q., Gao, Y., and Liu, P., "Simulation on the effect of cylinder liner and piston ring surface roughness on friction performance," *Mech. Ind.* 23:8, 2022, doi:10.1051/meca/2022007.
 14. Koch, F., Decker, P., Gülpen, R., Quadflieg, F.-J., and Loeprecht, M., "Cylinder Liner Deformation Analysis - Measurements and Calculations," *SAE Technical Paper Series*, 1998, doi:10.4271/980567.
 15. Selmani, E., Delprete, C., and Bisha, A., "Cylinder liner deformation orders and efficiency of a piston ring-pack," *E3S Web Conf.* 95:04001, 2019, doi:10.1051/e3sconf/20199504001.
 16. Flores, G.K., "Graded Freeform Machining of Cylinder Bores using Form Honing," *SAE Technical Papers 2015-01-1725*, 2015, doi:10.4271/2015-01-1725.
 17. Hong, S.-H., "Tribology in Marine Diesel Engines," *Tribology of Machine Elements - Fundamentals and Applications*, IntechOpen, 2022, doi:10.5772/intechopen.100547.
 18. Thigale, S., Kumar, M.N., Aghav, Y., Gokhale, N., and Gokhale, U., "Design and Analysis Aspects of Medium and Heavy-Duty Engine Crankcase," in: Lakshminarayanan, P. A. and Agarwal, A. K., eds., *Design and Development of Heavy Duty Diesel Engines*, 1st ed., Springer Singapore, ISBN 978-981-15-0972-8: 427–465, 2020, doi:10.1007/978-981-15-0970-4_12.
 19. Hassan Khuder, A.W., AL-Filfily, A.A., and M. Sowou, K., "Mechanical stresses analysis in cylinder liner for perkins 1306 diesel engine," *J. Mech. Eng. Res. Dev.* 42(4):09–13, 2019, doi:10.26480/jmerd.04.2019.09.13.
 20. Thiagarajan, C., Prabhakar, M., Prakash, S., Senthil, J., and Saravana Kumar, M., "Heat transfer analysis and optimization of engine cylinder liner using different materials," *Materials Today: Proceedings*, 2020, doi:10.1016/j.matpr.2020.06.173.
 21. Bayata, F. and Yildiz, C., "The analyses of frictional losses and thermal stresses in a diesel engine piston coated with different thicknesses of thermal barrier films using co-simulation method," *Int. J. Engine Res.* 24(3):856–872, 2023, doi:10.1177/14680874211065637.
 22. Edtmayer, J., Lösch, S., Hick, H., and Walch, S., "Comparative study on the friction behaviour of piston/bore interface technologies," *Automot. Engine Technol.* 4(3–4):101–109, 2019, doi:10.1007/s41104-019-00045-x.
 23. Bi, Y., Xu, Y., Liu, S., Chen, S., Shen, L., and Xu, Y., "Cylinder liner deformation characteristics based on fourier transform and impact on ring pack sealing and friction power," *J. Brazilian Soc. Mech. Sci. Eng.* 45(5):242, 2023, doi:10.1007/s40430-023-04124-x.
 24. Ahmad Abo Swerih, "Performance Study of Additively Manufactured Cylinder Liner," Master thesis, Institut für Technische Verbrennung, Leibniz Universität

- Hannover, 2021.
25. Usman, A. and Park, C.W., "Numerical investigation of tribological performance in mixed lubrication of textured piston ring-liner conjunction with a non-circular cylinder bore," *Tribol. Int.* 105:148–157, 2017, doi:10.1016/j.triboint.2016.09.043.
 26. Rahmani, R., Theodossiades, S., Rahnejat, H., and Fitzsimons, B., "Transient elasto-hydrodynamic lubrication of rough new or worn piston compression ring conjunction with an out-of-round cylinder bore," *Proc. Inst. Mech. Eng. Part J J. Eng. Tribol.* 226(4):284–305, 2012, doi:10.1177/1350650111431028.
 27. Lu, Y., Liu, C., Zhang, Y., Wang, J., Yao, K., Du, Y., and Müller, N., "Evaluation on the tribological performance of ring/liner system under cylinder deactivation with consideration of cylinder liner deformation and oil supply," *PLoS One* 13(9):1–27, 2018, doi:10.1371/journal.pone.0204179.
 28. Ganguly, A., Agarwal, V.K., and Santra, T., "Prediction and Reduction of Cylinder Liner Bore Deformation for a Two Wheeler Single Cylinder Gasoline Engine," *SAE Int. J. Engines* 8(4):2015-01–1742, 2015, doi:10.4271/2015-01-1742.
 29. Yang, Z., Li, B., and Yu, T., "Distortion Optimization of Engine Cylinder Liner Using Spectrum Characterization and Parametric Analysis," *Math. Probl. Eng.* 2016:1–11, 2016, doi:10.1155/2016/9212613.
 30. Dunaevsky, V. V., "Analysis of distortions of cylinders and conformability of piston rings," *Tribol. Trans.* 33(1):33–40, 1990, doi:10.1080/10402009008981927.
 31. Alshwawra, A., Pohlmann-Tasche, F., Stelljes, F., and Dinkelacker, F., "Cylinder Liner Deformation - An Investigation of its Decomposition Orders under Varied Operational Load," *SAE Powertrains, Fuels & Lubricants Conference & Exhibition*, SAE International, 2022, doi:10.4271/2022-01-1040.
 32. Ghasemi, R. and Elmquist, L., "A study on graphite extrusion phenomenon under the sliding wear response of cast iron using microindentation and microscratch techniques," *Wear* 320:120–126, 2014, doi:10.1016/j.wear.2014.09.002.
 33. Ghasemi, R., Elmquist, L., Ghassemali, E., Salomonsson, K., and Jarfors, A.E.W., "Abrasion resistance of lamellar graphite iron: Interaction between microstructure and abrasive particles," *Tribol. Int.* 120:465–475, 2018, doi:10.1016/j.triboint.2017.12.046.
 34. Trung, K.N., "The temperature distribution of the wet cylinder liner of v-12 engine according to calculation and experiment," *J. Therm. Eng.* 7(Supp 14):1872–1884, 2021, doi:10.18186/thermal.1051265.
 35. Rejowski, E.D., Soares, E., Roth, I., and Rudolph, S., "Cylinder liner in ductile cast iron for high loaded combustion diesel engines," *J. Eng. Gas Turbines Power* 134(7), 2012, doi:10.1115/1.4006071.
 36. Hitosugi, H., Nagoshi, K., Ebina, M., and Furuhashi, S., "Study on cylinder bore deformation of dry liner in engine operation," *JSAE Rev.* 17(2):113–119, 1996, doi:10.1016/0389-4304(95)00060-7.

37. Bi, Y., Wang, P., Luo, L., Wang, H., Xin, Q., Lei, J., and Shen, L., "Analysis of out-of-round deformation of a dry cylinder liner of a non-road high-pressure common-rail diesel engine based on multi-field coupling," *J. Brazilian Soc. Mech. Sci. Eng.* 43(1):50, 2021, doi:10.1007/s40430-020-02737-0.
38. Gintsburg, B.Y., "The Conformability of Piston Rings to Deformed Cylinders," Proc. TSIAM, Oborongiz, Moscow, 1946.
39. Gintsburg, B.Y., "Splitless-Type Piston Rings," *Russ. Eng. J.* 48(7):37–40, 1968.
40. Dunaevsky, V. and Alexandrov, S., "Development of Conformability Model of Piston Rings with Consideration of Their Three-Dimensional Torsional Distortions and Fourier Series Representation of Cylinder Bore Geometry," *SAE Tech. Pap. Ser.*, 2002-01–3131, 2002, doi:10.4271/2002-01-3131.
41. Dunaevsky, V. and Rudzitis, J., "Clarification of a Semi-Empirical Approach in Piston Ring-Cylinder Bore Conformability Prediction," *J. Tribol.* 129(2):430–435, 2007, doi:10.1115/1.2647800.
42. (Val) Dunaevsky, V. and Alexandrov, S., "Three-Dimensional Engineering Approach to Conformability Analysis of Piston Rings," *Tribol. Trans.* 48(1):108–118, 2005, doi:10.1080/05698190590903105.
43. Dunaevsky, V. V., Sawicki, J.T., Frater, J., and Chen, H., "Analysis of Elastic Distortions of a Piston Ring in the Reciprocating Air Brake Compressor Due to the Installation Stresses," *SAE Tech. Pap. Ser.*, 1999-01–3770, 1999, doi:10.4271/1999-01-3770.
44. Liang, X., Wang, Y., Huang, S., Yang, G., Tang, L., and Cui, G., "Investigation on Cylinder Bore Deformation under Static Condition Based on Fourier Decomposition," *SAE Tech. Pap. Ser.* 2017-01–03(March), 2017, doi:10.4271/2017-01-0366.
45. Abe, S. and Suzuki, M., "Analysis of Cylinder Bore Distortion During Engine Operation," *SAE Tech. Pap. Ser.*, 950541, 1995, doi:10.4271/950541.
46. Zhu, X., Cheng, Y., and Wang, L., "Study on Deformation Characteristics of Diesel Engine Cylinder Liner under Different Influencing Factors," *J. Phys. Conf. Ser.* 1885(3):032019, 2021, doi:10.1088/1742-6596/1885/3/032019.
47. Li, G., Gu, F., Wang, T., Lu, X., Zhang, L., Zhang, C., and Ball, A., "An Improved Lubrication Model between Piston Rings and Cylinder Liners with Consideration of Liner Dynamic Deformations," *Energies* 10(12):2122, 2017, doi:10.3390/en10122122.
48. Kang, J., Lu, Y., Yang, X., Zhao, X., Zhang, Y., and Xing, Z., "Modeling and experimental investigation of wear and roughness for honed cylinder liner during running-in process," *Tribol. Int.* 171:107531, 2022, doi:10.1016/j.triboint.2022.107531.
49. Kang, J., Lu, Y., Zhao, B., Jiang, C., Li, P., Luo, H., and Zhang, Y., "Experimental study of the tribological characteristics of a honed cylinder liner during the running-in

- process," *Mech. Sci.* 13(1):101–110, 2022, doi:10.5194/ms-13-101-2022.
50. Grabon, W., Pawlus, P., Wos, S., Koszela, W., and Wieczorowski, M., "Effects of cylinder liner surface topography on friction and wear of liner-ring system at low temperature," *Tribol. Int.* 121:148–160, 2018, doi:10.1016/j.triboint.2018.01.050.
 51. Hitosugi, H., Nagoshi, K., Komada, M., and Furuham, S., "Study on Mechanism of Lubricating Oil Consumption Caused by Cylinder Bore Deformation," *SAE Technical Paper Series*, 2010, doi:10.4271/960305.
 52. Fujimoto, H., Yoshihara, Y., Goto, T., and Furuham, S., "Measurement of Cylinder Bore Deformation During Actual Operating Engines," *SAE Tech. Pap. Ser.*, 910042, 1991, doi:10.4271/910042.
 53. Iijima, N., Sakurai, T., Takiguchi, M., Harigaya, Y., Yamada, T., and Yoshida, H., "An Experimental Study on Relationship between Lubricating Oil Consumption and Cylinder Bore Deformation in Conventional Gasoline Engine," *SAE Int. J. Engines* 2(1):2009-01–0195, 2009, doi:10.4271/2009-01-0195.
 54. Hasse, C., "Scale-resolving simulations in engine combustion process design based on a systematic approach for model development," *Int. J. Engine Res.* 17(1):44–62, 2016, doi:10.1177/1468087415597842.
 55. Pierce, D., Haynes, A., Hughes, J., Graves, R., Maziasz, P., Muralidharan, G., Shyam, A., Wang, B., England, R., and Daniel, C., "High temperature materials for heavy duty diesel engines: Historical and future trends," *Prog. Mater. Sci.* 103:109–179, 2019, doi:10.1016/j.pmatsci.2018.10.004.
 56. Michelberger, B., Jaitner, D., Hagel, A., Striemann, P., Kröger, B., Leson, A., and Lasagni, A.F., "Combined measurement and simulation of piston ring cylinder liner contacts with a reciprocating long-stroke tribometer," *Tribol. Int.* 163:107146, 2021, doi:10.1016/j.triboint.2021.107146.
 57. Maassen, F., Koch, F., Schwaderlapp, M., Ortjohann, T., and Dohmen, J., "Analytical and Empirical Methods for Optimization of Cylinder Liner Bore Distortion," *SAE Technical Paper Series*, 2001, doi:10.4271/2001-01-0569.
 58. Alshwawra, A., Pasligh, H., Hansen, H., and Dinkelacker, F., "Increasing the roundness of deformed cylinder liner in internal combustion engines by using a non-circular liner profile," *Int. J. Engine Res.* 22(4):1214–1221, 2021, doi:10.1177/1468087419893897.
 59. Koeser, P.S., Berbig, F., Pohlmann-Tasche, F., Pasligh, H., and Dinkelacker, F., "Predictive Piston Cylinder Unit Simulation - Part I: Novel Findings on Cyclic Inter-Ring Pressure Measurements and Piston Ring Dynamic Simulation Validation," *SAE Tech. Pap. Ser.*, 2021-01–0650, 2021, doi:10.4271/2021-01-0650.
 60. Koeser, P.S., Berbig, F., Pohlmann-Tasche, F., Dinkelacker, F., Wang, Y., and Tian, T., "Predictive Piston Cylinder Unit Simulation - Part II: Novel Methodology of Friction Simulation Validation Utilizing Floating-Liner Measurements," *SAE Tech. Pap. Ser.*, 2023-01–0415, 2023, doi:10.4271/2023-01-0415.

61. Alshwawra, A., Pohlmann-Tasche, F., Stelljes, F., and Dinkelacker, F., "Enhancing the geometrical performance using initially conical cylinder liner in internal combustion engines-A numerical study," *Appl. Sci.* 10(11):3705, 2020, doi:10.3390/app10113705.
62. Roy, S., Ganesh, N., Kumarasamy, A., and Viswanathan, P., "Thermomechanical Analysis of a Cylindrical Liner BT - Advances in Engineering Design and Simulation," in: Li, C., Chandrasekhar, U., and Onwubolu, G., eds., Springer Singapore, Singapore, ISBN 978-981-13-8468-4: 33–40, 2020.
63. Abouchi, M. and Basturk, S., "An investigation on the friction losses between cylinder liner and piston rings," *Sustain. Eng. Innov.* 4(2):146–155, 2022, doi:10.37868/sei.v4i2.id161.
64. Barbieri, S.G., Mangeruga, V., Giacomini, M., Laurino, C., and Lorenzini, M., "A finite element numerical methodology for the fatigue analysis of cylinder liners of a high performance internal combustion engine," *Key Eng. Mater.* 827, 2019, doi:10.4028/www.scientific.net/kem.827.288.
65. Barbieri, S.G., Giacomini, M., Mangeruga, V., Bianco, L., and Mastrandrea, L.N., "A Simplified Methodology for the Analysis of the Cylinder Liner Bore Distortion: Finite Element Analyses and Experimental Validations," *14th International Conference on Engines & Vehicles*, SAE International, 2019, doi:10.4271/2019-24-0164.
66. Youssef, A.M., Calderbank, G., Sherrington, I., Smith, E.H., and Rahnejat, H., "A Critical Review of Approaches to the Design of Floating-Liner Apparatus for Instantaneous Piston Assembly Friction Measurement," *Lubricants* 9(1):10, 2021, doi:10.3390/lubricants9010010.
67. Mufti, R.A. and Priest, M., "Experimental Evaluation of Piston-Assembly Friction Under Motored and Fired Conditions in a Gasoline Engine," *J. Tribol.* 127(4):826–836, 2005, doi:10.1115/1.1924459.
68. Winklhofer, E., Loesch, S., Satschen, S., and Thonhauser, B., "Reduction of Friction Losses by Means of Cylinder Liner Offset in a Floating Liner Single Cylinder Engine," *Int. J. Automot. Eng.* 9(4):20184124, 2018, doi:10.20485/jsaeijae.9.4_304.
69. Pohlmann-Tasche, F., Köser, P., Pasligh, H., Haase, H., and Dinkelacker, F., "Influence of Topring Coating and Oil Specification on Crank Angle-Resolved Piston Group Friction in Medium-Duty Diesel Engines," *29th CIMAC World Congress*, Vancouver: 1–16, 2019.
70. Pohlmann-Tasche, F., Köser, P.S., Berbig, F., and Dinkelacker, F., "Stroke-dependent Coated Cylinder Liners for Large Industrial Gas Engines," *MTZ Worldw.* 83(7–8):16–23, 2022, doi:10.1007/s38313-022-0807-7.
71. Ma, Liu, Wang, Wang, Huang, and Xu, "The Effect of Honing Angle and Roughness Height on the Tribological Performance of CuNiCr Iron Liner," *Metals (Basel)*.

- 9(5):487, 2019, doi:10.3390/met9050487.
72. Grabon, W., Pawlus, P., Wos, S., Koszela, W., and Wieczorowski, M., "Evolutions of cylinder liner surface texture and tribological performance of piston ring-liner assembly," *Tribol. Int.* 127:545–556, 2018, doi:10.1016/j.triboint.2018.07.011.
 73. Söderfjäll, M., Herbst, H.M., Larsson, R., and Almqvist, A., "Influence on friction from piston ring design, cylinder liner roughness and lubricant properties," *Tribol. Int.* 116:272–284, 2017, doi:10.1016/j.triboint.2017.07.015.
 74. Yousfi, M., Mezghani, S., Demirci, I., and Mansori, M. El, "Smoothness and plateauness contributions to the running-in friction and wear of stratified helical slide and plateau honed cylinder liners," *Wear* 332–333:1238–1247, 2015, doi:10.1016/j.wear.2014.11.011.
 75. Mezghani, S., Demirci, I., Yousfi, M., and Mansori, M. El, "Mutual influence of crosshatch angle and superficial roughness of honed surfaces on friction in ring-pack tribo-system," *Tribol. Int.* 66:54–59, 2013, doi:10.1016/j.triboint.2013.04.014.
 76. Alshwawra, A., Pohlmann-Tasche, F., Stelljes, F., and Dinkelacker, F., "Effect of Freeform Honing on the Geometrical Performance of the Cylinder Liner— Numerical Study," *SAE Int. J. Engines* 16(4):03-16-04–0027, 2022, doi:10.4271/03-16-04-0027.
 77. Landerl, C., Rüllicke, M., Spanring, D., and Schmuck-Soldan, S., "The Next Generation Gasoline Engine Family from BMW," *MTZ Worldw.*, 2018, doi:10.1007/s38313-017-0175-x.
 78. Halbhuber, J. and Wachtmeister, G., "Effect of Form Honing on Piston Assembly Friction," *SAE Technical Paper 2020-01-5055*, SAE International, 2020, doi:10.4271/2020-01-5055.
 79. Stelljes, F., "Tribologische Untersuchung und Analyse einer geometrisch optimierten Zylinderlaufbuchse," Master thesis, Institut für Technische Verbrennung, Leibniz Universität Hannover, 2022.
 80. Denkena, B., Handrup, M., Schmidt, C., Pillkahn, P., Katzsch, D., Reuter, L., and Stelljes, F., "Energieeffiziente Prozessketten zur Herstellung eines reibungs-, gewichts- und lebensdaueroptimierten Antriebsstrangs, 'Antriebsstrang 2025' - "Energieeffiziente Prozessketten zur Herstellung eines reibungs-, gewichts- und lebensdaueroptimierten Antriebstrang," 2022, doi:10.2314/KXP:1839641614.
 81. J. F. Nye, "Physical Properties Of Crystals: Their Representation by Tensors and Matrices," Reprint ed, Oxford University Press, U.S.A, ISBN 978-0198511656, 2002.
 82. Migita, R., "Effects of Material Properties on Bore Deformation of Engine Cylinder Liner," Master thesis, Kyushu University, 2020.
 83. Pasligh, H., Oehlert, K., Dinkelacker, F., and Ulmer, H., "Crank angle resolved floating-liner friction measurements on microstructured cylinder liner surfaces,"

- in: Bargende, M., Reuss, H., and Wiedemann, J., eds., *16. Internationales Stuttgarter Symposium*, Springer, Wiesbaden: 969–981, 2016, doi:10.1007/978-3-658-13255-2_72.
84. Sieg, G., Ulmer, H., and Dinkelacker, F., “Vorrichtung und Verfahren zur Reibkraftmessung,” 10 2015 109 332, Deutsches Patent, Deutschland, 2016.
 85. Denkena, B., Bergmann, B., Wichmann, M., Handrup, M., Katzsch, D., Pillkahn, P., Reuter, L., Schmidt, C., and Stelljes, F., “Resource-Efficient Process Chains for the Production of High-Performance Powertrain Components in the Automotive Industry,” in: Kohl, H., Seliger, G., and Dietrich, F., eds., *Manufacturing Driving Circular Economy. GCSM 2022*, Springer, Cham: 410–418, 2023, doi:10.1007/978-3-031-28839-5_46.
 86. Denkena, B., Bergmann, B., and Handrup, M., “Piezo-actuated hybrid tool for the micro structuring of cylinder liners in an energy-efficient process chain,” *Procedia Manuf.* 52:138–143, 2020, doi:10.1016/j.promfg.2020.11.025.

A large, bold, green letter 'I' is centered on a light green rectangular background. The letter has a classic serif font style with a thick vertical stem and horizontal top and bottom bars.


Link: <https://doi.org/10.1177/1468087419893897>



Standard Article

Increasing the roundness of deformed cylinder liner in internal combustion engines by using a non-circular liner profile

Ahmad Alshwawra , Henning Pasligh, Hauke Hansen and Friedrich Dinkelacker

International J of Engine Research
1–8
© IMechE 2019
Article reuse guidelines:
sagepub.com/journals-permissions
DOI: 10.1177/1468087419893897
journals.sagepub.com/home/jer


Abstract

Increasing the efficiency of internal combustion engines is of major interest for reduced greenhouse gas emission. A significant improvement potential is given with the reduction of friction losses. Here, especially the friction between the piston ring and the cylinder liner is of interest. This article describes a study with the target to enhance the piston ring–cylinder liner conformation through increasing the roundness of the deformed liner during the warm operation state. The approach is based on the assumption that a non-circular liner in the cold state can deform due to thermal and mechanical stresses toward a circular shape under typical hot operation conditions. To test this hypothesis, a computational model for a gasoline engine was built and simulated using advanced finite element methods. The simulation describes the deformation process of the liner from the thermal and mechanical stresses. First, the deformation of a circular liner is simulated, showing asymmetric deformations of up to 30 μm in the warm state for the cylinder positioned at the end of the four-cylinder bank. As experimental data are readily available, a comparison was possible, showing good agreement. Then, three liner configurations with non-circular shape in the cold stage are investigated. For an elliptically shaped configuration, a nearly circular-shaped liner is reached under typical operation conditions. This numerical approach shows the potential for reduced friction of the piston–liner arrangement within internal combustion engines. The planned next step is the extension of this method to three-dimensional shape aspects and the application to the geometry of our test engine of our lab where friction can be measured in detail with a floating-liner measurement system.

Keywords

Cylinder liner, finite element method, engine design, thermal deformation, piston ring–cylinder liner conformation, non-circular liner

Date received: 17 September 2019; accepted: 13 November 2019



Article

Enhancing the Geometrical Performance Using Initially Conical Cylinder Liner in Internal Combustion Engines—A Numerical Study

Ahmad Alshwawra * , Florian Pohlmann-Tasche, Frederik Stelljes and Friedrich Dinkelacker

Institute for Technical Combustion, Leibniz Universität Hannover, 30823 Garbsen, Germany; tasche@itv.uni-hannover.de (F.P.-T.); stelljes@itv.uni-hannover.de (F.S.); dinkelacker@itv.uni-hannover.de (F.D.)

* Correspondence: alshwawra@itv.uni-hannover.de

Received: 2 May 2020; Accepted: 24 May 2020; Published: 27 May 2020



Abstract: Reducing friction is an important aspect to increase the efficiency of internal combustion engines (ICE). The majority of frictional losses in engines are related to both the piston skirt and piston ring–cylinder liner (PRCL) arrangement. We studied the enhancement of the conformation of the PRCL arrangement based on the assumption that a suitable conical liner in its cold state may deform into a liner with nearly straight parallel walls in the fired state due to the impact of mechanical and thermal stresses. Combining the initially conical shape with a noncircular cross section will bring the liner even closer to the perfect cylindrical shape in the fired state. Hence, a significant friction reduction can be expected. For the investigation, the numerical method was first developed to simulate the liner deformation with advanced finite element methods. This was validated with given experimental data of the deformation for a gasoline engine in its fired state. In the next step, initially conically and/or elliptically shaped liners were investigated for their deformation between the cold and fired state. It was found that, for liners being both conical and elliptical in their cold state, a significant increase of straightness, parallelism, and roundness was reached in the fired state. The combined elliptical-conical liner led to a reduced straightness error by more than 50% compared to the cylindrical liner. The parallelism error was reduced by 60% to 70% and the roundness error was reduced between 70% and 80% at different liner positions. These numerical results show interesting potential for the friction reduction in the piston–liner arrangement within internal combustion engines.

Keywords: cylinder liner; piston ring–cylinder liner conformation; conical liner; noncircular liner; thermal deformation; internal combustion engine; finite element method; tapered bore liner; gasoline engine; engine design

1. Introduction

The piston ring–cylinder liner (PRCL) assembly contributes to 20% to 50% of the total mechanical energy loss of internal combustion engine (ICE) [1]. In passenger cars, approximately 4%–7.5% of fuel energy is used to overcome the frictional losses by the piston assembly, and the oil control ring alone corresponds to 0.23% to 2.8% of the fuel energy in the diesel engine [2]. Piston rings need to be conformed to the bore shape to prevent lubricant oil consumption and corresponding emission of particular and hydrocarbons. However, high piston ring tension leads to increased friction losses, which means more fuel consumption and greenhouse gas (GHG) emissions [3,4]. This implies that decreasing the friction in this contact without altering the sealing function can both increase the efficiency of the engine and reduce GHG emissions, which is a major challenge for the automotive industry [5,6].

Many researchers have discussed the tribological performance of the PRCL friction pair. Most of them have focused on the honing texture, roughness, and orientation [7–11]. Only few published

works have discussed the enhancement of the PRCL conformation through the increase of the shape accuracy in the fired state. Increasing the roundness of the deformed liner in the fired state provides a significant opportunity for improving the PRCL performance [12,13]. The authors of [14] studied the performance of initially noncircular liners numerically. In this study, it was shown that an engine with noncircular liners in the cold state can increase the roundness of the liners in its fired state significantly. The authors of [15] studied the effects of liner bore shape on the friction using a floating liner research engine. They found that using a larger bore diameter in the bottom of the liner decreased the friction.

There are many reasons which cause the liner to deform from its ideal circular shape. This includes manufacturing inaccuracies, the assembly process, thermal expansion variations between different engine components, temperature gradients during the fired state, and mechanical load during fired operations [16,17]. More than 85% of the accumulated deformation in the liner is referred to the operational mechanical and thermal loads [13]. The shape, the way, and the value of this deformation, in both longitudinal and radial directions, must have a great influence on any design improvement. Hence, the prediction of those deformation factors is important to enhance engine performance.

The rate of radial liner deformation along the longitudinal direction is influenced by the uneven distribution of combustion heat to the cylinder. The cylinder wall temperature increases toward the top section resulting in increased liner diameter in the upper part of the liner. As the piston diameter increases as well, eventually, the lower part causes more friction [18]. This problem can be solved by applying a specific honing profile on the liner, offering a greater liner diameter in the lower part of the liner. This technology is already implemented by some manufacturers [12,18,19]. However, detailed work on the quantification of the parallelism and straightness of the liner in the fired state has not been published so far. The present article describes a methodology to analyze the uneven deformation of the liner between the cold and a hot state with numerical methods.

The aim of this article was to find a defined methodology to reduce the engine friction and achieve better PRCL conformation through increasing the liner's straightness, roundness, and parallelism during the fired operation state. To reach that, a tapered bore liner in the cold state should be used. The main hypothesis in this work is that a suitable formed conical liner will be deformed to a more cylindrical shape in the fired state, such that the friction will decrease. Furthermore, mixing the conical shape with elliptical cross sections can be supposed to enhance the roundness, parallelism, and straightness of the liner.

To investigate that, the deformation model was first validated through the comparison with experiments for a defined gasoline engine. Next, the local deformation of the liner was simulated for the originally cylindrical liner with circular cross sections for an operation condition with predefined thermal loads in the different regions of the liner, as can be seen realistic for an operating engine. In the next step, the local deformation was subtracted from the originally cylindrical liner shape so that the liner had a conical shape in the cold state. Moreover, the cross sections were taken here in predefined noncircular shape. With this shaped liner, the deformations were calculated for the assumed hot conditions, and the resulting shape was investigated for the fired operation conditions.

The main contribution of this article is to provide a quantitative study for the deformation and the deformation trends of honed liners. In this study, the geometrical aspects of honed liners were regarded. For that, quantitative parameters like straightness, roundness, and parallelism were introduced. To date, a combined conical-elliptical shaped liner has not been published.

2. Theoretical Background

The cylinder liner deformation can be represented by a Fourier series [20]. The deviation ΔR of the liner bore from the perfect circular shape can be written as:

$$\Delta R = A_0 + A_1 \cos \theta + B_1 \sin \theta + A_2 \cos 2\theta + B_2 \sin 2\theta + \dots + A_n \cos n\theta + B_n \sin n\theta \quad (1)$$

where A_n, B_n are the Fourier's coefficients, θ is the angular position, and n is the deformation order. For each n th order, the maximum bore deformation $U_{max,n}$ and the phase angle \varnothing_n can be calculated with

$$U_{max,n} = \sqrt{A_n^2 + B_n^2} \quad (2)$$

$$\varnothing_n = \frac{1}{n} \tan^{-1} \frac{B_n}{A_n} \quad (3)$$

Using the harmonic series, the ΔR can be rewritten as:

$$\Delta R = A_0 + \sum_{n=1}^i \left[\frac{U_{max,n}}{2} \cos\{n(\theta - \varnothing_n)\} \right] \quad (4)$$

Different deformation orders describe different distortion patterns. The zeroth order describes the round bore, the first order describes the eccentric bore, the second order describes the oval bore, third order describes the three-lobe-shaped bore, and the fourth order describes the four-lobe-shaped bore. Generally, the first four deformation orders dominate the total liner deformation, while the higher orders deformations are commonly neglected [13].

3. Physical and Computational Model

For the simulation of the liner deformation, the complex three-dimensional thermal effects, as well as the local stresses and strains, have to be regarded. This can be done with Finite Element Methods (FEM) [21]. The main challenge for FEM is the computational requirement and capacity, namely computational power, memory, and computational time. Therefore, it is important to work with sufficiently simple yet accurate models. The current study was done with the ANSYS mechanical software, which is able to study liner deformation [22–26]. It is attractive due to its capability of handling dynamic, thermal, material, geometric, and contact nonlinearities in the finite element model.

The simulated engine in this work was based on a NISSAN CA18 gasoline engine, which had a piston stroke of 83.6 mm, cylinder bore of 83 mm, and total displacement of 1809 cm³. The liner thickness was 1.6 mm, with a clearance of 80 μ m from the engine block. More details about this engine dimensions and specifications have been described by the author of [27]. The cylinder block and the cylinder liner were made of cast iron, while the cylinder head was made of an aluminum alloy. The physical material properties for the grey cast iron are shown in Table 1. The deformation of this cylinder liner was measured at 4000 rpm under full load [25]. The measured temperature at this operation points varied between 123 °C to 185 °C at the engine block and between 150 °C to 197 °C at the cylinder liner. The coolant temperature was 80 °C, and the used bolt pretension was 80,000 N. The top deck was restrained from the movement in the axial direction. Further details about the physical model have been described by the authors of [14].

Table 1. Physical properties for grey cast iron [28].

| | |
|---|------------------------|
| Density | 7200 kg/m ³ |
| Thermal expansion coefficient (20–200 °C) | 11.7 μ m/mK |
| Heat conductivity (200 °C) | 47.5 W/mK |
| Elastic modulus | 103–118 GPa |
| Tensile strength | 250–350 MPa |

The numerical study was done on the terminal cylinder located at the end of the four-cylinder engine. The deformation of the terminal cylinder is different from the other intermediate cylinders due to uneven supply of the combustion heat in the front-rear direction. This leads to a third-order deformation pattern for the terminal cylinder in addition to the first-, second-, and fourth-order

deformations that also appear in the intermediate cylinders. One and a half cylinders were simulated to include the effects of the thermal load from the adjacent cylinder and the surrounding (see Figure 1). The simulated deformations were found to be in the range of up to 30 μm for the fired conditions. Both the trends and the values of the deformations have good agreement with experimental data described by the authors of [25]. The detailed model configuration, boundary conditions, temperature distributions, mesh properties, grid independence test, circumferential position dependent deformation, and model validation have been explained by the authors of [14].

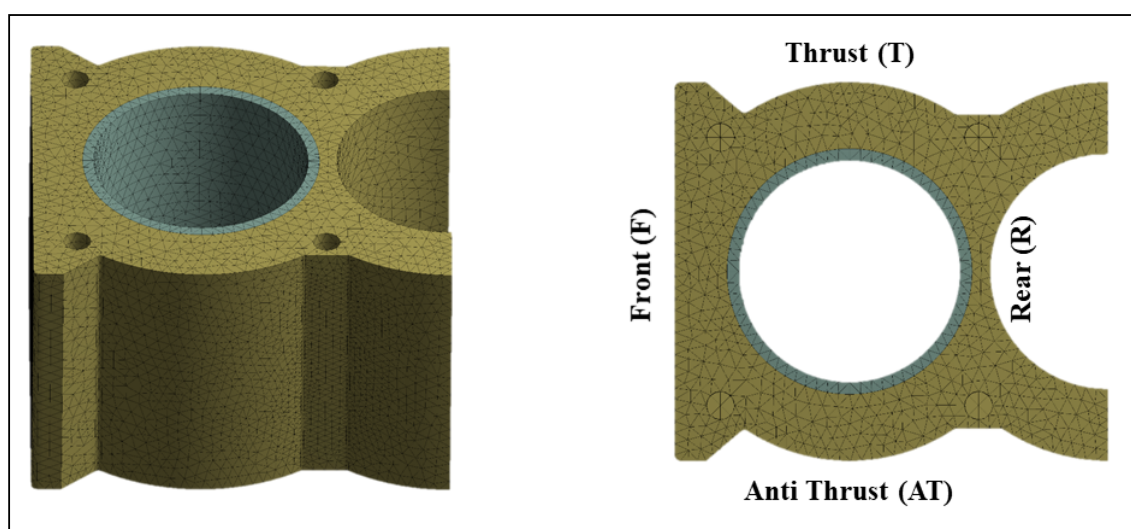


Figure 1. One and half cylinder model used in this study with the different sides of the cylinder.

4. Conical Liners

The selection of the tapering angle for the conical liner was based on reversing the angle resulted from the cylindrical liner. Figure 2 shows the resulting bore deformation for the circular liner on the thrust, antithrust, front, and rear sides. The figure shows the deformation in a strongly exaggerated representation to highlight the differences between the upper and lower part deformations. It is noticeable that this difference varies from one side to another. The upper part is always more deformed than the lower part. The difference of the deformation is about 5 μm on the thrust and antithrust sides 7 μm on the front and rear sides. For the setup of an optimized liner, a conical shaped liner was assumed for the cold state. It was formed with 5- μm increments of the lower radius (see Figure 3). This design is compatible with the generally known shapes for noncylindrical liners used by some manufacturers [18,19]. For the sake of simplicity, the design proposed in this work was based on one fixed operation point. In later applications, an optimal inclination design should be determined on the basis of a statistical analysis for different operation points of the engine.

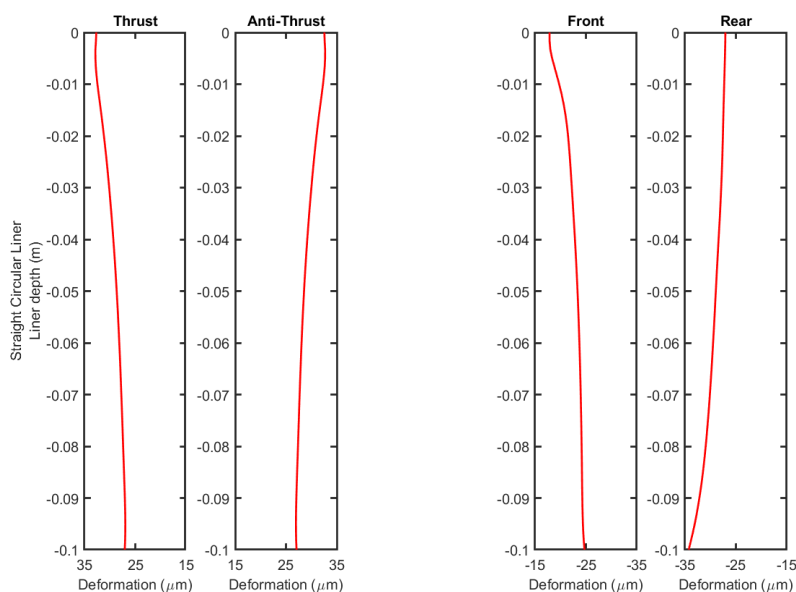


Figure 2. Simulation of the bore deformation for fired conditions for the originally straight circular liner for the four sides of the terminal cylinder.

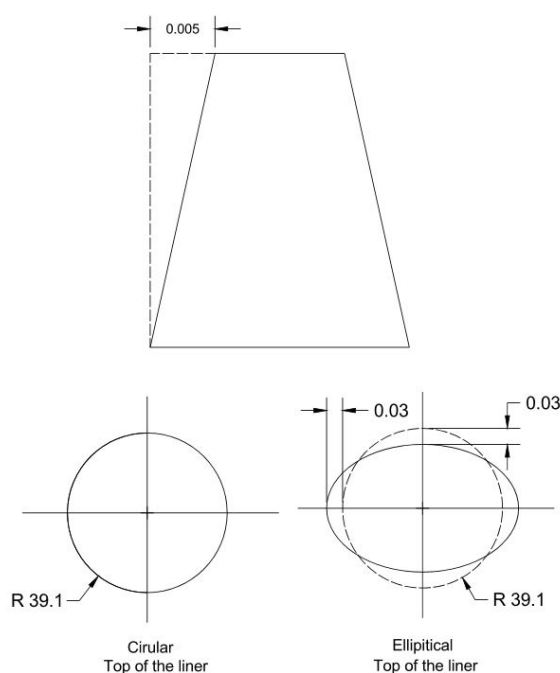


Figure 3. Dimensions and cross sections for conical liners (Dimensions in millimeter).

Figure 3 also shows the cross section in the top plane of the conical liner. Two designs were investigated here. Commonly, the cross section has a circular form. In a preceding work [14], it was shown that an elliptical liner cross section in the cold state can reduce the roundness error in the fired state by more than 75% for the terminal cylinder in four-cylinder gasoline engine due to the inhomogeneous thermal conditions. It was found that the deformation of a circular liner leads to a nearly elliptical shape in the fired state, while an initially elliptic liner with opposite ellipticity in the cold state deforms to an almost circular shape in the fired state. This does not affect the piston shape, since the amount of ellipticity is small and can be absorbed by the piston rings in the cold state. Furthermore, it can be assumed that the piston itself keeps its circular shape in the fired state due to its geometry.

The deformation of both the conical circular and the conical elliptical liners in the cold state were simulated at the same operational conditions (4000 rpm at full load). The results for the bore deformation for circular and elliptical conical liners are presented in Figures 4 and 5. For comparison, the figures also show the deformations of the initially straight wall liners, being either circular (Figure 4) or elliptical (Figure 5). The comparison between the straight and conical liners shows that the conical liners deformed to a better straight and parallel shape in the fired state. This led to friction reduction due to both increasing the oil film thickness between piston ring and cylinder liner and eliminating the secondary movement [12,15,18]. It is worth noting that although the values and trends for circular and elliptical liners look the same, the final shape of deformation was totally different, as explained previously.

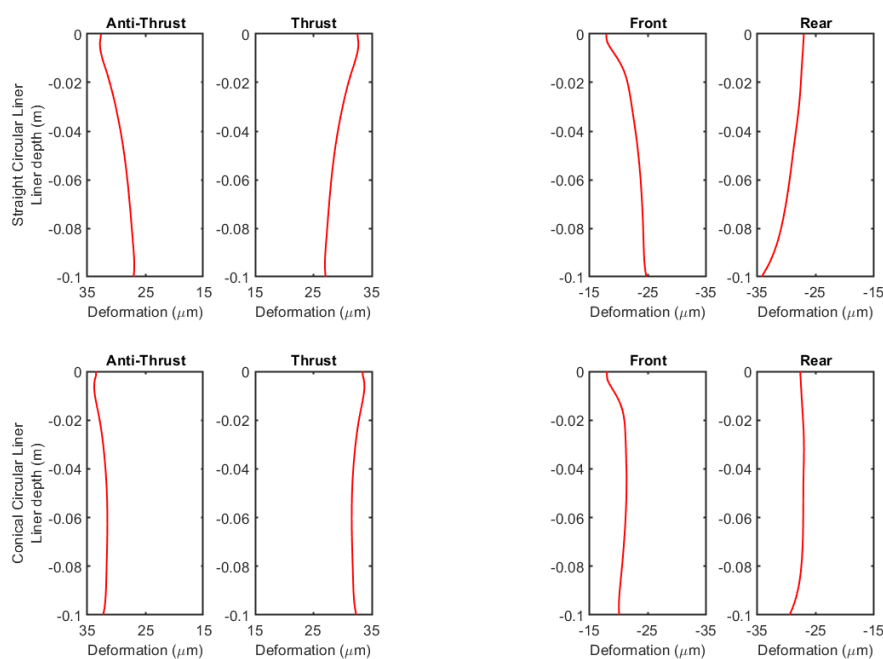


Figure 4. Bore deformation for straight (top) and conical circular liners (bottom) for the hot operation case.

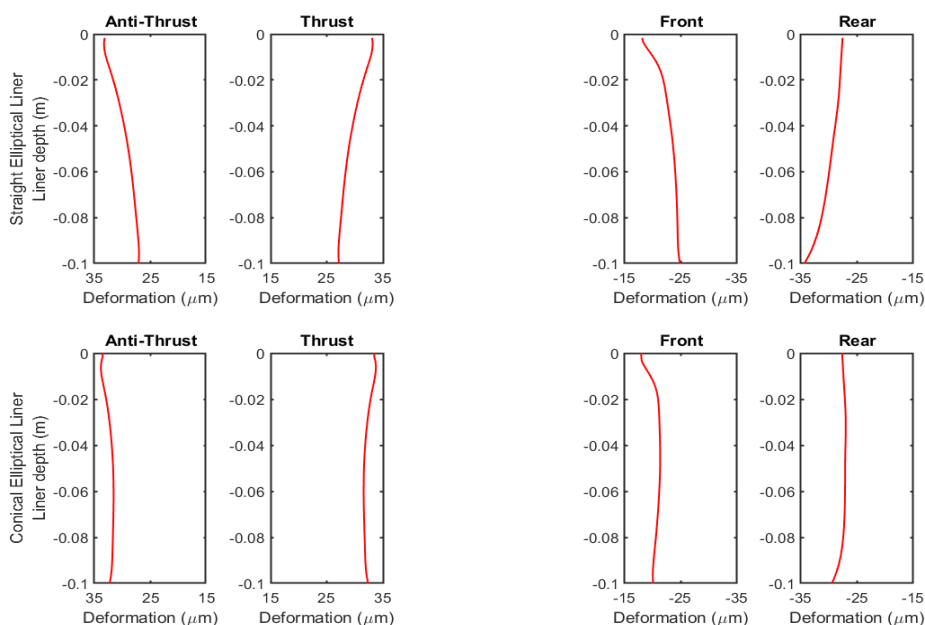


Figure 5. Bore deformation for straight (top) and conical elliptical liners (bottom) for the hot operation case.

5. Geometric Deformation Indicators

To check if the use of the conical liner affected the roundness of the liner's cross sections, the roundness errors were calculated at different elevations. The roundness was evaluated with the least squares circle method [14]. Briefly, the roundness error is the difference between the maximum and minimum circles that confine all the data points in the cross section (see Figure 6a). Furthermore, the straightness error is calculated as the minimum distance between two straight lines that contain all the points as explained in Figure 6b. The straightness error represents the change of the radius over the length, while the roundness error represents the change of the radius over the circumference. The parallelism error equals the difference between maximum and minimum distances between points at identical elevations in two lines facing each other, as explained in Figure 6c and Equation (5).

$$\text{Parallelism error} = d_{\max} - d_{\min} \quad (5)$$

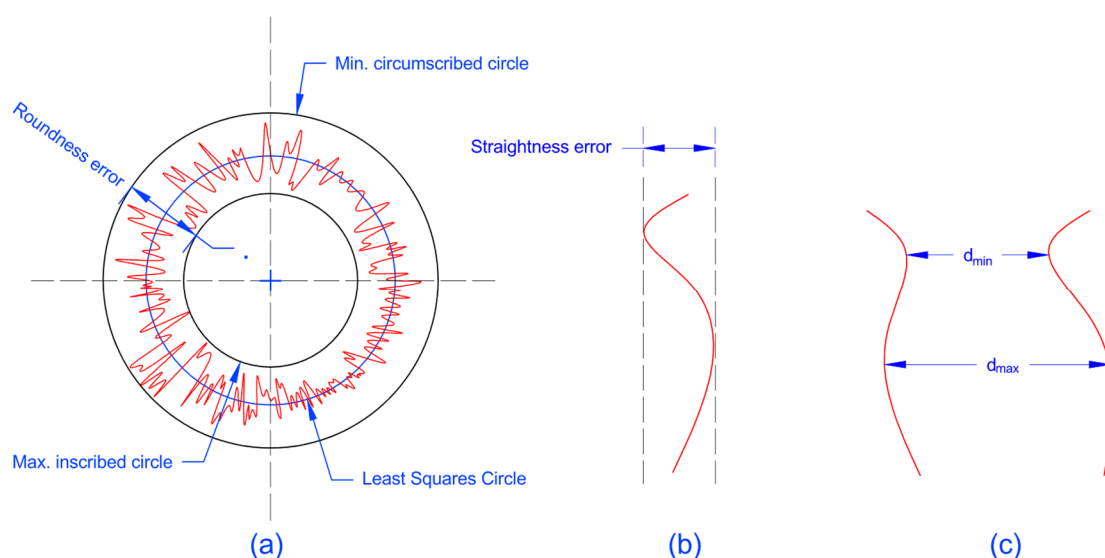


Figure 6. (a) Roundness error; (b) Straightness error; (c) Parallelism error.

The maximum value of the parallelism error is the summation of the straightness error of these two lines. The parallelism represents the change of the diameter over length, and thus shows the change in the bore tightness in a certain direction. This error is critical for both engine friction and PRCL performance. The reason for the use of both straightness and parallelism error is to predict the closeness of the liner's wall to the required straight parallel shape, since the parallelism error alone cannot predict the existence of parallel curved walls. The results are summarized in Tables 2–4.

Table 2. Parallelism deviation in the axial direction for the liner in both the cold state and under typical fired operational conditions. (Numbers are given in micrometers).

| Shape | Side | Cold State | | Fired State | |
|------------------------|------|-------------------|------------|-------------------|------------|
| | | Thrust-Antithrust | Front-Rear | Thrust-Antithrust | Front-Rear |
| Straight circle (ref.) | | 0.0 | 0.0 | 11.6 | 13.5 |
| Conical circle | | 9.8 | 9.8 | 4.4 | 5.4 |
| Straight ellipse | | 0.0 | 0.0 | 12.3 | 13.5 |
| Conical ellipse | | 9.8 | 9.8 | 4.4 | 4.0 |

Table 3. Straightness deviation for the liner in both the cold state and under typical fired operational conditions. (Numbers are given in micrometers).

| Shape \ Side | Cold State | | | | Fired State | | | |
|------------------------|------------|-------------|-------|------|-------------|-------------|-------|------|
| | Thrust | Anti-Thrust | Front | Rear | Thrust | Anti-Thrust | Front | Rear |
| Straight circle (ref.) | 0.0 | 0.0 | 0.0 | 0.0 | 5.7 | 5.9 | 6.8 | 7.2 |
| Conical circle | 4.9 | 4.9 | 4.9 | 4.9 | 2.2 | 2.2 | 3.4 | 3.4 |
| Straight ellipse | 0.0 | 0.0 | 0.0 | 0.0 | 6.1 | 6.2 | 6.8 | 6.8 |
| Conical ellipse | 4.9 | 4.9 | 4.9 | 4.9 | 2.2 | 2.2 | 3.5 | 3.4 |

Table 4. Roundness deviation for the liner in both the cold state and under typical fired operational conditions at different heights within the liner. (Numbers are given in micrometers).

| Shape \ Liner Height | Cold State | | | Fired State | | |
|------------------------|------------|-------|-------|-------------|-------|-------|
| | 10 mm | 50 mm | 90 mm | 10 mm | 50 mm | 90 mm |
| Straight circle (ref.) | 0.9 | 0.9 | 0.9 | 59.8 | 57.1 | 58.6 |
| Conical circle | 1.0 | 1.1 | 1.3 | 71.9 | 69.4 | 70.4 |
| Straight ellipse | 60.6 | 60.5 | 60.5 | 15.3 | 9.4 | 8.1 |
| Conical ellipse | 61.4 | 61.4 | 61.4 | 17.3 | 10.8 | 14.0 |

Tables 2 and 3 show that both the parallelism and straightness of the liner increased in the fired state when a conical liner was used. The parallelism deviation decreased by a factor of three from values of around 12 μm to values around 4 μm . Simultaneously, the straightness error decreased from values of around 6 μm to values around 3 μm , which indicates that the walls of the liner became straighter and more parallel. They also showed almost the same values for both elliptical and circular cross sections, which indicates that the parallelism and straightness were independent of the liner cross section. In the thrust–antithrust direction, the liner was almost straight and parallel. An identical deviation of two micrometers out of a straight line was found at the top region of the liner on both sides. Here, the reason was given essentially from the pre-tightening load [25]. It can be assumed that this deviation could also be reduced if the longitudinal bore shape of the liner in its cold state was processed with a detailed nonlinear shape. Then, this shape could be derived from the reverse deviation of the fired state deformation. For the front–rear direction, a deviation from a straight shape occurred in the lower part in the rear side due to an uneven supply for the combustion heat from the terminal side and from the side of the adjacent cylinders. This led to a certain eccentricity in the lower part of the liner.

From Table 4, it can be seen that the roundness error increased significantly in the fired state if a circular shape was used in the cold state. This holds true for both the straight and the conical circular liner. If the cold state has an elliptical shape in the assumed parameters of the ellipse (see Figure 3), the roundness error is reduced in the fired state significantly from values between 60 μm and 70 μm to values between 10 μm and 15 μm . This holds true for both the initially straight and the initially conically shaped liners. The roundness error is mainly related to blow-by and oil leakage to the combustion chamber. A larger roundness error implies that the piston rings need an increased pretension to prevent the leakage. This increases the frictional losses to a certain extent. This contribution is, however, rather small.

The parallelism error influences the friction losses more directly. On the one hand, the deviation from the straight parallel shape of the liner leads to varying oil film thickness between the piston ring and skirt and the cylinder liner. This can increase the friction. In the extreme case of the bore diameter being locally smaller than the piston diameter, the friction would increase drastically. On the

other hand, the clearance between piston ring/skirt and cylinder liner can also increase, which can lead to increased secondary movement of the piston, which affects the friction. This implies that the parallelism error can possibly have more influence on the friction than the roundness error, even if it has smaller values. Although the roundness error is slightly smaller for the initially straight elliptical liner, the influence on the parallelism must be regarded. In sum, both influences are therefore regarded best with the initially conically and elliptically shaped liners.

These results agree with and explain the results found in the literature. For example, the study done by Edtmayer et al. [15] showed that using a larger bore diameter in the bottom of the liner decreases the friction. This can be referred to the fact that this type of honing increases the straightness and parallelism of the deformed liner in the hot state.

6. Conclusions

The uneven distribution of combustion heat within an internal combustion engine leads to a significant increase of the diameter at the upper part of the liner compared to that at the lower part. This leads to increased friction and oil losses. This study assumed that an originally conical liner in its cold state could be used to reach a nearly cylindrical form in its fired operation state. This would improve the PRCL conformation and thus reduce the friction and the oil losses. To study that, a numerical validated gasoline engine model was used. With a numerical FEM simulation model, the deformation behavior of the liner was investigated between the cold state and a typical operation point of the engine at 4000 rpm.

The simulation case was based on a four-cylinder NISSAN CA18 gasoline engine, and experimental data of the roundness influence was given as a validation case. The study was done for the terminal cylinder located at the end of the engine with regard to the asymmetric thermal load from the neighbor cylinder on one side. From the first simulations of the deformation of the initially cylindrical liner for experimentally given temperature profiles, the resulting deformation was determined as a function of height. The larger temperatures in the upper section of the liner led to increased deformation. In the given case, the radius was increased by 30 μm .

In order to reach a nearly cylindrical liner shape, an initially conical liner was designed where the inclination angle was derived from the inverse of the calculated difference of the deformation between the upper and the lower section of the liner. Based on an earlier study [14], the cross section of the liner was also regarded and was varied to be either circular in the cold state or to be slightly elliptical in such a way that the uneven thermal load led to a circular cross section in the fired state. In this study, both effects were regarded in a combined way. Using the validated FEM model, the detailed liner deformation was simulated for the thermal and stress conditions which were relevant for a full load operation point of the engine at 4000 rpm.

The numerical simulation results showed that the use of the conical liner in the cold state enhanced the parallelism in the fired state by a factor of three in such a way that the parallelism error reduced from about 12 μm to values in the range of 4 μm . Moreover, the straightness in the fired state enhanced by a factor of two in such a way that the straightness deviation error reduced from about 6 μm to values in the range of 3 μm . This indicates that the liner's walls became more parallel and straighter. The remaining straightness error occurred at the upper part of the liner and was the result of the pre-tightening load. The utilization of a conical elliptical liner also reduced the roundness error in the fired state significantly from roundness error values of 60 μm to 70 μm to values in the range of 10 μm to 15 μm . The combination of both effects in conically and elliptically shaped liners has a great potential for increasing roundness, parallelism, and straightness in the fired engine state. This can possibly lead to reduced friction. Moreover, the oil losses can be reduced. With that, it might be possible to reduce the contact pressure of the piston rings, which, by itself, would additionally reduce the friction loss of the engine.

The approach and methodology described in this article provide a good starting point to analyze one of the most complex and critical areas in internal combustion engines. It has to be seen, if such

complex shaped liners, i.e., the combination of a conically and elliptically shaped liners, will lead to advantages in real engines. For that, detailed measurements of the crank-angle resolved friction forces are planned in the near future on the single cylinder diesel test engine at the Leibniz University of Hannover [29–31].

Author Contributions: Conceptualization, A.A., F.P.-T. and F.D.; methodology, A.A.; software, A.A.; validation, A.A. and F.P.-T.; formal analysis, A.A.; investigation, A.A.; writing—Original draft preparation, A.A.; writing—Review and editing, A.A., F.P.-T., F.S. and F.D.; visualization, A.A.; supervision, F.D.; project administration, F.S.; funding acquisition, F.D. All authors have read and agreed to the published version of the manuscript.

Funding: A partial fund for this work was provided by the German Jordanian University (GJU) through a research scholarship. German Federal Ministry for Economic Affairs and Energy (BMWi) funded another part within the cooperation project “Energieeffiziente Prozessketten zur Herstellung eines reibungs-, gewichts- und lebensdaueroptimierten Antriebsstrangs” (Antriebsstrang 2025). The publication of this article was funded by the Open Access Fund of the Leibniz Universität Hannover.

Conflicts of Interest: The authors declare that they have no conflict of interest.

References

- Gu, C.; Meng, X.; Xie, Y.; Zhang, D. The influence of surface texturing on the transition of the lubrication regimes between a piston ring and a cylinder liner. *Int. J. Engine Res.* **2017**, *18*, 785–796. [[CrossRef](#)]
- Anderberg, C.; Dimkovski, Z.; Rosén, B.G.; Thomas, T.R. Low friction and emission cylinder liner surfaces and the influence of surface topography and scale. *Tribol. Int.* **2019**, *133*, 224–229. [[CrossRef](#)]
- Styles, G.; Rahmani, R.; Rahnejat, H.; Fitzsimons, B. In-cycle and life-time friction transience in piston ring-liner conjunction under mixed regime of lubrication. *Int. J. Engine Res.* **2014**, *15*, 862–876. [[CrossRef](#)]
- Delprete, C.; Razavykia, A. Piston dynamics, lubrication and tribological performance evaluation: A review. *Int. J. Engine Res.* **2018**, *21*, 725–741. [[CrossRef](#)]
- Pierce, D.; Haynes, A.; Hughes, J.; Graves, R.; Maziasz, P.; Muralidharan, G.; Shyam, A.; Wang, B.; England, R.; Daniel, C. High temperature materials for heavy duty diesel engines: Historical and future trends. *Prog. Mater. Sci.* **2019**, *103*, 109–179. [[CrossRef](#)]
- Song, Y.; Zheng, Z.; Peng, T.; Yang, Z.; Xiong, W.; Pei, Y. Numerical investigation of the combustion characteristics of an internal combustion engine with subcritical and supercritical fuel. *Appl. Sci.* **2020**, *10*, 862. [[CrossRef](#)]
- Grabon, W.; Pawlus, P.; Wos, S.; Koszela, W.; Wiczorowski, M. Evolutions of cylinder liner surface texture and tribological performance of piston ring-liner assembly. *Tribol. Int.* **2018**, *127*, 545–556. [[CrossRef](#)]
- Söderfjäll, M.; Herbst, H.M.; Larsson, R.; Almqvist, A. Influence on friction from piston ring design, cylinder liner roughness and lubricant properties. *Tribol. Int.* **2017**, *116*, 272–284. [[CrossRef](#)]
- Yousfi, M.; Mezghani, S.; Demirci, I.; El Mansori, M. Smoothness and plateau contributions to the running-in friction and wear of stratified helical slide and plateau honed cylinder liners. *Wear* **2015**, *332*, 1238–1247. [[CrossRef](#)]
- Mezghani, S.; Demirci, I.; Yousfi, M.; El Mansori, M. Mutual influence of crosshatch angle and superficial roughness of honed surfaces on friction in ring-pack tribo-system. *Tribol. Int.* **2013**, *66*, 54–59. [[CrossRef](#)]
- Hu, Y.; Meng, X.; Xie, Y.; Fan, J. Mutual influence of plateau roughness and groove texture of honed surface on frictional performance of piston ring-liner system. *Proc. Inst. Mech. Eng. Part J J. Eng. Tribol.* **2017**, *231*, 838–859. [[CrossRef](#)]
- Flores, G.K. Graded Freeform Machining of Cylinder Bores using Form Honing. In *SAE Technical Paper*; SAE International: Warrendale, PA, USA, 2015. [[CrossRef](#)]
- Koch, F.; Decker, P.; Gülpen, R.; Quadflieg, F.-J.; Loeprecht, M. Cylinder Liner Deformation Analysis—Measurements and Calculations. In *SAE Technical Paper Series*; SAE International: Warrendale, PA, USA, 2010. [[CrossRef](#)]
- Alshwawra, A.; Pasligh, H.; Hansen, H.; Dinkelacker, F. Increasing the roundness of deformed cylinder liner in internal combustion engines by using a non-circular liner profile. *Int. J. Engine Res.* **2019**. [[CrossRef](#)]
- Edtmayer, J.; Lösch, S.; Hick, H.; Walch, S. Comparative study on the friction behaviour of piston/bore interface technologies. *Automot. Engine Technol.* **2019**, *4*, 101–109. [[CrossRef](#)]

16. Lu, Y.; Liu, C.; Zhang, Y.; Wang, J.; Yao, K.; Du, Y.; Müller, N. Evaluation on the tribological performance of ring/liner system under cylinder deactivation with consideration of cylinder liner deformation and oil supply. *PLoS ONE* **2018**, *13*, e0204179. [[CrossRef](#)]
17. Yang, Z.; Li, B.; Yu, T. Distortion Optimization of Engine Cylinder Liner Using Spectrum Characterization and Parametric Analysis. *Math. Probl. Eng.* **2016**, *2016*, 9212613. [[CrossRef](#)]
18. Landerl, C.; Rüllicke, M.; Spanring, D.; Schmuck-Soldan, S. The Next Generation Gasoline Engine Family from BMW. *MTZ Worldw.* **2018**, *79*, 38–45. [[CrossRef](#)]
19. Axel, P.; Wild, M.; Rothe, A.; Audi, A.G. Internal Combustion Engine. Property right DE102011117660B4, 2014.
20. Dunaevsky, V.V. Analysis of distortions of cylinders and conformability of piston rings. *Tribol. Trans.* **1990**, *33*, 33–40. [[CrossRef](#)]
21. Reitz, R.D.; Ogawa, H.; Payri, R.; Fansler, T.; Kokjohn, S.; Moriyoshi, Y.; Agarwal, A.K.; Arcoumanis, D.; Assanis, D.; Bae, C.; et al. IJER editorial: The future of the internal combustion engine. *Int. J. Engine Res.* **2019**, *21*, 3–10. [[CrossRef](#)]
22. Liang, X.; Wang, Y.; Huang, S.; Yang, G.; Tang, L.; Cui, G. Investigation on Cylinder Bore Deformation under Static Condition Based on Fourier Decomposition. *SAE Tech. Pap. Ser.* **2017**. [[CrossRef](#)]
23. Ganguly, A.; Agarwal, V.K.; Santra, T. Prediction and Reduction of Cylinder Liner Bore Deformation for a Two Wheeler Single Cylinder Gasoline Engine. *SAE Int. J. Engines* **2015**, *8*, 1913–1923. [[CrossRef](#)]
24. Maassen, F.; Koch, F.; Schwaderlapp, M.; Ortjohann, T.; Dohmen, J. Analytical and Empirical Methods for Optimization of Cylinder Liner Bore Distortion. *SAE Tech. Pap. Ser.* **2010**. [[CrossRef](#)]
25. Hitosugi, H.; Nagoshi, K.; Ebina, M.; Furuhashi, S. Study on cylinder bore deformation of dry liner in engine operation. *JSAE Rev.* **1996**, *17*, 113–119. [[CrossRef](#)]
26. Nguyen, D.V.; Duy, V.N. Numerical analysis of the forces on the components of a direct diesel engine. *Appl. Sci.* **2018**, *8*, 761. [[CrossRef](#)]
27. Flammang, J.M. *Standard Catalog of Imported Cars 1946–1990*, 1st ed.; Kp Books: Iola, WI, USA, 1992.
28. *European Standard: DIN EN 1561: 2012-01, Founding Grey Cast IRON*; German Version; Beuth: Brussel, Belgium, 2012. [[CrossRef](#)]
29. Pasligh, H.; Oehlert, K.; Dinkelacker, F.; Ulmer, H. Crank angle resolved floating-liner friction measurements on microstructured cylinder liner surfaces. In *16. Internationales Stuttgarter Symposium*; Springer: Wiesbaden, Germany, 2016.
30. Pasligh, H.; Ulmer, H.; Dinkelacker, F. Friction investigations on locally microstructured cylinder liner surfaces using a floating-liner measurement system. In *Proceedings of the CIMAC Congress, Helsinki, Finland, 6–10 June 2016*; paper no. 295. pp. 1–9.
31. Pohlmann-Tasche, F.; Köser, P.; Pasligh, H.; Haase, H.; Dinkelacker, F. Influence of Topring Coating and Oil Specification on Crank Angle-Resolved Piston Group Friction in Medium-Duty Diesel Engines. In *Proceedings of the 29th CIMAC World Congress, Vancouver, BC, Canada, 10–14 June 2019*; pp. 1–16.



© 2020 by the authors. Licensee MDPI, Basel, Switzerland. This article is an open access article distributed under the terms and conditions of the Creative Commons Attribution (CC BY) license (<http://creativecommons.org/licenses/by/4.0/>).

III

Link: <https://doi.org/10.4271/2022-01-1040>

| | |
|---|--|
| 2022-01-1040 Published 30 Aug 2022 | |
|  | <h2 style="text-align: center;">Cylinder Liner Deformation - An Investigation of its Decomposition Orders under Varied Operational Load</h2> <p style="text-align: center;">Ahmad Alshwawra, Florian Pohlmann-Tasche, Frederik Stelljes, and Friedrich Dinkelacker Leibniz Universität Hannover</p> <p><i>Citation:</i> Alshwawra, A., Pohlmann-Tasche, F., Stelljes, F., and Dinkelacker, F., "Cylinder Liner Deformation - An Investigation of its Decomposition Orders under Varied Operational Load," SAE Technical Paper 2022-01-1040, 2022, doi:10.4271/2022-01-1040.</p> |

Received: 12 Apr 2022

Revised: 11 Jul 2022

Accepted: 11 Jul 2022

Abstract

Enhancing the efficiency of the internal combustion engine is of most interest to achieve sustainability, for instance in connection with sustainable fuels, like hydrogen or biofuels. Regardless of the type of fuel, great development possibilities are seen in reducing the friction of the piston group. Analyzing the cylinder liner deformation is essential to understanding the behavior of the piston rings-cylinder liner (PRCL) coupling in the hot operation state. This paper describes the liner deformation at the hot operation state over the liner depth for different operational points. To do so, a validated mathematical model based on a physical model of a terminal cylinder in an internal combustion engine has been introduced. The validated mathematical model is then simulated using FEM software to numerically calculate liner

deformations at different operational conditions. Subsequently, the deformations are analyzed using Fourier decomposition to find the variation trends for each order of deformation over the liner's depth and engine operational points. It is found that the second-order deformation is dominant over the liner depth. This deformation order is highly dependent on the operational load. The fourth-order deformation is highly dependent on the liner depth with low dependency on the operational load. The trends for first and third orders are also discussed. The simulation was repeated for aluminum alloy as a different engine material to investigate the material effects. The results show that although the deformation values differ significantly with different materials, the trends for the deformation's order remain almost the same. In an outlook, the possible application to real engines is discussed.

IV

Link: <https://doi.org/10.4271/03-16-04-0027>



Effect of Freeform Honing on the Geometrical Performance of the Cylinder Liner—Numerical Study

Ahmad Alshwara,¹ Florian Pohlmann-Tasche,¹ Frederik Stelljes,¹ and Friedrich Dinkelacker¹

¹Leibniz Universität Hannover, Institute for Technical Combustion, Germany

Abstract

Reducing the friction of the internal combustion engine (ICE) is of major interest to reduce fuel consumption and greenhouse gas (GHG) emissions. A huge potential for friction reduction is seen in the piston ring-cylinder liner (PRCL) coupling. Approaching the cylindrical liner shape in the hot operation state will enhance the PRCL conformation. Recently, newly developed freeform honing techniques can help to achieve this perfect cylinder shape. This article presents a numerical study of the effect of freeform honing on the geometrical performance of the liner in the hot operation state. The freeform honed liner (TR) concept is based on the approach of reversing the local deformation of a conventional circular liner. A validated computational model for a gasoline engine is used to compare the geometrical performance of those TR cases with circular, elliptical (EL), and conical elliptical liners (NEL) at different operational points. It was found that the TR concept can reduce the roundness error by 92-95% and the straightness error by 70-75% when the reference load equals the operational one. Quite a good compromise is found to be the initial NEL shape, which probably would be easier for the manufacturing process. In this study, the influence of the reference load on the shape, and with that on friction, is also investigated at different operational loads. It was found that the reference load should be selected at a medium level since commonly the deviations at higher operational loads are less problematic for friction than vice versa. The numerical studies with optimal freeform-shaped cylinder liners—or with the compromise of NEL shapes—show a promising approach to enhance the PRCL conformation and reduce engine friction.

History

Received: 03 Dec 2021
 Revised: 21 Mar 2022
 Accepted: 15 Aug 2022
 e-Available: 01 Sep 2022

Keywords

Cylinder liner, Engine design, Thermal deformation, Piston ring-cylinder liner conformation, Non-circular liner, Conical liner, Tapered bore liner, Freeform honed liner

Citation

Alshwara, A., Pohlmann-Tasche, F., Stelljes, F., and Dinkelacker, F., "Effect of Freeform Honing on the Geometrical Performance of the Cylinder Liner—Numerical Study," *SAE Int. J. Engines* 16(4):2023, doi:10.4271/03-16-04-0027.

ISSN: 1946-3936
 e-ISSN: 1946-3944

A large, bold, green letter 'V' is centered on a light green rectangular background. The letter is a simple, sans-serif font with a slight shadow effect.

Article

Structural Performance of Additively Manufactured Cylinder Liner—A Numerical Study

Ahmad Alshwawra ^{1,*} , Ahmad Abo Swerih ¹, Ahmad Sakhrieh ^{2,3}  and Friedrich Dinkelacker ¹ 

¹ Institute for Technical Combustion, Leibniz Universität Hannover, 30823 Garbsen, Germany

² Mechanical and Industrial Engineering Department, School of Engineering, American University of Ras Al Khaimah, Ras Al-Khaimah 10021, United Arab Emirates

³ Mechanical Engineering Department, The University of Jordan, Amman 11942, Jordan

* Correspondence: alshwawra@itv.uni-hannover.de

Abstract: Climate change is exacerbated by vehicle emissions. Furthermore, vehicle pollution contributes to respiratory and cardiopulmonary diseases, as well as lung cancer. This requires a drastic reduction in global greenhouse gas emissions for the automobile industry. To address this issue, researchers are required to reduce friction, which is one of the most important aspects of improving the efficiency of internal combustion engines. One of the most important parts of an engine that contributes to friction is the piston ring cylinder liner (PRCL) coupling. Controlling the linear deformation enhances the performance of the engine and, as a result, contributes positively to its performance. The majority of the tests to study the conformability between cylinder liner and piston were carried out on cylinder liners made of cast iron. It is possible to improve the performance of piston ring cylinder liner couplings by implementing new and advanced manufacturing techniques. In this work, a validated finite element model was used to simulate the performance when advanced manufactured materials were adapted. The deformation of the cylinder liner due to thermal and mechanical loads is simulated with five different additive manufactured materials (Inconel 625, Inconel 718, 17-4PH stainless steel, AlSi10Mg, Ti6Al4V). Simulated roundness and straightness errors, as well as maximum deformation, are compared with conventional grey cast iron liner deformation. Some additive manufactured materials, especially Ti6Al4V, show a significant reduction in deformation compared to grey cast iron, both in bore and circumferential deformation. Results show that Ti6Al4V can reduce maximum liner deformation by 36%. In addition, the roundness improved by 36%. The straightness error when Ti6Al4V was used also improved by 44% on one side, with an average of 20% over the four sides. Numerical results indicate that additive manufactured materials have the potential to reduce friction within the piston liner arrangement of internal combustion engines.

Keywords: additive manufacturing; additively manufactured cylinder liner; finite element method; engine design; thermal deformation; cylinder liner; internal combustion engine



Citation: Alshwawra, A.; Abo Swerih, A.; Sakhrieh, A.; Dinkelacker, F. Structural Performance of Additively Manufactured Cylinder Liner—A Numerical Study. *Energies* **2022**, *15*, 8926. <https://doi.org/10.3390/en15238926>

Academic Editors: Haifeng Liu and Zongyu Yue

Received: 20 October 2022

Accepted: 21 November 2022

Published: 25 November 2022

Publisher's Note: MDPI stays neutral with regard to jurisdictional claims in published maps and institutional affiliations.



Copyright: © 2022 by the authors. Licensee MDPI, Basel, Switzerland. This article is an open access article distributed under the terms and conditions of the Creative Commons Attribution (CC BY) license (<https://creativecommons.org/licenses/by/4.0/>).

1. Introduction

The increase in the number of automotive vehicles worldwide indicates a need to improve fuel economy and reduce emissions in an effort to improve sustainability [1,2]. Reducing the energy loss inside the engine would improve fuel efficiency and maximize the benefit of conversion to sustainable fuels such as hydrogen and biofuels in internal combustion engines [3]. Power cylinders account for roughly half of the mechanical friction losses in an engine [4,5]. According to a study by Holmberg et al. [6], friction within the piston assembly accounts for 45% of energy losses in an internal combustion engine. The performance of internal combustion engines depends significantly on cylinder liners, one of the most important components of these engines. This has led in recent years to intensive research to improve the performance of piston ring cylinder liner (PRCL) couplings.

Conformability between piston rings and cylinder liners is crucial since it affects the consumption of lubricating oil and greenhouse gas emissions [7]. This conformability

is altered by the liner deformation in the hot state [8]. The failure of the piston ring to adapt to the deformed cylinder liner bore decreases the engine efficiency and increases emissions due to the loss of combustion pressure and the leak of lubricant oil into the combustion chamber. Therefore, additional tightness is required for the piston rings to maintain the required sealing capabilities. This additional tightness decreases the engine efficiency due to the increase in frictional losses and increases the emission as more fuel will be consumed [7,9]. Enhancing the geometrical performance of the cylinder liner to increase its roundness in the hot state represents a good solution for this dilemma [10–13].

Enhancing the geometrical performance of the cylinder liner can be achieved through controlling its deformation from the cold state to the hot state. One of the methods is to start the engine in the cold state with a non-circular liner. Alshwawra et al. [14] showed through advanced simulation techniques that starting the engine with an elliptical liner can reduce the roundness error significantly in the hot state. Further enhancement in the liner's geometrical performance can be achieved with a superposition of this elliptical shape with a conical liner form in the cold state [15]. Flores [13] presented a methodology to control the liner deformation and to enhance its geometrical performance through advanced honing techniques. Alshwawra et al. [16] studied the improvement of the geometrical performance of a freeform honed liner at different operational loads. Edtmayer et al. [17] experimentally found that friction can be reduced by using a liner with a larger bore diameter in its lower half.

Another method to control the liner deformation in the hot state is changing the liner material [12]. Materials or processes for the in-cylinder components of internal combustion engines have been investigated for better friction and performance [18,19]. The majority of the tests to study the conformability between cylinder liner and piston were carried out on cylinder liners made of cast iron [20]. Other materials for cylinder liners are rarely investigated. Thermal stress in cylinder liners made of magnesium alloy and titanium and varying in thickness by 0.5, 1, and 1.5 mm were analyzed. In comparison to cast iron and magnesium alloy, titanium alloy used for cylinder liners has a high heat transfer rate [21]. The grey cast iron liner shows a better geometrical performance compared to an aluminum alloy liner. However, the trends of the deformation and the influence of deformation orders are almost the same for both materials [12]. The thermal expansion coefficient dominates other material properties, including thermal conductivity, Young's modulus, and Poisson's ratio, in terms of the deformation of the liner to improve the conformability between cylinder liner and piston. The conformability between the cylinder liner and piston can be greatly improved by materials with a negative thermal expansion coefficient [22].

Furthermore, the deformation of the liner can be controlled by redesigning the liner to apply an advanced internal local heating and cooling system. In this regard, advanced additive manufacturing (AM) techniques can be useful. Recently, additive manufacturing technologies have gained a lot of attention and have great potential in the engine manufacturing industry [23]. The main advantage of AM over traditional manufacturing processes is the ability to freely shape complex parts without using traditional manufacturing methods such as extrusion, forging, casting and secondary machining processes [24–27]. The near net shaping capability makes AM a cost-effective technique because it minimizes waste [25]. In addition, AM offers great flexibility in terms of the type of raw materials [21]. By using AM techniques, non-traditional liner design can be achieved to improve the geometrical performance of the liner and therefore to enhance the engine efficiency [16].

To be able to use the AM techniques for cylinder liner manufacturing, it is important to investigate the compatibility of AM materials for this type of application. Although AM techniques were considered for the production of some of the parts of the internal combustion engine such as the piston [28,29], they have still not been fully investigated for cylinder liners. This work aims for the investigation of the compatibility of AM materials for the fabrication of a cylinder liner from a structural and the geometrical perspective. This article provides a quantitative study of the deformation of AM liners and the trends in their deformation. Cast iron is used as a reference material since it is the most common

material used for cylinder liners today. Thermal and mechanical bore deformation of the liner has been investigated. The finite-element model is established in this study to predict bore roundness changes for several AM liners and for the reference liner.

The significance of this work can be summarized by: (i) investigation of the structural compatibility for using AM materials in a cylinder liner, (ii) analyzing the geometrical performance of an additively manufactured cylinder liner, and (iii) providing a comparative analysis for the geometrical performance of different AM materials compared to the conventional grey cast iron.

2. Methodology

2.1. Finite Element Techniques

The changes in conformability between piston rings and cylinder liners have also been attributed to mechanical and thermal factors [30,31]. Many researchers have tested the deformation of the cylinder liner and its influencing factors experimentally [32,33]. However, it is often difficult to quantify frictional losses at full scale when examining different engine configurations. Cycle-to-cycle variations, vibrations, thermal effects, and other factors contributing to noise often overshadow frictional differences [34]. Therefore, researchers used simplified rig component testing. Alternatively, different computational approaches have been used for the prediction and modeling of liner deformation [10,35]. An important and useful tool for analyzing and optimizing the geometry of cylinder liners is the use of finite element analyses (FEA) [36]. Structural analysis of cylinder liners is one of the areas where FEA can be efficiently used [37,38]. Applying this method to the engine's cylinder liner can predict its deformation and stress distribution, which can be used to improve the design and reliability of the cylinder liner [39]. Additionally, FEA is powerful for studying the dynamic phenomena associated with piston assembly components [40].

This work uses the ANSYS mechanical solver to calculate the liner deformation numerically. This solver has been used in earlier works as well as in the literature to simulate the liner deformation due to its capability to handle the various non-linearities in the finite element model [14,30,41]. The greatest challenge for FEA is the computing requirements and computing capacity, namely computing power, memory and computing time. It is therefore very important to work with sufficiently simple but accurate models [14].

2.2. Physical Model

The simulation model is developed based on the NISSAN CA18 engine. It is a four-stroke, water-cooled, four-cylinder gasoline engine, arranged in a row, with 83 mm cylinder bore, 83.6 mm piston stroke, and a displacement of 1809 cm. The engine was modified to utilize a 1.6 mm thick cylinder dry liner that is made of grey cast iron. The clearance between the engine block and the liner was 80 μm . The liner deformation was measured experimentally for this modified engine at different operational loads [32,33]. The measured deformation was performed at depths varying between 10 mm from the top of the liner and 90 mm from the top of the liner. For the simulation work, the operational point of 4000 rpm/full load was selected, as it represents the highest thermal load and therefore the highest deformation. Further information about this engine, including its detailed specifications and dimensions, can be found in [42].

2.3. Simulation Model

The simulation in this research followed the model validated by Alshwawra et al. [14]. The model focused on the first and half of the second cylinder to capture the different thermal loads generated by adjacent cylinders and their surroundings. It is expected that the deformation of the first and fourth cylinder liners would be more complicated and asymmetric than that of the second or third cylinder liner due to the asymmetric thermal load [12]. The first and half of the second cylinders are shown in Figure 1 as well as their positions in the engine.

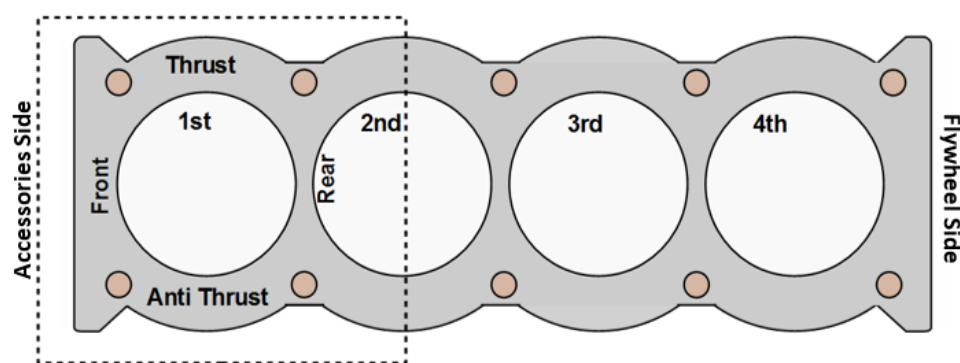


Figure 1. One and a half cylinder model used in this study with the different sides of the cylinder.

At any specific point, the directional local deformation can be found using the following equation:

$$d\delta_i = \varepsilon(i)di \quad (1)$$

where δ_i and $\varepsilon(i)$ represent the local deformation and local strain in i direction, respectively. The above-mentioned local strain is the total summation of elastic strain ε_{el} and thermal strain ε_{th} . Hook's law can be used to find the elastic strain:

$$\{\varepsilon_{el}\} = [D]^{-1}\{\sigma\} \quad (2)$$

Here, $\{\sigma\}$ represents the stress vector, and $[D]$ represents a matrix related to the material's mechanical properties. To find the thermal strain:

$$\varepsilon_{th} = \int_{T_{ref}}^T \alpha(T)dT \quad (3)$$

with the thermal expansion coefficient $\alpha(T)$, the strain free temperature T_{ref} , and the operating temperature T .

2.4. Computational Mesh

Finite element analysis (FEA) simulation requires accurate meshing in order to produce realistic results. On one hand, a high-density mesh provides the best results, but it also requires a lot of computing time and storage space. On the other hand, the coarse mesh can lead to unrealistic results. Therefore, an adaptive mesh that is neither too fine nor too coarse is used. Grid independency was tested for multiple mesh sizes starting from 25 thousand nodes and 16 thousand elements up to one million nodes and half a million elements. Based on this test, a mesh size of 197,666 elements and 112,944 nodes was selected. The average calculation time for a supercomputer with 96 processors is 25 h per run. The detailed mesh properties, grid independence test and circumferential position dependent deformation are provided in [14].

2.5. Boundary Conditions

The temperatures of the liner and block inner wall at 4000 rpm/full load were measured experimentally [32]. The measured liner temperature varies between 155 and 198 °C while the measured block temperature varies between 103 and 180 °C. The temperature of the coolant is given to be 80 °C. It was also assumed that the temperature of the outer walls of the block is equal to the coolant temperature, and the bolt pre-tension is 80,000 N. For the calculations, it is assumed that the upper surface is fixed in the axial direction (from top to bottom). As the model is subjected to both thermal and mechanical loads, it is numerically solved using the direct coupled approach, in which the mechanical and thermal matrices are solved in parallel. The accuracy in this case is higher compared to the use of sequential approaches. However, more computational time is required.

The thermal deformation increases with the physical time until it reaches the steady state. The simulated liner deformations were compared with the measured line deformations for the terminal cylinder at 4000 rpm/full load. The simulated deformations showed a good agreement in term of values and trend with the corresponding experimental deformations at different elevations. Based on that, the model is considered to be valid. The detailed model configuration, boundary conditions, temperature distributions, and model validation are explained in [14] for this reference case (grey cast iron liner at 4000 rpm/full load).

2.6. Liner's Materials

The validated model was used to simulate the liner deformation for different AM materials at 4000 rpm/full load. For the purpose of this study, five additive manufactured materials (Inconel 625, Inconel 718, 17-4PH stainless steel, AlSi10Mg, Ti6Al4V) were analyzed along with the reference cast iron material. Despite having different properties, all the selected materials were used in high-quality, complex-designed products that are exposed to strong mechanical and thermal loads. The properties of the materials are summarized in Table 1.

Table 1. Properties of AM materials vs. grey cast iron [36–39].

| | | Grey Cast Iron | Inconel 625 | Inconel 718 | 17-4PH | AlSi10Mg | Ti6Al4V |
|-------------------------------|--|----------------|-------------|-------------|-----------|----------|-----------|
| Density | g/cm^3 | 7.2 | 8.44 | 8.2 | 7.75 | 2.68 | 4.4 |
| Melting Range | $^{\circ}\text{C}$ | 1180–1380 | 1290–1350 | 1260–1335 | 1400–1450 | 557–596 | 1692–1698 |
| Thermal expansion coefficient | $\mu\text{m/m } ^{\circ}\text{C}$ (150 $^{\circ}\text{C}$) | 11.7 | 12.8 | 13 | 10.7 | 23.6 | 10 |
| Elastic modulus | GPa | 110 | 162 | 165 | 204 | 76 | 107 |
| Tensile strength | MPa | 250 | 655 | 648 | 970 | 251 | 1098 |
| Thermal Conductivity | W/mk (200 $^{\circ}\text{C}$) | 47.5 | 12.5 | 13.7 | 18.3 | 113 | 7.5 |

3. Results and Discussion

The deformation of the liner was simulated at three different depths from the top deck, as well as 10, 50 and 90 mm. The analysis considered front, rear, thrust and anti-thrust sides as shown in Figure 2.

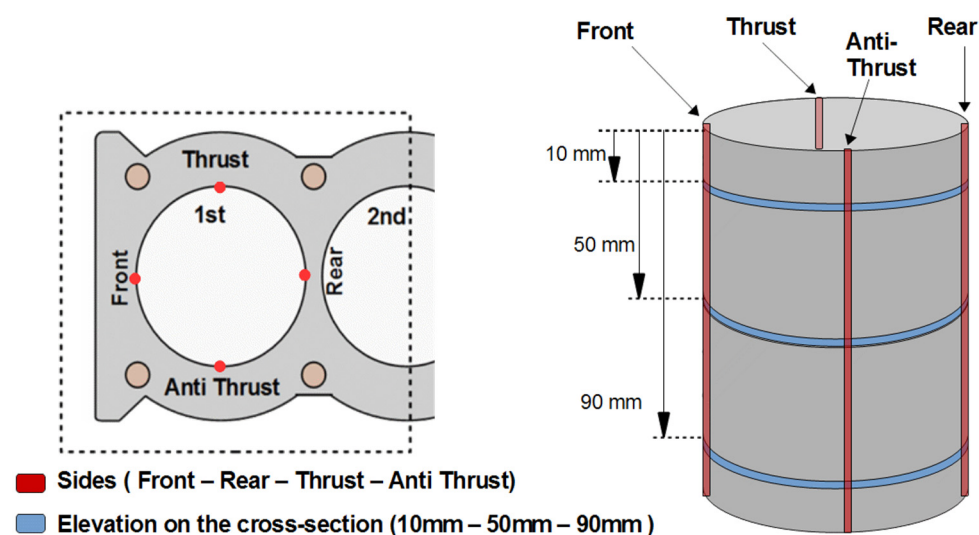


Figure 2. Locations and orientations of the deformation paths for the cylinder liner.

A variety of methods were used to assess the compatibility of additive manufacturing materials for the cylinder liner. As a starting point, the maximum deformation method was used, since it is the simplest method to study the influence of different materials on the structural behavior of the liner. Data can be collected directly from the ANSYS interface, which shows an overview of the direction and the amplitude of liner deformations. The deformations in the Z direction are very small compared to the deformations in the XY plane; thus, the maximum deformation in the Z direction can be ignored and the comparison is only conducted in the XY plane. The maximum deformation at the three mentioned depths is depicted in Figure 3.

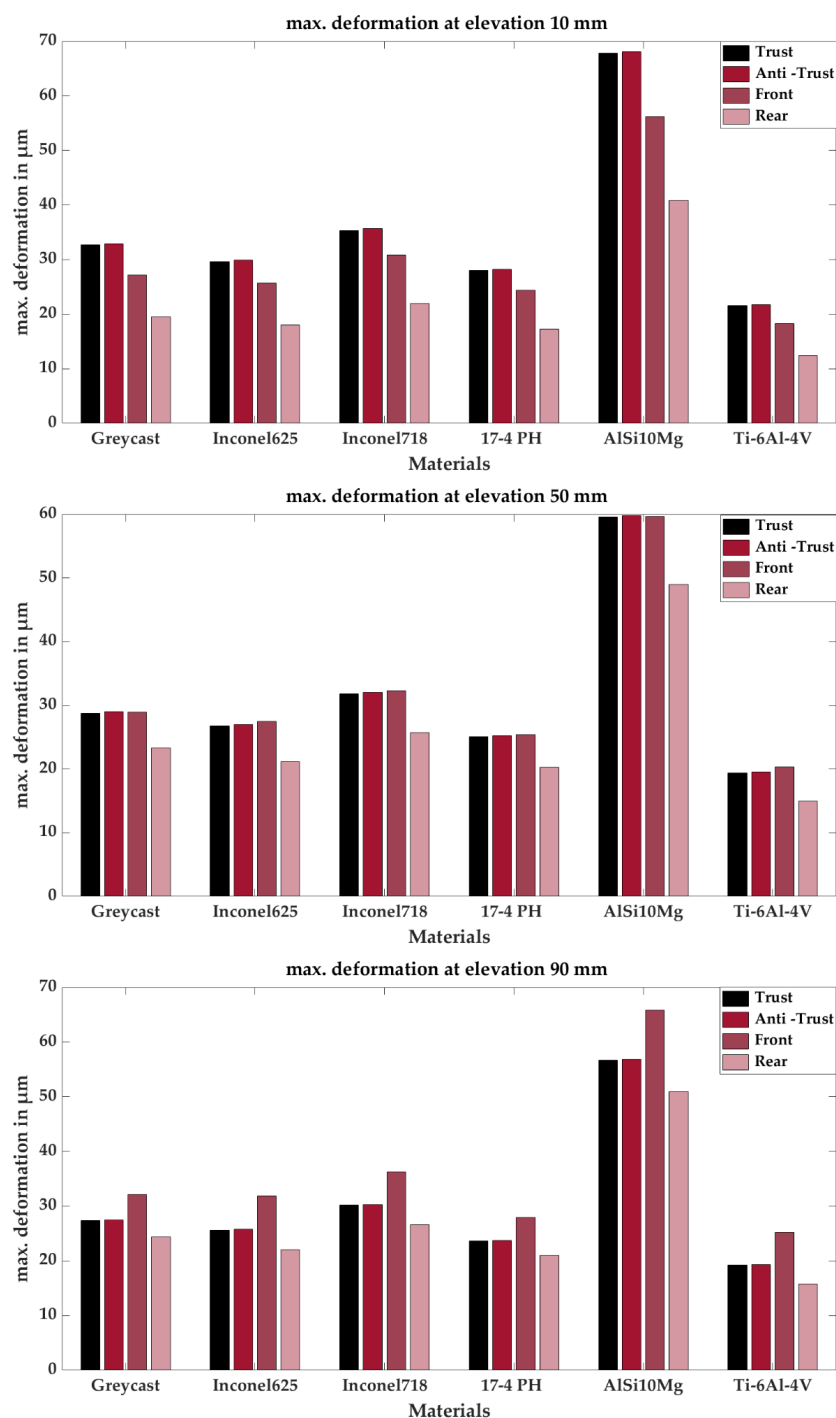


Figure 3. Maximum deformation at 10, 50 and 90 mm from the top.

It can be seen from the figure that the maximum deformation in the thrust and anti-thrust directions is almost equal but varies in the front and rear directions. This is expected due to the different heat boundary conditions in the front–rear direction. AlSi10Mg increases the maximum deformation of the cylinder liner, as the deformations are almost twice as large as the reference material. This can be referred to as the high thermal expansion coefficient of AlSi10Mg alloy compared with grey cast iron as shown in Table 1. The maximum deformation of the liner decreased when using the Ti6Al4V alloy. Other materials show close maximum deformations to the grey cast iron. Table 2 summarizes the maximum deformation deviations from the grey cast iron.

Table 2. Deviation of max. deformation at elevations of 10, 50 and 90 mm from the top compared with the reference material.

| Deviation of Max. Deformation at Elevation 10 mm (in %) | | | | | |
|--|-----------------------|--------|-------------|-------|-------|
| Material | Side | Thrust | Anti-Thrust | Front | Rear |
| | Grey cast iron (ref.) | | - | - | - |
| Inconel625 | | -9.5 | -9.2 | -5.5 | -7.9 |
| Inconel718 | | 8.2 | 8.4 | 13.4 | 12.5 |
| 17-4PH | | -14.3 | -14.3 | -10.2 | -11.7 |
| AlSi10Mg | | 107.5 | 106.9 | 106.5 | 109.4 |
| Ti6Al4V | | -34.1 | -33.9 | -32.7 | -36.5 |
| Deviation of Max. Deformation at Elevation 50 mm (in %) | | | | | |
| Material | Side | Thrust | Anti-Thrust | Front | Rear |
| | Grey cast iron (ref.) | | - | - | - |
| Inconel625 | | -7.1 | -6.8 | -5.1 | -9.3 |
| Inconel718 | | 10.5 | 10.7 | 11.6 | 10.1 |
| 17-4PH | | -12.8 | -12.8 | -12.2 | -13.3 |
| AlSi10Mg | | 107.0 | 106.4 | 106.2 | 110.0 |
| Ti6Al4V | | -32.8 | -32.5 | -29.8 | -35.9 |
| Deviation of Maximum Deformation at Elevation 90 mm (in %) | | | | | |
| Material | Side | Thrust | Anti-Thrust | Front | Rear |
| | Grey cast iron (ref.) | | - | - | - |
| Inconel625 | | -6.6 | -6.3 | -0.9 | -9.7 |
| Inconel718 | | 10.1 | 10.1 | 12.6 | 9.2 |
| 17-4PH | | -13.8 | -13.8 | -13.1 | -14.0 |
| AlSi10Mg | | 107.0 | 106.6 | 104.6 | 109.2 |
| Ti6Al4V | | -29.8 | -29.6 | -21.8 | -35.3 |

Table 2 shows the percent deviation of maximum deformation from the reference material (grey cast iron). Compared to the reference material, the distortions are greater when the deviation is positive but less when it is negative. Inconel625, 17-4PH and Ti6Al4V decreased the maximum deformation by different percentages. Ti6Al4V alloy shows the maximum reduction (-36.5%) at 10 mm from the deck. The other AM materials (AlSi10Mg and Inconel718) increase the maximum deformations. The tables also show that the deviation of maximum deformation is consistent at all sides for each material. This means that the deviation is either positive or negative at all sides.

The structural compatibility of the additive manufactured materials for the cylinder liner was also evaluated through the analysis of the change in liner radius. This method enables determining the deformation at all points of the cylinder liner circumference. The radial deformation is calculated at each point using the following set of equations:

$$R = \sqrt{(X_{new}^2 + Y_{new}^2)} \quad (4)$$

where

$$X_{new} = X_o + Def_x \quad (5)$$

$$Y_{new} = Y_o + Def_y \quad (6)$$

X_{new} : X-coordinate of the points after deformation;

Y_{new} : Y-coordinate of the points after deformation;

X_o : Initial x-coordinate (before deformation);

Y_o : Initial y-coordinate (before deformation);

Def_x : Value of deformation in x-direction;

Def_y : Value of deformation in y-direction.

Figure 4 shows the radius of the liner cross-section changes at different levels when using AM materials. This change, whether increasing or decreasing, is due to the thermal deformation in the liner. The changes are not in the same direction. The radius increases on the thrust and anti-thrust sides but decreases on the other two sides (front and rear). All materials, including the grey cast iron, show the same behavior. Based on this observation, it can be concluded that more comprehensive details about liner deformation can be obtained by analyzing the deformation at those four points.

AlSi10Mg has a significantly higher change in radius than the other materials. There is a difference of 60–70 μm between the ideal shape radius (0.0391 m) and the radius on the four main sides of the liners (thrust, anti-thrust, front, and rear). The radius of the Ti6Al4V alloy liner was the closest to the non-deformed liner. Other additive manufactured materials showed different deformation behaviors. Inconel625 and 17-4PH show a slight improvement in the radius curve compared to the grey cast iron.

This figure illustrates the circumferential deformations at the different main elevations of the cylinder liner (10, 50, and 90 mm). Due to the observed differences in radius between the elevation layers, the bore deformation along the elevation was studied. The investigation of the bore deformation plays an important role in obtaining a comprehensive description of the deformations of the additively manufactured liners. As observed previously, the greatest deformation in the cylinder liners occurs on the four main sides (thrust, anti-thrust, front, and rear). These four sides were therefore selected for investigation, as shown in Figure 5.

It is apparent in Figure 5 that deformation varies from side to side. There is usually more deformation in the upper part than in the lower part. Inconel625, 17-4P, Ti6Al4V and Inconel718 have a very similar bore deformation trend similar to the grey cast iron. These liners were deformed into a conical shape in the thrust–anti-thrust direction. The difference in deformation on the thrust and anti-thrust was less than 5 μm . In the case of AlSi10Mg, the bore deformation looked different. The top part was even more deformed than the other materials. There could have been a difference of up to 15 μm , and the shape remained conical.

In order to determine whether additive manufactured materials affect the roundness of the liner's cross-section, the roundness errors were calculated at different elevations (10, 50, and 90 mm) using the least squares circle (LSC) method. In this method, a specific center point of the circle is set in such a way that the sum of the squares of the deviation is minimized for the measured profile. The inscribed circle and the circumscribed circle are drawn next. The roundness error ΔR is the difference between the radius of the inscribed circle and the radius of the circumscribed circle as shown in Figure 6a.

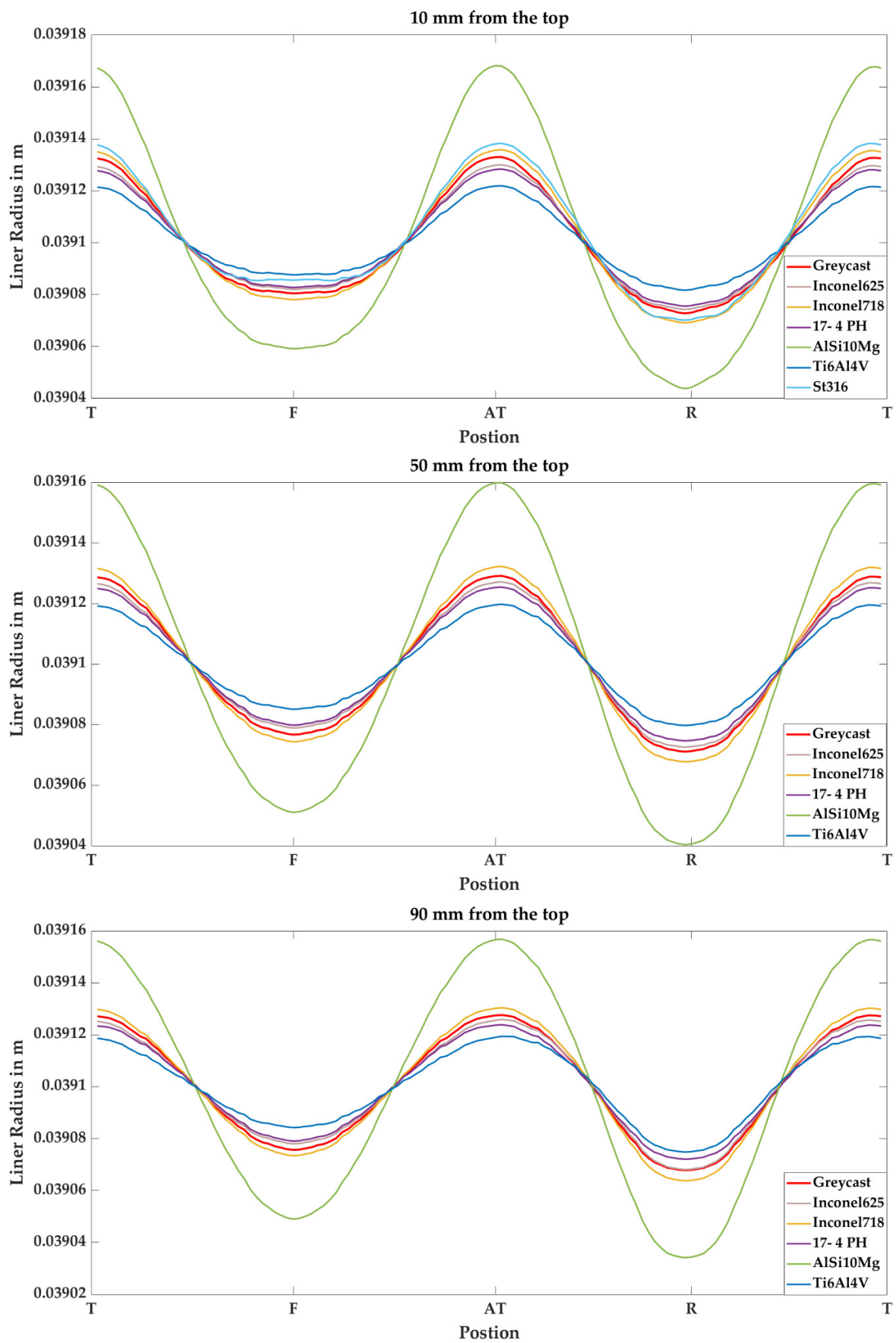
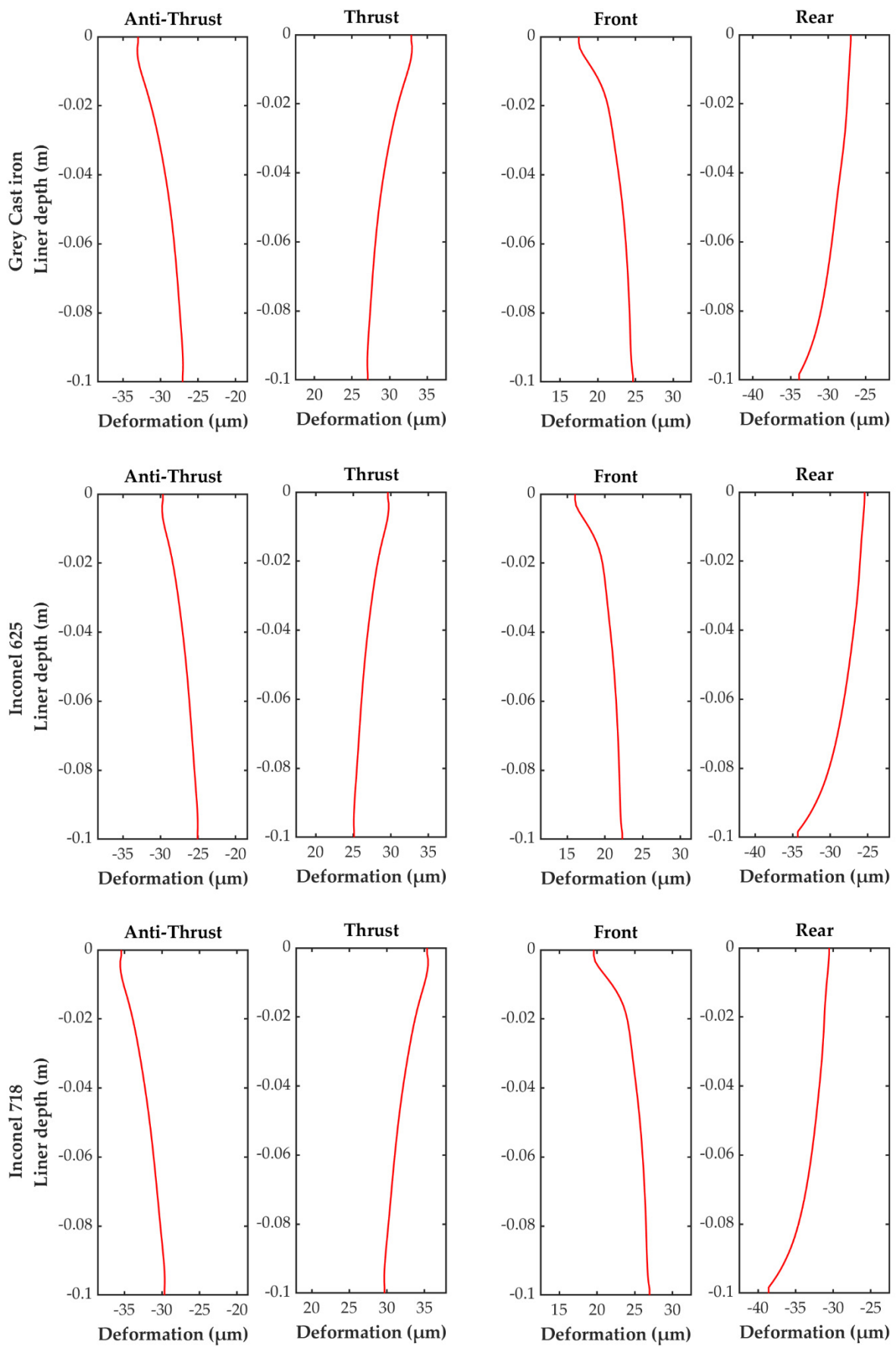


Figure 4. Radius of the cylinder liner at elevations 10, 50 and 90 mm.



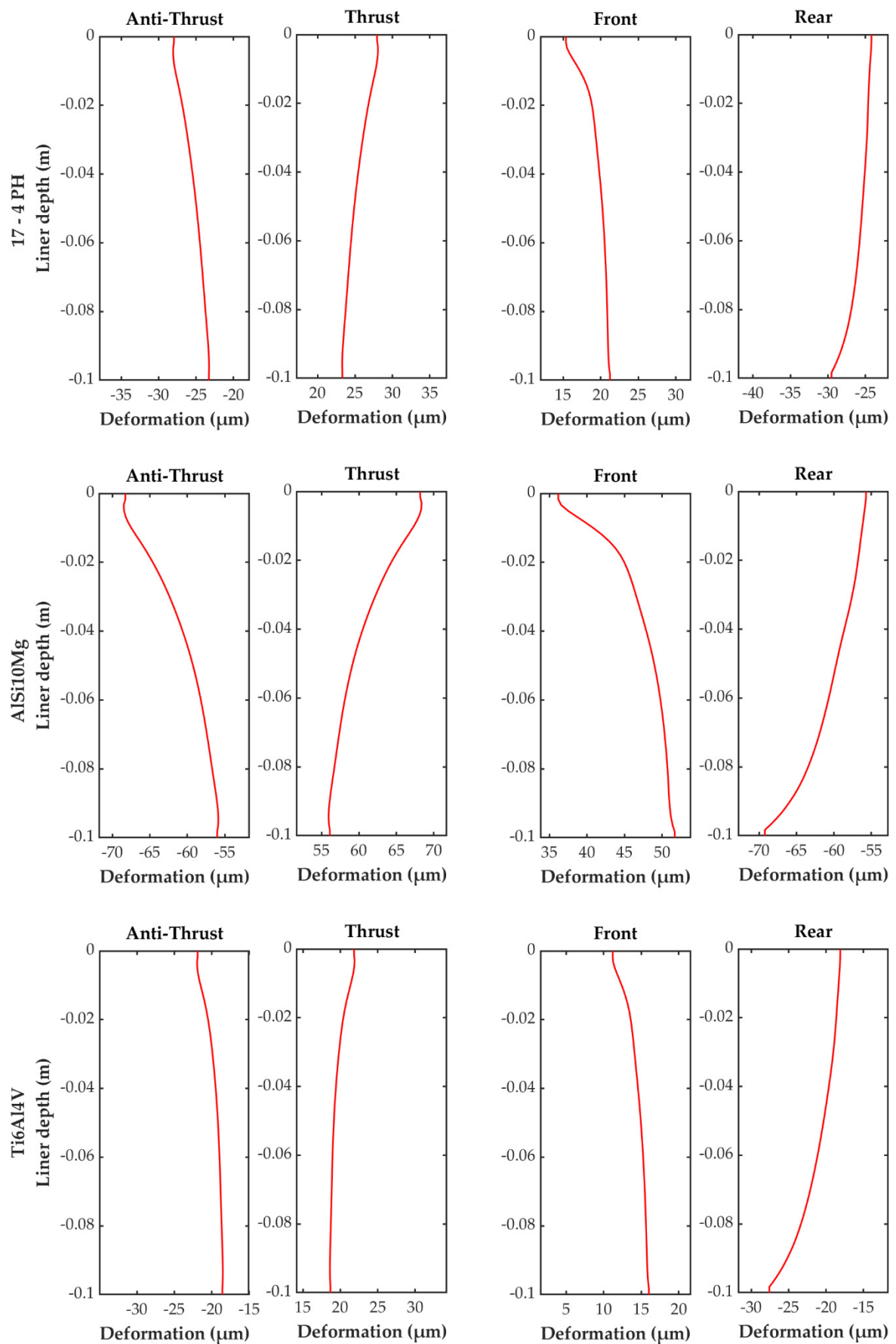


Figure 5. Bore deformation for grey cast iron and AM material.

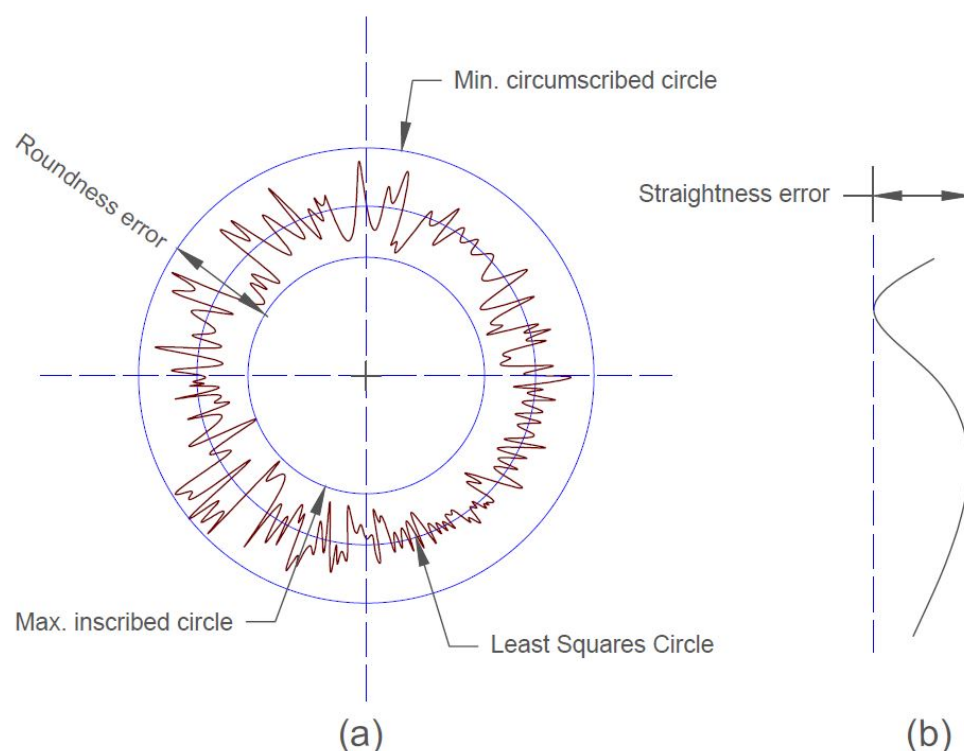


Figure 6. (a) Roundness error; (b) straightness error.

While the straightness error represents the change in radius over depth, the roundness error represents the change in radius over circumference. Figure 6b shows how to calculate the straightness error as the minimum distance between two straight lines that contain all the points. Table 3 shows the roundness error of the six liners (five additive manufactured materials and grey cast iron). Keeping in mind that in the cold state, all materials exhibited no roundness error, the roundness errors in the fired state increased significantly. There was a variation in the roundness error of the six liners. Figure 7 shows the deviation of the roundness error (RE) from the roundness error of the grey cast iron liner.

Table 3. Roundness deviation of the liner in μm .

| Material | Liner Height | Fired State | | |
|-----------------------|--------------|-------------|-------|-------|
| | | 10 mm | 50 mm | 90 mm |
| Grey cast iron (ref.) | | 59.5 | 57.2 | 58.5 |
| Inconel625 | | 54.8 | 53.5 | 56.4 |
| Inconel718 | | 65.8 | 63.5 | 65.3 |
| 17-4PH | | 52.0 | 49.9 | 50.6 |
| AlSi10Mg | | 123.2 | 118.2 | 120.5 |
| Ti6Al4V | | 39.6 | 39.2 | 43.4 |

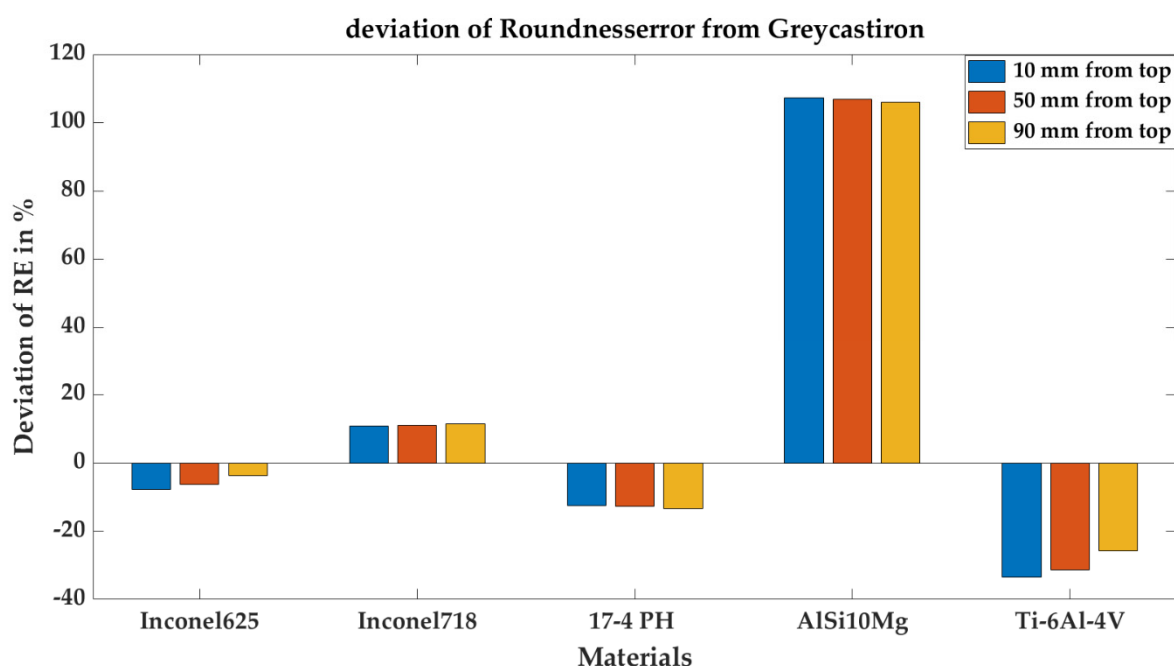


Figure 7. Deviation of roundness error of AM materials from grey cast iron.

Materials such as Ti6Al4V and 17-4PH have a significant improvement in roundness compared to grey cast iron. With an approximate roundness error of 39 μm , Ti6Al4V had the lowest roundness error. The two Inconel materials show different performances. While Inconel 625 had better roundness values than grey cast iron, the roundness error was greater for Inconel 718 than for grey cast iron. AlSi10Mg had about a 120 μm roundness error, which is very high compared to the grey cast iron. A larger roundness error implies that the piston rings need increased pretension to prevent leakage. This increases the frictional losses to a certain extent [1]; therefore, the friction with AlSi10Mg could increase compared to the grey cast iron. In contrast, friction can be reduced when Ti6Al4V and 17-4PH materials are used.

Table 4 shows the straightness error of the six liners (five AM materials and grey cast iron), while Figure 8 shows a deviation in the straightness error (SE) of the AM materials from the straightness error of the grey cast iron. Note that there was no straightness error in the cold state. The table shows that Ti6Al4V had the best and smallest straightness error between all material alloys but not from all sides. On the rear side, the straightness error value (9.5 μm) was higher than the value for the reference material. The straightness error with Inconel625 on the rear also had a higher value compared with grey cast iron. Again, AlSi10Mg had the largest straightness error on both sides: front and rear (15.5 and 13.5 μm). In general, the ranking from this analysis remains the same as for the elevation of the roundness error.

Table 4. Straightness deviation of the liner in μm .

| Material | Side | Fired State | | | |
|-----------------------|------|-------------|-------------|-------|------|
| | | Thrust | Anti-Thrust | Front | Rear |
| Grey cast iron (ref.) | | 5.9 | 6.1 | 7.2 | 6.9 |
| Inconel625 | | 4.6 | 4.7 | 6.3 | 8.9 |
| Inconel718 | | 5.8 | 5.9 | 7.4 | 8.0 |
| 17-4PH | | 4.8 | 4.8 | 5.9 | 5.3 |
| AlSi10Mg | | 12.4 | 12.6 | 15.5 | 13.5 |
| Ti6Al4V | | 3.3 | 3.4 | 4.8 | 9.5 |

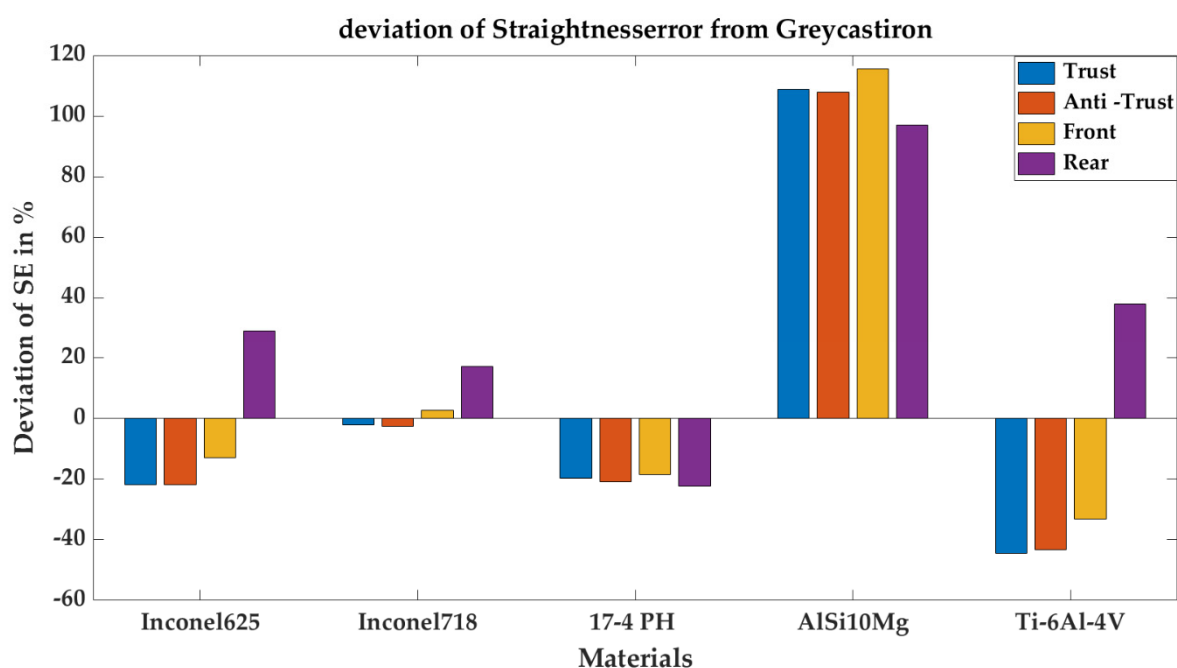


Figure 8. Deviation of straightness error of AM materials from grey cast iron.

These results show that AM materials can be used as an alternative to conventional materials from a structural point of view. Some of these AM alloys will even enhance the geometrical performance of the cylinder liner and therefore enhance the overall efficiency of the engine. For example, the Ti6Al4V alloy reduces the average roundness error by 30% and the average straightness error by 21% compared with the grey cast iron.

4. Conclusions

Materials used in additive manufacturing have proven themselves in many fields for years. Thus, this technology can possibly be used in new areas that require revolutionary design and manufacturing processes. This technology provides a good development opportunity for the piston ring cylinder liner coupling, which is considered as an important component of internal combustion engines. The utilization of AM techniques for the manufacturing process of liners can allow for new degrees of freedom in terms of cooling and forming of the liner. This can improve the conformability of the piston ring to the cylinder liner, which is essential since the lack of conformability can affect engine performance and energy consumption.

One of the biggest barriers for using additive manufacturing in liners is the lack of knowledge about whether AM materials are suitable for use in cylinder liners. In this work, the structural compatibility of additive manufactured materials for the cylinder liner was investigated using a validated finite-element model. The influences and effects of the AM materials on the liner deformation at 4000 rpm/full load were simulated and compared to the conventional grey cast iron. Based on simulation results, the maximum deformation, the bore and circumferential deformation, and the roundness and straightness errors were determined.

The results show that the maximum liner deformation as well as the bore and circumferential deformations of the AM liners are comparable to the grey cast iron. Ti6Al4V, Inconel 625 and 17-4PH materials can reduce the maximum deformation on average by 32%, 7%, and 13%, respectively, while AISi10Mg and Inconel 718 increase the maximum deformation on average by 107% and 11%, respectively. From a geometrical performance aspect, the roundness error at hot state decreased by using Ti6Al4V, Inconel 625 and 17-4PH materials. Maximum reduction of 36% compared to grey cast iron was achieved when using Ti6Al4V material. The straightness error at hot state was reduced by about 20% for the 17-4PH material. The enhancement of the geometrical performance of the liner using

Ti6Al4V, Inconel 625 and 17-4PH materials can be reflected on the efficiency on the PRCL coupling and therefore on the total energy efficiency.

These results indicate that additive manufactured materials can be used as a liner material from a structural point of view. However, a full understanding of the additively manufactured cylinder liners and their impacts on the tribological performance of the piston group would require more detailed investigations. Moreover, a revolutionary design for cylinder liners can be achieved in order to control the liner deformation and tribological behavior. This can improve internal combustion engine technology and maximize the benefits of conversion to fuels. The findings of this work present a step in this direction.

Author Contributions: Conceptualization, A.A.; methodology, A.A.; software, A.A. and A.A.S.; validation, A.A.; formal analysis, A.A.S. and A.S.; investigation, A.A.S.; resources, F.D.; data curation, A.A. and A.S.; writing—original draft preparation, A.S.; writing—review and editing, A.A., A.A.S., A.S. and F.D.; visualization, A.A.S. and A.S.; supervision, F.D.; project administration, A.A.; funding acquisition, A.A. and F.D. All authors have read and agreed to the published version of the manuscript.

Funding: Partial fund is given from Leibniz University Hannover. The study is based on earlier funded research work from German Federal Ministry for Economic Affairs and Energy (BMWi) within the cooperation project (Antriebsstrang 2025). The study is intended as a preparation for a new research project in conjunction with additive manufacturing. The publication of this article was funded by the Open Access Fund of the Leibniz Universität Hannover.

Acknowledgments: This publication was made possible with the support and within the interdisciplinary setting of the Arab–German Young Academy of Sciences and Humanities (AGYA). AGYA is supported by the German Federal Ministry of Education and Research (BMBF). The authors also would like to thank F. Pohlmann-Tasche and F. Stelljes for sharing their experiences and fruitful discussions.

Conflicts of Interest: The authors declare no conflict of interest.

References

- Dargay, J.; Gately, D.; Sommer, M. Vehicle Ownership and Income Growth, Worldwide: 1960–2030. *Energy J.* **2007**, *28*, 143–170. [[CrossRef](#)]
- King, J. *The King Review of Low-Carbon Cars*; LowCVP: London, UK, 2007.
- Rahmani, R.; Rahnejat, H.; Fitzsimons, B.; Dowson, D. The Effect of Cylinder Liner Operating Temperature on Frictional Loss and Engine Emissions in Piston Ring Conjunction. *Appl. Energy* **2017**, *191*, 568–581. [[CrossRef](#)]
- Heywood, J.B. *Internal Combustion Engine Fundamentals*, 2nd ed.; McGraw-Hill Education: New York, NY, USA, 2018; Volume 2012.
- Kurbet, S.N.; Malagi, R.R. Review on Effects of Piston and Piston Ring Dynamics Emphasis with Oil Consumption and Frictional Losses in Internal Combustion Engines. In Proceedings of the 8th International Conference on Engines for Automobiles, SAE Technical Papers, Capri, Italy, 16 September 2007.
- Holmberg, K.; Andersson, P.; Erdemir, A. Global Energy Consumption Due to Friction in Passenger Cars. *Tribol. Int.* **2012**, *47*, 221–234. [[CrossRef](#)]
- Styles, G.; Rahmani, R.; Rahnejat, H.; Fitzsimons, B. In-Cycle and Life-Time Friction Transience in Piston Ring-Liner Conjunction under Mixed Regime of Lubrication. *Int. J. Engine Res.* **2014**, *15*, 862–876. [[CrossRef](#)]
- Liu, N.; Wang, C.; Xia, Q.; Gao, Y.; Liu, P. Simulation on the Effect of Cylinder Liner and Piston Ring Surface Roughness on Friction Performance. *Mech. Ind.* **2022**, *23*, 8. [[CrossRef](#)]
- Delprete, C.; Razavykia, A. Piston Dynamics, Lubrication and Tribological Performance Evaluation: A Review. *Int. J. Engine Res.* **2018**, *21*, 725–741. [[CrossRef](#)]
- Koch, F.; Decker, P.; Gülpen, R.; Quadflieg, F.-J.; Loeprecht, M. Cylinder Liner Deformation Analysis—Measurements and Calculations. *SAE Tech. Pap.* **1998**, *107*, 838–847. [[CrossRef](#)]
- Selmani, E.; Delprete, C.; Bisha, A. Cylinder Liner Deformation Orders and Efficiency of a Piston Ring-Pack. *E3S Web Conf.* **2019**, *95*, 04001. [[CrossRef](#)]
- Alshwawra, A.; Pohlmann-Tasche, F.; Stelljes, F.; Dinkelacker, F. Cylinder Liner Deformation—An Investigation of Its Decomposition Orders under Varied Operational Load. *SAE Tech. Pap.* **2022**, 2022-01-1040. [[CrossRef](#)]
- Flores, G.K. Graded Freeform Machining of Cylinder Bores Using Form Honing. *SAE Tech. Pap.* **2015**, 2015-01-1725. [[CrossRef](#)]
- Alshwawra, A.; Pasligh, H.; Hansen, H.; Dinkelacker, F. Increasing the Roundness of Deformed Cylinder Liner in Internal Combustion Engines by Using a Non-Circular Liner Profile. *Int. J. Engine Res.* **2021**, *22*, 1214–1221. [[CrossRef](#)]
- Alshwawra, A.; Pohlmann-Tasche, F.; Stelljes, F.; Dinkelacker, F. Enhancing the Geometrical Performance Using Initially Conical Cylinder Liner in Internal Combustion Engines—A Numerical Study. *Appl. Sci.* **2020**, *10*, 3705. [[CrossRef](#)]

16. Alshwawra, A.; Pohlmann-Tasche, F.; Stelljes, F.; Dinkelacker, F. Effect of Freeform Honing on the Geometrical Performance of the Cylinder Liner—Numerical Study. *SAE Int. J. Engines* **2022**, *16*, 2023. [[CrossRef](#)]
17. Edtmayer, J.; Lösch, S.; Hick, H.; Walch, S. Comparative Study on the Friction Behaviour of Piston/Bore Interface Technologies. *Automot. Engine Technol.* **2019**, *4*, 101–109. [[CrossRef](#)]
18. Rejowski, E.D.; Soares, E.; Roth, I.; Rudolph, S. Cylinder Liner in Ductile Cast Iron for High Loaded Combustion Diesel Engines. *J. Eng. Gas Turbines Power* **2012**, *134*, 072807. [[CrossRef](#)]
19. Baby, A.K.; Priyaranjan, M.; Deepak Lawrence, K.; Rajendrakumar, P.K. Tribological Behaviour of Hypereutectic Al-Si Automotive Cylinder Liner Material under Dry Sliding Wear Condition in Severe Wear Regime. *Proc. Inst. Mech. Eng. Part J J. Eng. Tribol.* **2021**, *235*, 1450–1462. [[CrossRef](#)]
20. Abouchi, M.; Basturk, S. An Investigation on the Friction Losses between Cylinder Liner and Piston Rings. *Sustain. Eng. Innov.* **2022**, *4*, 146–155. [[CrossRef](#)]
21. Seifi, M.; Salem, A.; Beuth, J.; Harrysson, O.; Lewandowski, J.J. Overview of Materials Qualification Needs for Metal Additive Manufacturing. *JOM* **2016**, *68*, 747–764. [[CrossRef](#)]
22. Migita, R. *Effects of Material Properties on Bore Deformation of Engine Cylinder Liner*; Kyushu University: Kyushu, Japan, 2020.
23. Gray, J.; Depcik, C. Review of Additive Manufacturing for Internal Combustion Engine Components. *SAE Int. J. Engines* **2020**, *13*, 617–632. [[CrossRef](#)]
24. Liu, S.; Shin, Y.C. Additive Manufacturing of Ti6Al4V Alloy: A Review. *Mater. Des.* **2019**, *164*, 107552. [[CrossRef](#)]
25. Nemova, D.; Kotov, E.; Andreeva, D.; Khorobrov, S.; Olshevskiy, V.; Vasileva, I.; Zaborova, D.; Musorina, T. Experimental Study on the Thermal Performance of 3D-Printed Enclosing Structures. *Energies* **2022**, *15*, 4230. [[CrossRef](#)]
26. Frazier, W.E. Metal Additive Manufacturing: A Review. *J. Mater. Eng. Perform.* **2014**, *23*, 1917–1928. [[CrossRef](#)]
27. Guo, N.; Leu, M.C. Additive Manufacturing: Technology, Applications and Research Needs. *Front. Mech. Eng.* **2013**, *8*, 215–243. [[CrossRef](#)]
28. Millo, F.; Piano, A.; Roggio, S.; Bianco, A.; Pesce, F.C.; Vassallo, A.L. Numerical Assessment of Additive Manufacturing-Enabled Innovative Piston Bowl Design for a Light-Duty Diesel Engine Achieving Ultra-Low Engine-Out Soot Emissions. *SAE Int. J. Engines* **2021**, *15*, 427–443. [[CrossRef](#)]
29. Kumaran, M.; Senthilkumar, V.; Justus Panicker, C.T.; Shishir, R. Concept Design and Analysis of Multi-Layer and Multi-Process Piston of SS316L and AlSi10Mg by Additive Manufacturing. In *Recent Advances in Materials and Modern Manufacturing*; Palani, I.A., Sathiya, P., Palanisamy, D., Eds.; Springer Nature: Singapore, 2022; pp. 441–446.
30. Lu, Y.; Liu, C.; Zhang, Y.; Wang, J.; Yao, K.; Du, Y.; Müller, N. Evaluation on the Tribological Performance of Ring/Liner System under Cylinder Deactivation with Consideration of Cylinder Liner Deformation and Oil Supply. *PLoS ONE* **2018**, *13*, 0204179. [[CrossRef](#)] [[PubMed](#)]
31. Yang, Z.; Li, B.; Yu, T. Distortion Optimization of Engine Cylinder Liner Using Spectrum Characterization and Parametric Analysis. *Math. Probl. Eng.* **2016**, *2016*, 9212613. [[CrossRef](#)]
32. Hitosugi, H.; Nagoshi, K.; Ebina, M.; Furuhashi, S. Study on Cylinder Bore Deformation of Dry Liner in Engine Operation. *JSAE Rev.* **1996**, *17*, 113–119. [[CrossRef](#)]
33. Fujimoto, H.; Yoshihara, Y.; Goto, T.; Furuhashi, S. Measurement of Cylinder Bore Deformation during Actual Operating Engines. *SAE Tech. Pap.* **1991**, 910042. [[CrossRef](#)]
34. Johansson, S.; Nilsson, P.H.; Ohlsson, R.; Rosén, B.G. Experimental Friction Evaluation of Cylinder Liner/Piston Ring Contact. *Wear* **2011**, *271*, 625–633. [[CrossRef](#)]
35. Maassen, F.; Koch, F.; Schwaderlapp, M.; Ortjohann, T.; Dohmen, J. Analytical and Empirical Methods for Optimization of Cylinder Liner Bore Distortion. *SAE Tech. Pap.* **2001**, 2001-01-0569. [[CrossRef](#)]
36. Barbieri, S.G.; Mangeruga, V.; Giacomini, M.; Laurino, C.; Lorenzini, M. A Finite Element Numerical Methodology for the Fatigue Analysis of Cylinder Liners of a High Performance Internal Combustion Engine. *Key Eng. Mater.* **2019**, *827*, 288–293. [[CrossRef](#)]
37. Murakami, H.; Nakanishi, N.; Ono, N.; Kawano, T. New Three-Dimensional Piston Secondary Motion Analysis Method Coupling Structure Analysis and Multi Body Dynamics Analysis. *SAE Int. J. Engines* **2012**, *5*, 42–50. [[CrossRef](#)]
38. Jafari, A.A.; Khalili, S.M.R.; Azarafza, R. Transient Dynamic Response of Composite Circular Cylindrical Shells under Radial Impulse Load and Axial Compressive Loads. *Thin-Walled Struct.* **2005**, *43*, 1763–1786. [[CrossRef](#)]
39. Li, M.H.; Dong, D.D. Finite Element Analysis of the Cylinder Liner of a 280 Diesel Engine. *Adv. Mater. Res.* **2013**, *616–618*, 1745–1750. [[CrossRef](#)]
40. Malagi, R.R.; Kurbet, S.N.; Gowrishenkar, N. Finite Element Study on Piston Assembly Dynamics in Multicylinder Internal Combustion Engine. *SAE Tech. Pap.* **2011**, 2011-01-1075. [[CrossRef](#)]
41. Liang, X.; Wang, Y.; Huang, S.; Yang, G.; Tang, L.; Cui, G. Investigation on Cylinder Bore Deformation under Static Condition Based on Fourier Decomposition. *SAE Tech. Pap.* **2017**, 2017-01-0366. [[CrossRef](#)]
42. Flammang, J.M. *Standard Catalog of Imported Cars 1946–1990*, 1st ed.; Kp Books: Iola, WI, USA, 1992; ISBN 0873411587.

List of publications

Alshwawra, A., Almuhtady, A., and Sakhrieh, A., “Electricity system security in Jordan: A response for arab uprising,” *Heliyon* 9(5):e15961, 2023, doi:10.1016/j.heliyon.2023.e15961.

Alawadhi, G., Almehiri, M., Sakhrieh, A., **Alshwawra, A.**, and Asfar, J. Al, Cost Analysis of Implementing In-Pipe Hydro Turbine in the United Arab Emirates Water Network, *Sustainability* 15(1), 2023, doi:10.3390/su15010651.

Alshwawra, A., Abo Swerih, A., Sakhrieh, A., and Dinkelacker, F., Structural Performance of Additively Manufactured Cylinder Liner—A Numerical Study, *Energies* 15(23), 2022, doi:10.3390/en15238926.

Alshwawra, A., Pohlmann-Tasche, F., Stelljes, F., and Dinkelacker, F., “Effect of Freeform Honing on the Geometrical Performance of the Cylinder Liner—Numerical Study,” *SAE Int. J. Engines* 16(4):03-16-04-0027, 2022, doi:10.4271/03-16-04-0027.

Alshwawra, A., Pohlmann-Tasche, F., Stelljes, F., and Dinkelacker, F., “Cylinder Liner Deformation - An Investigation of its Decomposition Orders under Varied Operational Load,” *SAE Powertrains, Fuels & Lubricants Conference & Exhibition*, SAE International, 2022, doi:10.4271/2022-01-1040.

Alshwawra, A., “Syrian refugees’ integration policies in jordanian labor market,” *Sustain.*, 2021, doi:10.3390/su13137234.

Alshwawra, A., Pasligh, H., Hansen, H., and Dinkelacker, F., “Increasing the roundness of deformed cylinder liner in internal combustion engines by using a non-circular liner profile,” *Int. J. Engine Res.* 22(4):1214–1221, 2021, doi:10.1177/1468087419893897.

Alshwawra, A. and Almuhtady, A., “Impact of Turmoil and Gas Resources in the Eastern Mediterranean on Jordanian Energy Security and Foreign Policy,” *Insight Turkey* 22(3):237–255, 2020, doi:10.25253/99.2020223.13.

Alshwawra, A., Pohlmann-Tasche, F., Stelljes, F., and Dinkelacker, F., “Enhancing the geometrical performance using initially conical cylinder liner in internal combustion engines-A numerical study,” *Appl. Sci.* 10(11):3705, 2020, doi:10.3390/app10113705.

Asfar, J. Al, **Alshwawra, A.**, Shaban, N.A., Alrbai, M., Qawasmeh, B.R., Sakhrieh, A., Hamdan, M.A., and Odeh, O., “Thermodynamic analysis of a biomass-fired lab-scale power plant,” *Energy* 194, 2020, doi:10.1016/j.energy.2019.116843.

Alshwawra, A. and Almuhtady, A., “DOĞU AKDENİZ DOĞALGAZ KAYNAKLARI VE BÖLGESEL KRİZLERİN ÜRDÜN ENERJİ GÜVENLİĞİ VE DIŞ POLİTİKASINA ETKİLERİ,” in: ŞAHİN, M. and YILMAZ, M. L., eds., *Akdeniz’de Devlet ve Düzen*, Polis Akademisi Başkanlığı, ISBN 978-605-7822-38-3: 195–214, 2020.

Alshwawra, A. and Almuhtady, A., "Impact of regional conflicts on energy security in Jordan," *Int. J. Energy Econ. Policy* 10(3):45–50, 2020, doi:10.32479/ijeep.9031.

Almuhtady, A., **Alshwawra, A.**, Alfaouri, M., Al-Kouz, W., and Al-Hinti, I., "Investigation of the trends of electricity demands in Jordan and its susceptibility to the ambient air temperature towards sustainable electricity generation," *Energy. Sustain. Soc.* 9(39), 2019, doi:10.1186/s13705-019-0224-1.

AlShwawra, A. and Asfar, J. Al, "Simulation of olive cake combustion in a fluidized bed burner," *Int. J. Mech. Eng. Robot. Res.*, 2018, doi:10.18178/ijmerr.7.5.483-488.

Asfar, J.J. Al, **AlShwawra, A.**, Sakhrieh, A., and Hamdan, M.A., "Combustion characteristics of solid waste biomass, oil shale, and coal," *Energy Sources, Part A Recover. Util. Environ. Eff.* 40(3):335–342, 2018, doi:10.1080/15567036.2017.1416707.

Hammad, A. and Asfar, J. Al, "Comparative study on direct burning of oil shale and coal," *AIP Conf. Proc.* 1863(1):030024, 2017, doi:10.1063/1.4992177.

Asfar, J.J. Al, **Hammad, A.**, Sakhrieh, A., and Hamdan, M.A., "Two-dimensional numerical modeling of combustion of Jordanian oil shale," *Energy Sources, Part A Recover. Util. Environ. Eff.* 38(9):1189–1196, 2016, doi:10.1080/15567036.2014.880091.

Hammad, A. and Batayneh, S., "Design and installation of grid interactive solar system for building of Ministry of energy and mineral resources," in: Dinçer, I., ed., *Proceedings of the 13th International Conference on Clean Energy*, ISBN: 978-605-64806-0-7, Istanbul, Turkey: 1653–1658, 2014.

Hammad, A. and Al-Momani, H., "Politics and Energy Security in Jordan," *Global Conference on Renewable energy and Energy Efficiency for Desert Regions 2013*, Amman, Jordan: Paper No. 100, 2013.

Supervised Thesis

Master thesis:

Migita, R., "Effects of Material Properties on Bore Deformation of Engine Cylinder Liner,"
Kyushu University, 2020.

Student thesis:

Ahmad Abo Swerih, "Performance Study of Additively Manufactured Cylinder Liner,"
Leibniz Universität Hannover, 2021.

Bachelor thesis:

Anas Guizani, "Effects of Material Properties on Bore Deformation of Engine Cylinder Liner," Leibniz Universität Hannover, 2022.

Resume

Personal Data

Name: Ahmad Alshwawra
 Date of birth: 12.11.1984
 Citizenship: Jordanian

Education

2018 – 2023 Doctoral research in Mechanical Engineering, Institute of Technical Combustion, Leibniz University Hannover, Germany
 2013 – 2015 Master of Science in Conflict Management, Faculty of International Relations, University of Jordan, Jordan
 2008 – 2012 Master of Science in Mechanical Engineering, Faculty of Engineering and Technology, University of Jordan, Jordan
 2003 – 2007 Bachelor of Science in Mechanical Engineering, Faculty of Engineering and Technology, University of Jordan, Jordan

Work Experience

2018 – 2023 Research Assistance in Institute of Technical Combustion, Leibniz University Hannover, Germany
 2015 – 2018 Lecturer in Mechanical Engineering Department, German Jordanian University, Amman, Jordan
 2008 – 2015 Mechanical Engineer in Ministry of Energy and Mineral Resources, Amman, Jordan.
 2007 – 2008 Maintenance Engineer in Saudi Steel Pipes, Dammam, Saudi Arabia